Finite element analysis of two-dimensional reinforced concrete structures, taking account of non-linear physical behaviour and the development of discrete cracks

H. J. GROOTENBOER

Delftse Universitaire Pers

Finite element analysis of two-dimensional reinforced concrete structures, taking account of non-linear physical behaviour and the development of discrete cracks

Finite element analysis of two-dimensional reinforced concrete structures, taking account of non-linear physical behaviour and the development of discrete cracks

PROEFSCHRIFT
ter verkrijging van de graad van doctor
in te technische wetenschappen aan de
Technische Hogeschool Delft, op gezag
van de rector magnificus
prof. dr. ir. F.J. Kievits
voor een commissie aangewezen
door het college van dekanen te
verdedigen op woensdag 21 maart 1979
te 16.00 uur

door

HENDRICUS JOHANNES GROOTENBOER

civiel ingenieur
geboren te Amsterdam

Delftse Universitaire Pers, 1979

Dit proefschrift is goedgekeurd
door de promotor
PROF. IR. A.L. BOUMA
en de copromotor
LECTOR DR. ING. H.W. REINHARDT

Aan mijn Ouders
Aan Marjan

CONTENTS

Acknowledgements

The author thanks all who have contributed to the completion of this study, in particular dr. ir. J. Blaauwendraad and the direction of the Bridge departement of the Rijkswaterstaat.

INTRODUCTION

1.1 MOTIVE AND SCOPE OF THE RESEARCH

In the course of this century the material called concrete, reinforced or prestressed with steel, has become one of the most important building materials in civil and structural engineering. The design and execution of new structures which - in respect of shape, method of construction or manner of loading - are outside the range of standard experience make it necessary continually to investigate the behaviour of concrete structures.
Exemples of such structures are: offshore structures, nuclear power stations, and water engineering structures in or closely associated with the sea, such as the surge tide barrier in the Eastern Scheldt (Oosterschelde).
Increase in dimensional scale and the introduction of new techniques in the building of bridges and tunnels, however, also necessitate further research. In addition, the rise in the cost of all types of structure makes it essential to go on seeking less expensive alternative designs, materials and construction methods without lowering of safety standards.
Closely bound up with scale increase is the corresponding increase in the seriousness of the consequences of a disaster, so that careful and detailed structural safety analysis becomes more and more necessary. The central feature of such an analysis is an investigation of the loading and of the behaviour of the structure under all kinds of conditions such as cyclic loading (alternating loads), its time-dependent behaviour and especially its behaviour under overloading.

Investigation of the behaviour of concrete structures has hitherto chiefly been based on the results of tests performed on model structures or on structural components in the laboratory. Such tests provide good insight into the deformation of the structure and the magnitude of its failure load. But they yield only limited information on the strains and relative displacements of the embedded steel. Because of this, the interpretation of the behaviour and the detection of the causes thereof are made much more difficult. Knowledge of the causes of a certain behaviour is important in order to predict the behaviour of other structures or of similar structures under different loads.

The possibilities of mathematically predicting the behaviour of a concrete structure have been greatly extended as a result of the development of the computer. What are needed, besides a numerical model for describing the structure, are mathematical models embodying our knowledge of the behaviour of the constituent materials (steel and concrete) and of their manner of co-operation. One important condition for the attainment of an optimum result is the collaboration of investigators in these two fields of research. On the basis of these considerations the research project "Concrete analysis" has been initiated in the Netherlands within the framework of the Netherlands Committes for Concrete Research (C.U.R.). Collaborating in this project are the Technological Universities of Delft and Eindhoven, the Institute for

Applied Scientific Research on Building Materials and Building Structures (IBBC-TNO) and Rijkswaterstaat, a division of the Netherlands Ministry of Transport and Public Works.

The aim of the project is to achieve the further development of numerical models with the aid of which a deeper insight into the behaviour of concrete structures can be obtained and to make, on the basis thereof, a contribution to establishing new design rules and codes for practical use. The research will, for the time being, be confined to the static behaviour of two-dimensional concrete structures subject to in-plane loading. In addition to a study of the literature, the program of work comprises the following sub-projects:

- Experimental investigation of the transfer of force at a crack in a reinforced concrete structure.
- Investigation of a numerical model for describing the bond between steel and concrete.
- Development of a computer program for the analysis of two-dimensional framed structures (MACRO model).
- Development of a computer program for the analysis of the behaviour of two-dimensional thin plate structures (MICRO model).

The present thesis is the result of the above-mentioned research on a numerical model for the analysis of reinforced concrete plate structures subject to in-plane loading. In order to emphasize that, in the model developed here, each crack is described separately and that the displacements and forces are calculated in it, the name "MICRO" model has been applied. The numerical models, such as the above-mentioned program for framed structures, which are based on average properties of a reinforced concrete plate cracked in one or more places are called "MACRO" models in the "Concrete analysis" project.

1.2 BEHAVIOUR OF MATERIALS AND STRUCTURES

The behaviour of the material concrete is particularly complex. This is apparent from the following points:

- The maximum tensile stress that concrete can resist is much less than the maximum compressive stress that it can resist.
- The relation between compressive stress and strain deviates already at a relatively low level of stress from the linear relation in accordance with Hooke's law. Besides, this compressive strain is dependent not only on the stress acting at any particular instant, but also on the previous history of the stress.
- Concrete shrinks and swells. The magnitude and rate of these phenomena depend on, among other factors, the humidity of the environment and the dimensions of the structure.
- The creep deformation of concrete is considerable and may be as much as four times the elastic deformation. On removal of load, part of the creep is recoverable and part of it is irrecoverable.
- If a crack develops in concrete, transfer of shear forces across the crack nevertheless continues to be possible because the faces of the crack are not smooth, so that the irregularities on them will interlock if the width of the crack is small (aggregate interlock) (see Fig. 1.1). The magnitude of the maximum shear stress that can thus be transferred across a crack depends on the width of the latter. [1.1]

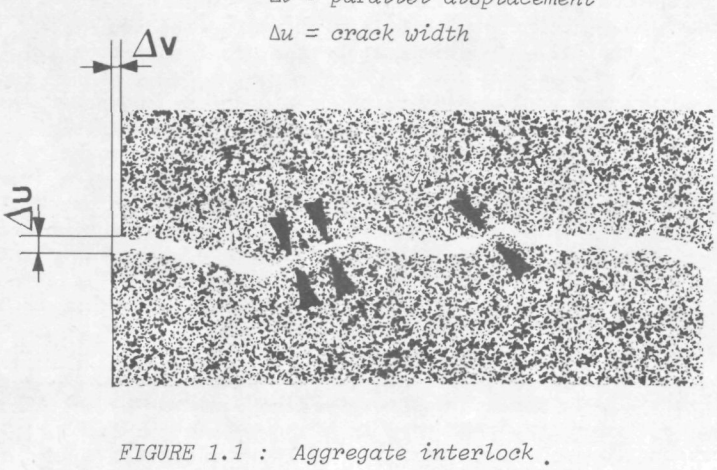

FIGURE 1.1 : Aggregate interlock .

To compensate for its low tensile strength, concrete is reinforced with steel bars and/or prestressed with tendons (high-tensile steel wires or bars). In the composite material formed in this way the steel, by virtue of its quality and shape, largely determines the co-operation of the two materials. Bond between concrete and steel, slip of the reinforcement and plastic deformation of the steel are important aspects with regard to this. In an unreinforced concrete structure, cracks develop already at low values of the loading. Cracks may considerably reduce the stiffness of the structure. When they are formed, the internal stress distribution is greatly changed. The reinforcing steel, which in the uncracked structure contributes only little to the actual loadbearing capacity, is now loaded to a high stress, as are also the contact surfaces between the steel and the concrete. The co-operation of the two materials now depends greatly on the quality of their bond and on the dowel action of the reinforcement at a crack in the concrete (see Fig. 1.2). The directions of the reinforcement and of the cracks have a major effect on the anisotropic behaviour of the cracked composite material.

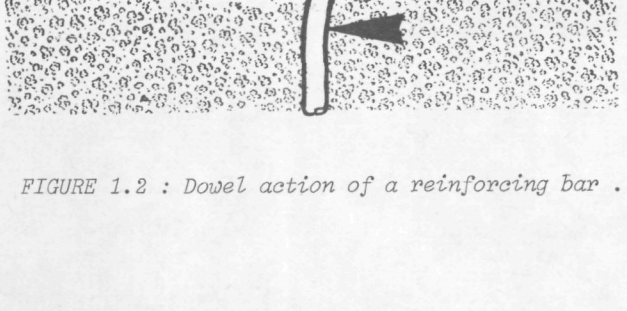

FIGURE 1.2 : Dowel action of a reinforcing bar .

Failure of a reinforced concrete structure may result from the occurrence of large deformations and thus exhibit a "ductile" character. Alternatively, however, it may be of a "brittle" character. This last-mentioned form of failure can be particularly dangerous because it is not initiated by large crack widths or deflections. In that case, too, the possibility of redistribution of forces which exists in a statically indeterminate structure cannot be sufficiently utilized.
Calculations for the design and analysis of reinforced concrete and prestressed concrete structures are usually based on linear elastic theory. This approach takes no account of the non-linear behaviour of the constituent materials, the reduction in stiffness due to cracking and the transition from isotropic to anisotropic properties for the composite material. Such calculations can therefore only provide insight into the behaviour of a structure at low values of loading. This is not necessarily a disadvantage with regard to structures within the conventional range of experience. The codes of practice often contain design rules to ensure that structures continue to conform to the relevant safety requirements also at higher loads.

A different situation exists with regard to new types of structures with which experience is as yet lacking. In most cases there are no codes or established design rules for them, and to test a prototype is often impracticable. For designing such structures and assessing their safety it is essential to have information on their behaviour under loads of large magnitude up to and including failure load. Since this behaviour is to a great extent determined by the above-mentioned non-linear behaviour of the materials, the analysis of these structures has to be based on models which take this behaviour into account. The calculations do indeed become much more complex in consequence of this and practically impossible to perform without the aid of a computer. The evolution that non-linear analysis models for reinforced concrete structures have undergone in the period from 1967 to the present time will be briefly outlined in the next section of the present chapter. All the models mentioned here are based on the finite element method. This numerical technique has proved to be particularly suitable for solving many kinds of problems in structural analysis with the aid of a computer.

1.3 NON-LINEAR ANALYSIS OF REINFORCED CONCRETE STRUCTURES BY THE FINITE ELEMENT METHOD

The purpose of this review of the subject is to give a general idea of the models that have been developed for the analysis of two-dimensional reinforced concrete structures loaded in their own plane. Confining the present treatment to these structures corresponds to the limitation of the scope of this study, as its title indicates. In the work of all the investigators in this field the emphasis is on the treatment of cracking. This is not surprising, since crack formation is of major influence on the stiffness, the internal stress distribution and the maximum loadbearing capacity of the structure. The first investigators to include cracking in their model were Ngo and Scordelis [1.2]. In their analysis of reinforced concrete beams they took account of the cracks by detaching the elements at their boundaries (see Fig. 1.3).

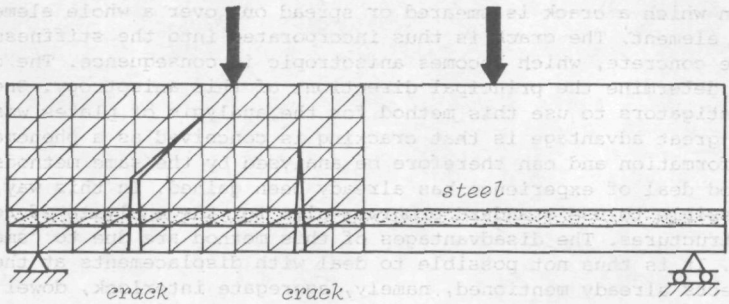

FIGURE 1.3 : Subdivision of a beam into elements by Ngo and Scordelis.

This schematization of cracking was later also used by Nilson [1.3] and by Stauder et al. [1.4]. In this method a crack is treated as a line on either side of which the displacements may differ in magnitude. This model offers the advantages that the displacements at a crack can be calculated and that these displacements can be taken into account in determining the effects such as aggregate interlock, dowel forces and yielding of the reinforcement. This model nevertheless was abandoned, the resons for this being:

- the limitation that cracks can occur only along the element boundaries. This results in a high degree of schematization of the cracking pattern and considerable dependence on the subdivision into elements. In Fig. 1.4 the cracking pattern calculated by Stauder for one of the concrete plates reported in [1.5] is compared with the actual experimental results. This comparison clearly illustrates the above-mentioned inflexibility of this approach;
- the second drawback relates to the method of analysis. In consequence of the detachment of the elements the system of equations must each time be established afresh and inverted or decomposed. In addition, the altered number of degrees of freedom has to be taken into account.

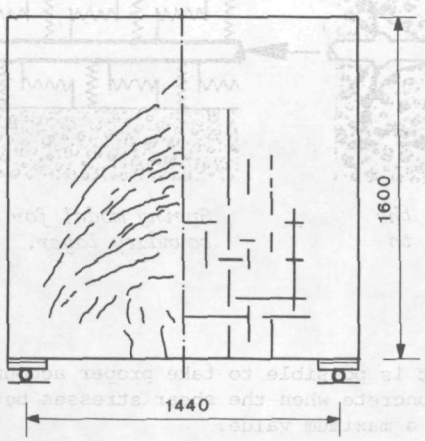

FIGURE 1.4 : Cracking pattern in a plate :
left : experimentally determined ;
right : as calculated by Stauder et al. [1.4]

In general, the discrete crack model has been abandoned in favour of the approach in which a crack is smeared or spread out over a whole element or over part of an element. The crack is thus incorporated into the stiffness properties of the concrete, which becomes anisotropic in consequence. The crack directions determine the principal directions of this anisotropy. One of the first investigators to use this method for the analysis of plates was Franklin [1.6]. Its great advantage is that cracking is conceived as a phenemenon like plastic deformation and can therefore be analysed by the same methods, with which a good deal of experience has already been gained. In this way, it becomes possible to use standard programs also for the analysis of reinforced concrete structures. The disadvantages of this method are due to "smearing out" the cracks. It is thus not possible to deal with displacements at the cracks in the aspects already mentioned, namely, aggregate interlock, dowel action and yielding of the steel. With this model the crack spacings and crack widths are difficult to calculate, even if a fine-meshed network of elements is used. Whether these drawbacks constitute a serious objection will depend on the kind of structure to be analysed. Experience shows that structures in which the bending moment is the determining quantity with regard to loadbearing capacity (ultimate strength) and which have a ductile load-deformation diagram can very suitable be analysed with these models. On the other hand, structures displaying brittle failure behaviour, which is frequently determined by one or a few dominant cracks, are not so suitable amenable to analysis on the basis of this model with "smeared-out" cracks. This frequently relates to shear cracks or flexural cracks in short cantilevers and comparable other structures.
Besides, not all the investigators adopt the same manner of schematization for the reinforcement. In those models that are based on discrete cracks the bars are always described with the aid of separate elements. These reinforcements elements are in many instances connected to the concrete elements by springs. The latter represent the behaviour at the boundary layer between steel and concrete (see Fig. 1.5).

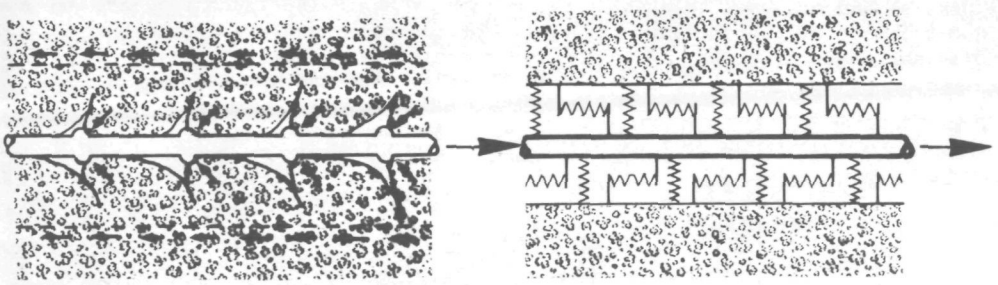

Transmission of force at the boundary layer according to Goto [1.7].

Spring model for the boundary layer.

FIGURE 1.5

With this schematization it is possible to take proper account of the slip of the reinforcement in the concrete when the shear stresses between the bar and the concrete have attained a maximum value.

In the models with "smeared-out" cracks the reinforcement is often incorporated into the properties of the plate element. For this element the aeolotropic properties of the composite material comprising concrete plus steel are then introduced into the analysis [1.8].

In that case, however, it is not possible to take account of displacement of the steel in relation to the concrete.

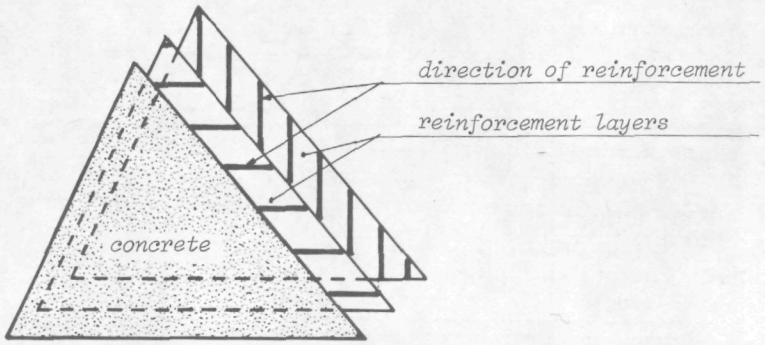

FIGURE 1.6 ; Composite reinforced concrete element

The method of dealing with the non-linear behaviour of concrete in the analysis presents less of a problem than does the choice of the model for describing this behaviour. Many different models to describe the behaviour of concrete under two-dimensional and three-dimensional states of stress are to be found in the literature. The results obtained with these respective models often differ considerably from one another, the reason being that as yet not enough is known concerning this behaviour. Lack of knowledge exists also with regard to the behaviour at a crack in the transfer of shear stresses (aggregate interlock) and the behaviour at the bounary layer between steel and concrete.

The main features of some important analytical models are summarized in Table 1.1. It indicates how the cracks are dealt with and what aspects of material behaviour are taken into account. A notable fact to emerge from these data is how little attention has hitherto been paid to aggregate interlock, shrinkage and creep, bond and - in particular - dowel action.

AUTHORS	BASIC MODELS	CONCRETE								STEEL			BOND			DOWEL ACTION			REFERENCES
		non-linear σ ε relation	discrete cracks	distributed cracks	model for agg. interlock	shrinkage and creep	2-dim. failure crit.	non-linear σ ε relation	yielding criterion	relaxation	linear τ Δv relation	non-linear τ Δv relation	failure criterion	linear σ Δu relation	non-linear σ Δu relation	failure criterion	
NGO & SCORDELIS			X								X			X			[1.2]
NILSON		X	X									X	X	X			[1.3]
FRANKLIN				X													[1.6]
CERVENKA				X													[1.9]
STAUDER, DORR a.o.		X	X									X	X	X			[1.4, 1.10]
SCHNOBRICH		X		X			X		X								[1.11, 1.19, 1.20]
HOSHINO				X		X					X						[1.12]
CEDOLIN & DEI POLI		X		X			X					X	X	X			[1.13]
VALLIAPPAN & DOOLAN				X			X		X								[1.14]
ZIENKIEWICZ a.o.		X		X			X		X								[1.15]
EBBINGHAUS		X		X	X		X		X								[1.8]
ARGYRIS a.o.		X		X			X										[1.16]
BUYUKOZTURK		X		X			X										[1.17]
LIN				X			X		X								[1.18]
KUSTERS		X		X			X		X								[1.21]

TABLE 1.1 : Summary of the facilities offered by various finite element models

1.4 AIM OF THE MICRO MODEL

First and foremost in connection with the development of the MICRO model was the desire to devise a model with which the behaviour of a structure can be analysed under various loads, enabling both the overall behaviour (e.g., a load-deflection diagram or a moment-curvature diagram for a portion of a beam) and the local occurrences within the structure to be described. The aim is to devise an instrument which can take the place of very expensive laboratory tests (with much internal recording of data) or which can assist in the interpretation of laboratory measurements with a limited number of recorded data. Of particalar interest is the behaviour after the occurrence of the first cracks and on attainment of the failure load. The model must be able to indicate the failure load, the cause of failure and the deformations that occur. In reinforced concrete structures the collapse mechanism is determined by the system of cracks that develops in the concrete, and the collapse load or, more generally, the failure load will depend on the stresses in the concrete and steel in the vicinity of the cracks.
Of special interest are those problems in which the structure, on reaching the failure load, displays brittle behaviour. Such behaviour occurs in failure due to shear or to a combination of shear and bending.
In these types of failure the dowel action of the reinforcement and the transfer of shear stresses at a crack play a major part. The deformation of the structure on attainment of the failure load will, in such cases, depend to a great extent on the slip of the reinforcement and the deformations of the concrete. Brittle failure of a structure is often the result of one dominant crack. The displacements at that crack determine the above-mentioned dowel forces, the shear stresses at the crack and the steel stresses in the vicinity of the crack.

It was endeavoured to find a model with discrete cracks, because in this way the displacements at a crack can suitably be determined and the effects of these displacements on the internal stresses can be taken into account. Also, this model can be expected to make the dominant crack distinctly discernible. The respective shares that the various forces have in the transfer of load at a section along a crack can then be analysed. An example of the various forces and stresses that may act at such a section is given in Fig. 1.7 for a beam loaded in bending and shear.

It should also be possible to use the model for the evaluation of the effects of the various types of non-linear material behaviour, in the boundary layer between steel and concrete and at a crack, upon the behaviour of a structure.

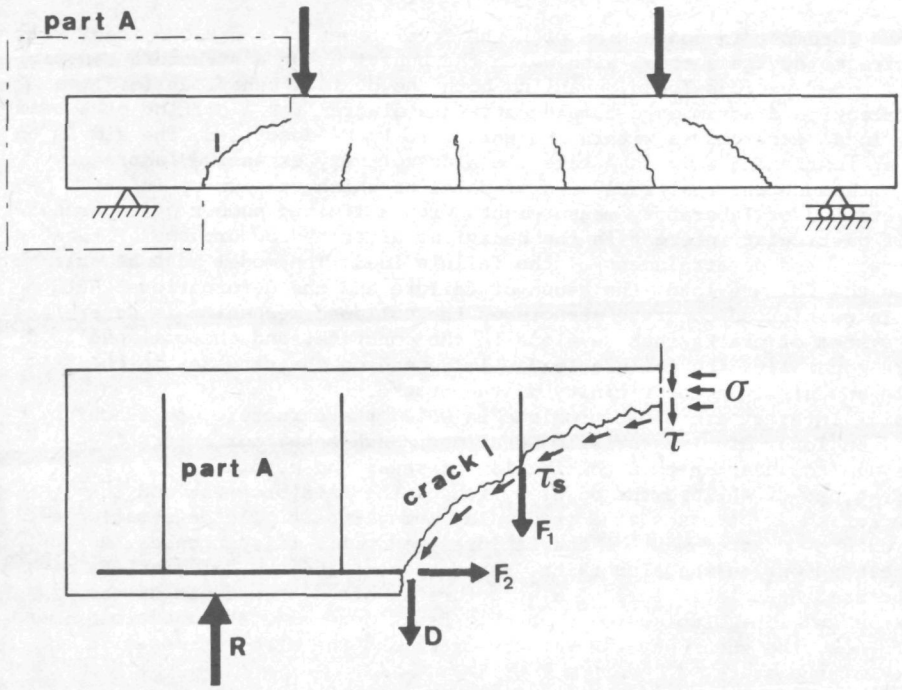

σ, τ	*stresses in uncracked concrete*
τ_s	*shear stress at a crack*
F_1	*force in stirrup reinforcement*
F_2	*force in tensile reinforcement*
D	*dowel force in tensile reinforcement*

FIGURE 1.7 : Forces and stresses at a section across a shear crack in a beam loaded in bending and shear.

2

FUNDAMENTALS

2.1 INTRODUCTION

The MICRO-model is a finite element analysis program based on the displacement method. This latter feature means that, in the system of equations ultimately to be solved, the displacements (degrees of freedom) of a number of points (nodes) are the unknowns.
This method has been chosen for the following reasons:

- a good deal of experience has already been gained with it,
- the system matrix of the system of equations is always positively definite,
- the number of degrees of freedom can be freely chosen,
- the equations can often be so arranged that a band matrix is obtained.

The hybrid mixed element model is used for the derivation of the force-deformation relations per element. In this model an assumption is made with regard to the distribution of the stresses in the element. The distribution of the displacements of the element boundaries is likewise assumed.
This model offers the following advantages:

- the distribution of the stresses in the various types of element can be suitably interadjusted,
- discontinuous distribution of the displacements in an element can be taken into account quite simply in this model. Such discontinuity occurs if a crack passes through the element,
- the favourable experience previously gained with this type of finite element model,
- the model offers the possibility of adding extra stress functions for describing special situations to the stress functions already existing,
- by adjusting the description of the displacements of element boundaries to the stress distribution at these boundaries it is ensured that the conditions of equilibrium are exactly satisfied at the boundaries. The advantage of this is that the stresses at a section along the element boundaries are always exactly in equilibrium with the external loads.

2.2 ELEMENTS USED, SCHEMATIZATION OF CRACKS

The structure is split up into two kinds of element, namely, a thin plate element for describing the concrete and a bar element by which the reinforcing steel (or prestressing steel) plus the boundary layer between steel and concrete are schematized.

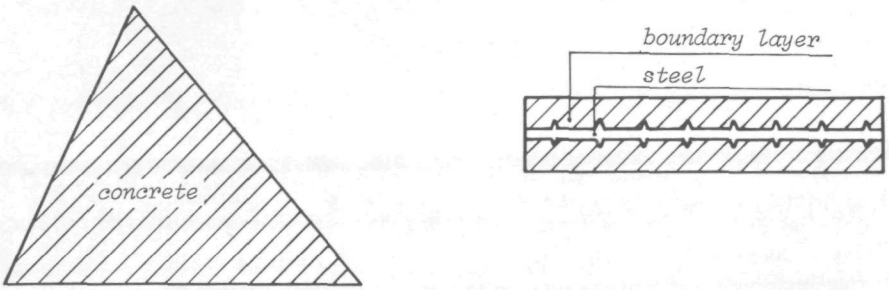

FIGURE 2.1 : Thin plate element and bar element

The bar elements must lie along the sides of the plate elements to enable transfer of stresses between the two types of element to occur.

The analysis takes account of the non-linear and time-dependent behaviour of the concrete, the non-linear behaviour of the steel and the behaviour in the boundary layer between steel and concrete. For a description of the various behaviour models for the materials and the boundary layer see Chapter 4.

If the stresses in a plate element attain the magnitudes at which, according to the cracking criterion, the concrete cracks a discrete crack is assumed to form, extending in a straight line from one boundary of the element to another. Not more than two cracks per plate element are permitted. For these cracks the limiting condition imposed is that they must intersect each other at an element boundary and that they must, from this point of intersection, each extend to a different side of the triangle. This requirement results from the rule applied in this program, namely, that at each side of the triangle only one point of intersection with a crack is allowed to occur.

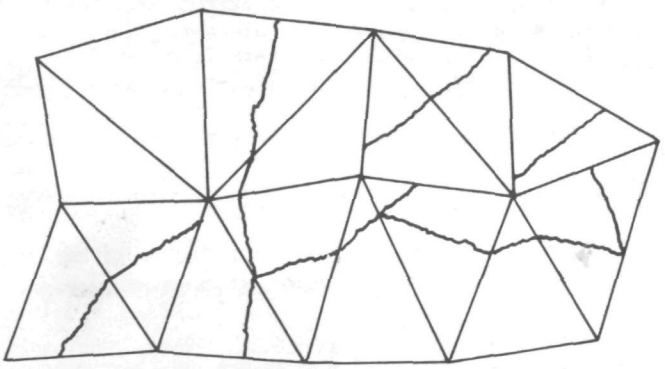

FIGURE 2.2 : Possible cracks in the triangular elements

The crack direction is taken to be perpendicular to the principal tensile stress. The position of a crack within a triangular element is so determined that the crack links up with a crack already present in an adjacent element. If the boundaries of the element under consideration have not yet been encountered by a crack in adjacent elements, the crack is assumed to pass through the centre of gravity of the triangle.

In each iteration only one new crack is applied. The next crack is not introduced into the model until the stresses perpendicular to the applied crack have become sufficiently small. This procedure is adopted in order to take account of the effect of the new crack on the internal stress distribution in the structure. In this way, with a sufficiently fine-meshed network of elements, it is possible to calculate the spacing of the cracks.

In a cracked element the three possible ways in which the parts thereof can undergo displacement as a rigid body are taken into account. To this end, the following are considered at a crack:

- the displacement of the two crack faces relatively to each other perpendicularly to the direction of the crack,
- the displacement of the two crack faces relatively to each other in the direction of the crack,
- the rotation of the two crack faces relatively to each other.

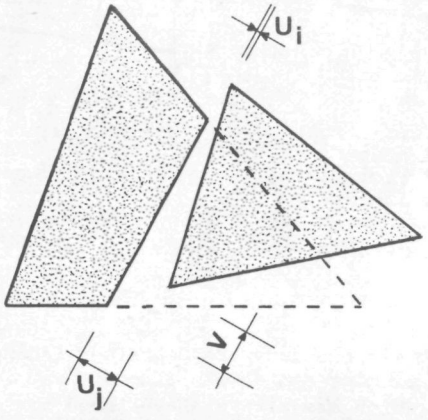

FIGURE 2.3 : Displacement possibilities at a crack

A crack, once it has been introduced into the model, remains in existence. The procedure does, however, take account of the possibility that, on further loading the structure, it may occur that a crack closes up again by compression, but as soon as tensile stresses act across a closed crack, the latter opens again. Transfer of compressive stresses across a crack is possible only for zero crack width.

In the uncracked element the stresses are assumed to be linearly distributed across it. Associated with this is the assumption of a quadratic distribution for the normal force and shear force in a bar element. The stress distribution diagrams corresponding to these assumptions - for the distribution along the plate element boundaries and in the bar element respectively - are indicated in Fig. 2.4.

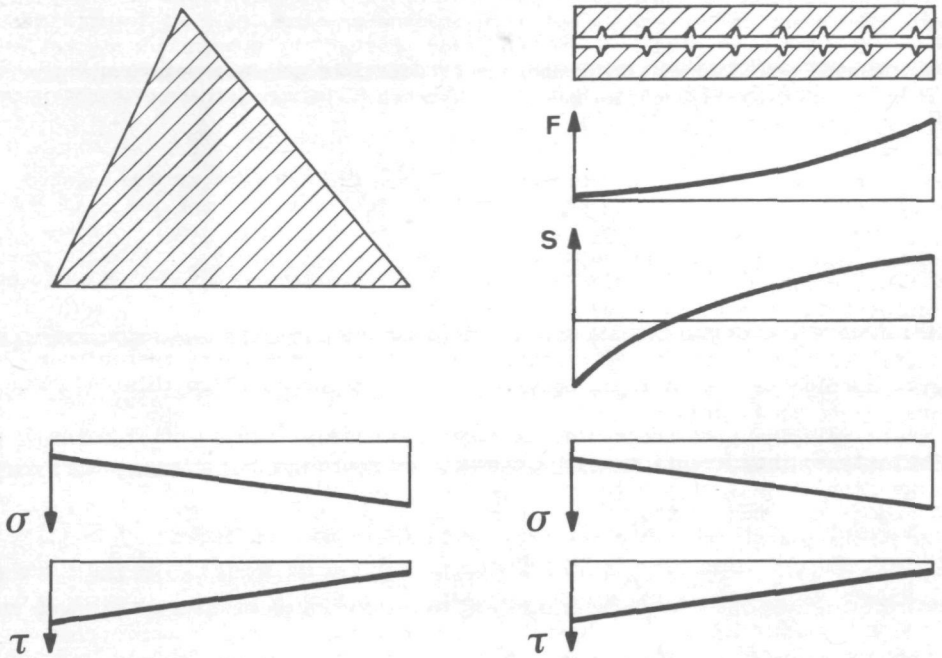

σ = *normal stress on side*

τ = *shear stress along side*

F = normal force

S = shear force

FIGURE 2.4 : Stress distribution along the plate element boundaries and in and along the bar element

The displacements of an element boundary are described independently of the displacements of the other element boundaries. In this way it is ensured that the equilibrium equations, which are always established for each displacement unknown, will relate only to the stresses at one element boundary. Now if the number of displacement unknowns per boundary is so chosen that the generalized nodal forces at these degrees of freedom uniquely represent the stresses at the boundary, this will ensure that, after solution of the system of equilibrium equations, the conditions of equilibrium are exactly satisfied at every point of a boundary.

This method of choosing the boundary displacements is called the method of natural boundary displacements [2.1]. For uniquely describing the linearly distributed stresses at the element boundaries it is necessary to describe both the normal displacement and the tangential displacement of the boundary likewise with a linear function. The degrees of freedom of the uncracked triangular element are indicated in Fig. 2.5 (a).

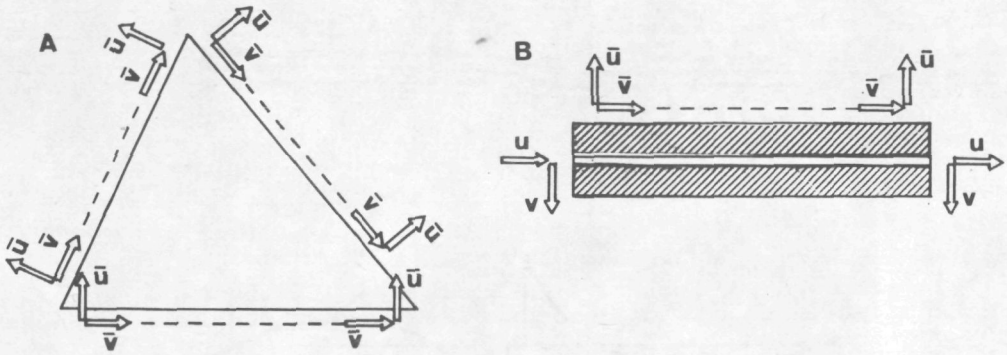

FIGURE 2.5 : Degrees of freedom of uncracked elements

In the case of the bar element a distinction is drawn between the degrees of freedom at the outside of the boundary layer ($\bar{u}$,$\bar{v}$) and the degrees of freedom at the end of the steel core (u,v). The first-mentioned degrees of freedom link up with those at the boundary of the thin plate element, while those at the ends of the steel core ensure continuity of connection with other bar elements (see Fig. 2.5(b)). In this way it is possible, in the model, to take account of the slip of the steel in relation to the surrounding concrete.

The stresses may vary greatly in the vicinity of a crack. This is most strikingly manifested in the dowel forces in the bar and in the associated stresses in the concrete. These forces and stresses are of maximum magnitude at a crack and are of opposite algebraic sign on either side thereof(see Fig. 2.6(b)).
The shear stresses acting between a reinforcing bar and the concrete may, if a crack intersects at an oblique angle the bar, display a disconuity in their distribution at the crack (see Fig. 2.6(c)).

Without extra arrangements these stress variations, and thus the effect of dowel action upon the loadbearing capacity, would be insufficiently expressed in the analysis. Therefore in the MICRO model, if a crack develops in an element, the number of possible stress fields is increased by fields which extend discontinuously across the crack. This applies to the bar element and the thin plate element (see Fig. 2.7). To make it possible to continue to satisfy exactly the equilibrium conditions at the boundaries of the elements also with these extra stress fields, it is necessary to increase the number of degrees of freedom at a boundary which is crossed by a crack and upon which discontinuously distributed boundary stresses may therefore act. These additional displacement quantities represent the discontinuity in the displacements at a crack.

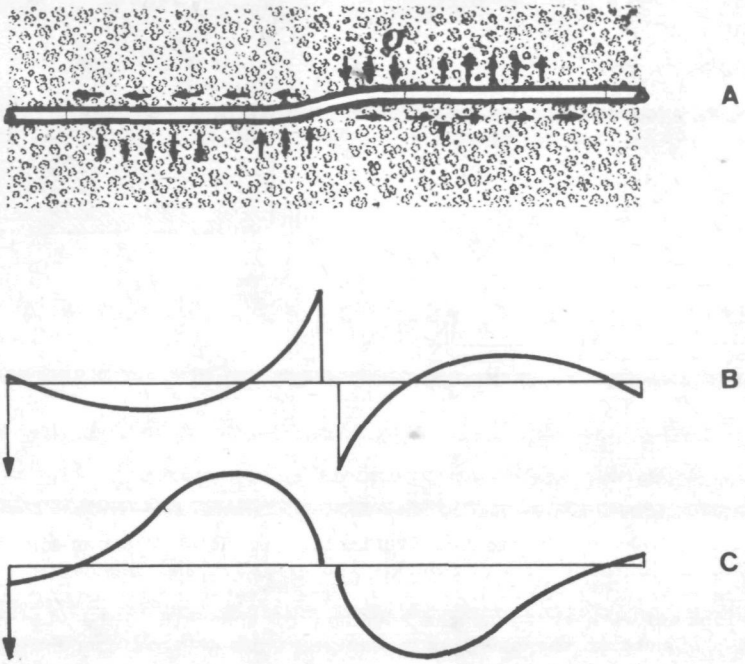

FIGURE 2.6 : Distribution of the stresses between the bar and the concrete in the vicinity of a crack

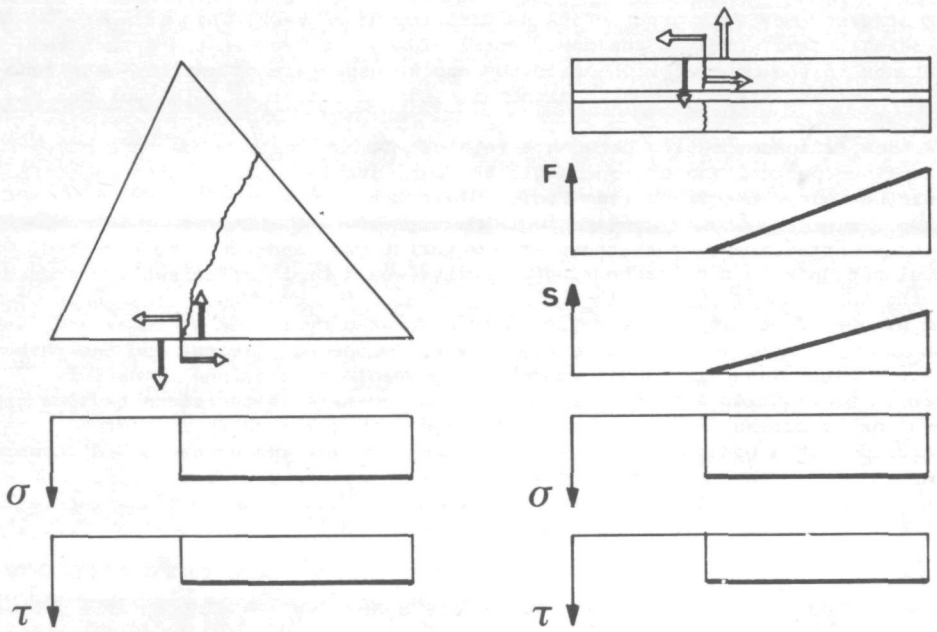

FIGURE 2.7 : Extra stress fields and degrees of freedom in a cracked thin plate element or bar element

The equilibrium equations for these extra degrees of freedom are assembled in a separate system of equations. In this way it is not necessary to modify the original system, which is highly advantageous from the viewpoint of computer efficiency.

2.3 METHOD OF ANALYSIS

In the MICRO model the "initial strain method" is used for dealing with the non-linear behaviour of the materials. To this end, the various stress-strain relationships are all written in the form:

$$\sigma = D\,(\varepsilon - \varepsilon^{I})$$

where: σ = stress(es)
D = initial modulus of elasticity (matrix)
ε_{I} = total strain(s)
ε^{I} = initial strain(s)

The initial strains may be due, inter alia, to the non-linear stress-strain relationship or the occurrence of displacements at cracks, but may also be caused by shrinkage and creep. An analysis by this method is based on an iterative procedure, as follows.
For the first iteration the initial strains are taken as zero. For a given load the stresses (σ_1) at the various points of the structure are calculated. Then the initial strains (ε^{I}_1) associated with these stresses are determined from the stress-strain diagram (Fig. 2.8). On the basis of these new initial strains the structure is again analysed for the same load. Next, with the new stresses (σ_2) at the various points of the structure the initial strains (ε^{I}_2) associated with these are calculted. Now if these newly calculated initial strains differ greatly from the previously calculated initial strains, the iteration process comprising the calculation of stresses and initial strains is continued until the difference between the newly calculated strains and those calculated in the previous iteration is sufficiently small. The way in which the iteration process proceeds depends on the structure and the way in which it is loaded and supported. In a statically determinate structure only one iteration is needed to reach the exact solution. For a statically indeterminate structure in which the total strain ε_o is prescribed the iteration process is given in Fig. 2.8. Successively the stresses and the initial strains σ_1, ε^{I}_1, σ_2, ε^{I}_2, σ_3, ε^{I}_3, σ_4, ε^{I}_4, etc. are calculated until the difference between ε^{I}_j and ε^{I}_{j+1} is sufficiently small.
The rate of convergence in this case can be increased by using a relaxation method with a relaxationfactor between zero and one.

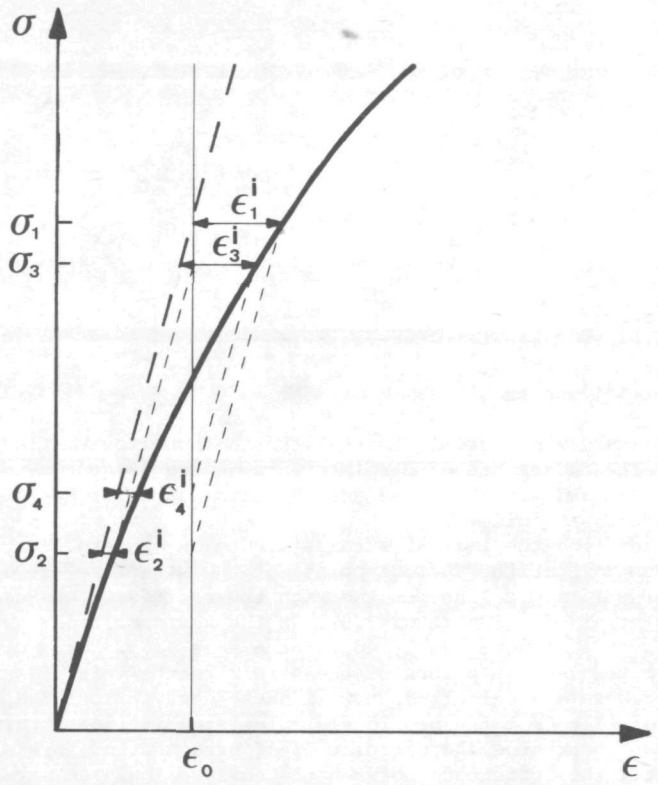

FIGURE 2.8 : Successively calculated initial strains for a structure in which the total strain ε_0 is prescribed

This method is employed because the modulus of elasticity (D) is kept constant in the analysis, the advantage being that the stiffness relationships need then be established only once and that the system of equations need be decomposed only once. The drawback of this method is that it cannot directly be used with materials having an ideal elasto-plastic behaviour (see Fig. 2.9) because for such materials the initial strains is not uniquely defined for each stress.

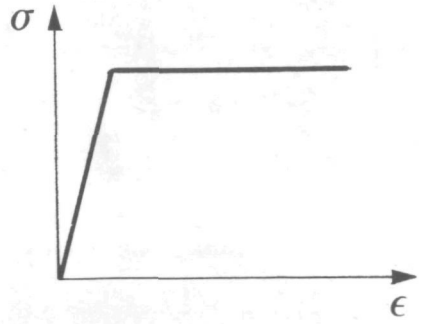

FIGURE 2.9 : Ideal elasto-plastic material behaviour

For determining the initial strain of an ideal plastic material the latter is conceived as being replaced by a visco-plastic material model. This means in effect that a viscous damper is placed parallel to the plastically deformable part (see Fig. 2.10).

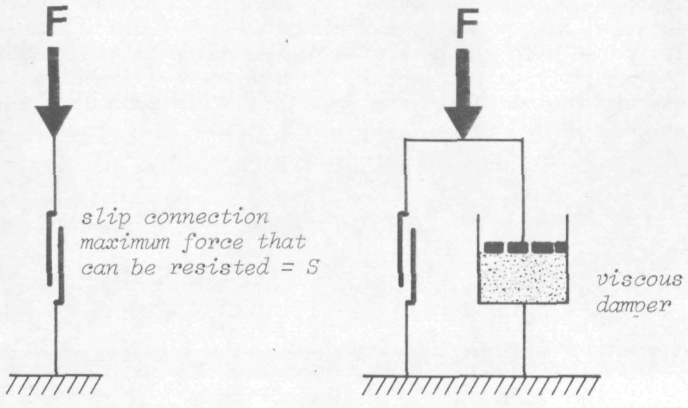

ideal plastic model *visco-plastic model*

FIGURE 2.10 :

If this visco-plastic model is loaded by a force P larger than the yielding force S, a force P-S will act upon the viscous damper. The rate of strain ($\dot{\varepsilon}_{vp}$) of this damper is dependent on the load and on the viscous stiffness K:

$$\dot{\varepsilon}_{vp} = K(P - S)$$

If the iteration process is conceived as a fictitious creep process with a time interval Δt between each two successive iterations, then the increase in visco-plastic strain per iteration is:

$$\Delta\varepsilon_{vp} = \dot{\varepsilon}_{vp}\Delta t = K\Delta t(P - S)$$

The iteration process (creep process) is continuied untill the difference P - S of the two forces has become sufficiently small. The viscous damper serves merely as a means for determining the initial strain. The viscous stiffness K and the time intervals Δt are therefore only auxiliary quantities. The magnitude of the product $K\Delta t$ determines whether the calculation converges and how rapidly. Carmeau, in [2.2], indicates what values should be adopted for $K\Delta t$ for the various plastic material models. In general, the process is found to converge satisfactorily if the following is conformed to:

$$\Delta\varepsilon_{vp} < \frac{2(P - S)}{D}$$

(where D is the modulus of elasticity of the material)
or:

$$K\Delta t < \frac{2}{D}$$

A disadvantage sometimes attributes to the initial strain method is that it has a more restricted range of convergence than the initial stress method. The stability of the iteration process is greatly increased by ensuring that the increments of the initial strains per iteration are not taken too large.

A guiding criterion for this is:

$$\Delta\varepsilon^{I} < \frac{\sigma}{D}$$

Alternatively to the possibility of incorporating the crack displacements in the initial strains, these displacements can be accommodated directly in the system of equations. This does not necessitate recalculating the stiffness relationships per element, but it will be necessary to re-establish and decompose the whole system of equations. Every time a number of cracks have formed, these are commodated in the equations. This procedure makes for more rapid iteration.

DERIVATION OF THE EQUATIONS

3.1 INTRODUCTION

The equations for the triangular thin plate element and for the bar element will be derived in this chapter. For this purpose tensor notation will be used because it enables the equations to be written in a compact form and clearly indicates the directions of the quantities concerned and their various partial derivatives. In the derivation it is assumed that the displacements remain small in relation to the dimensions of the structure and that the partial derivatives of the displacements are small in relation to unity. This means that the structure is presupposed to display geometrically linear behaviour.
Five basic equations are applicable in stress analysis. Three of these relate to each point of the structure, and two to its perimeter (boundaries).
The three equations that are valid for each point of a structure are:

1. The conditions of equilibrium:

$$\sigma_{ij,j} + q_i = 0 \tag{3.1a}$$

$$\sigma_{ij} - \sigma_{ji} = 0 \tag{3.1b}$$

These equations indicate the relationship between the volume load q and the stresses σ.

2. The constitutive equations:

$$\sigma_{ij} = D_{ijkl}\varepsilon_{kl} \tag{3.2}$$

The stiffness tensor D for a particular material expresses the relationship between the strains ε at a particular point and the stresses σ.

3. The kinematic equations:

$$\varepsilon_{ij} = \tfrac{1}{2}(u_{i,j} + u_{j,i}) \tag{3.3}$$

If the partial derivatives of the displacements u at a point are small in relation to unity, the strains are linearly dependent on them.

These three equations establish the relationships between the volume load, the stresses and the stress gradients, the strains and the displacement gradients at every point of the structure.
For every point of the perimeter of a structure, one of the following two conditions is always applicable separately in one direction.

4. The kinematic boundary conditions:

$$u_i = u_i^o \quad \text{on } A_u \tag{3.4}$$

For these points this means that, in the direction concerned, the magnitude of the displacement (u) is preassigned (u^o). The external force in this direction at the boundary is then unknown. A_u is the portion of the perimeter to which this condition applies.

5. The dynamic boundary conditions:

$$\sigma_{ij} e_j = p_i^o \quad \text{on } A_p \tag{3.5}$$

At these points of the boundary this means that, in the direction concerned, the external force is preassigned (p^o) and that the displacement is unknown. The vector e is the normal vector to the boundary at the point under consideration. A_p is the portion of the perimeter to which this condition applies.

The equations 3.4 and 3.5 relate the displacements and the stresses in the structure, respectively, to the conditions at the structure boundaries.

In the finite element method these five basic equations are used for the derivation of the equations. If the calculated stresses, strains and displacements for each point of the volume and the perimeter satisfy these conditions, then this solution is unique and exact. In general, it is possible only for one-dimensional structural components thus to satisfy all these conditions exactly. For two-dimensional or three-dimensional components (elements) a number of conditions can be satisfied exactly , the others approximately. Which conditions are satisfied exactly, and which only approximately, will depend on the element model employed.
The model that satisfies exactly the constitutive equations 3.2 and the kinematic equations 3.3 and 3.4 is called the compatible model. The counterpart to this is the so-called equilibrium model, which satisfies exactly the constituve equations 3.2 and the equilibrium conditions 3.1 and 3.5. Models which satisfy exactly neither the equilibrium conditions 3.1 nor the kinematic equations 3.3 are sometimes referred to as mixed models.

In the finite element method, interpolation functions and a number of parameters are used for describing the magnitude and distribution of the stresses, the strains and/or the displacements in an element. If, besides these functions which are valid over the whole element, interpolation functions and associated parameters are used which are valid only for the boundaries of an element, such a model is called a hybrid model. For a review of the various possible element models the relevant literature should be referred to [2.1] and [3.1] .
For describing the element behaviour the hybrid mixed model is used here. This is a generalization of the above-mentioned equilibrium model. It is based on an assumption for the distribution of the stresses in the element and for the distribution of the displacements of the element boundaries. For the triangular plate element the assumed stress distribution only approximately satisfies the moment equilibrium condition in equation 3.1b. The equations for the hybrid mixed model will here be established with the aid of Galerkin's method. This method is preferred to methods which make use of a variation principle, because with Galerkin's approach the element relationships can be derived directly from the five basic equations. Which conditions are satisfied exactly, and which only approximately, distinctly emerges from this derivation.

3.2 GALERKIN'S METHOD

Galerkin's method is based on the method of weighted residues [3.2]. With this approach the requirement that for every point of the element area it is necessary to satisfy each of the first three basic equations is eased. The equations which cannot be satisfied exactly are replaced by the conditions that the integrals over the area of the original equation, multiplied by a number of weighting functions, must become zero. By using several weighting functions it is not only possible to ensure that the stated condition is satisfied on average over the surface, but also that first-order and higher-order moments of the residue become zero.
The special feature of Galerkin's method is that for the weighting functions the same functions are used as for the description of the magnitude and distribution of the various quantities. This has the advantage that the formulas derived in this way are the same as those derived with the aid of the corresponding variation principle and that the stiffness matrix remains symmetric. The product of residue and weighting function always has the character of "work". Thus, residual forces are always weighted with displacement fields and residual strains are weighted with stress fields. What has been stated here with regard to the three conditions in the element is also valid for the boundary conditions : in the case of the latter it will be necessary to integrate over the perimeter instead of over the area.

The derivation of the equations starts from the consideration of one element. If the force-deformation relationships per element are known, the procedure for establishing an overall stiffness matrix and a load vector and for calculating the displacements conforms to the standard displacement method, which will not be further discussed.
For describing the stresses and displacements in an element, and also for describing the displacements of the element boundaries, separate functions and parameters are used in the hybrid mixed model.

Thus, the stresses are dependent on m parameters β and the co-ordinate functions P:

$$\sigma_{kl} = P_{kl\alpha}\beta_{\alpha} \qquad (\alpha = 1, .., m) \tag{3.6}$$

The displacements u in the element depend on k parameters V and the functions Q:

$$u_i = Q_{i\delta} V_{\delta} \qquad (\delta = 1, .., k) \tag{3.7}$$

And the displacements u^{o} of the element boundaries are described as a function of n displacements V^{o}:

$$u_i^{o} = L_{i\gamma} V_{\gamma}^{o} \qquad (\gamma = 1, .., n) \tag{3.8}$$

Of the two types of boundary condition, only one always has to be exactly satisfied at each point and for each direction. Here the kinematic boundary condition (equation 3.4) is used for all the boundaries of the element in all directions. In choosing the displacement quantities V^{o} and the interpolation functions L it is ensured that the displacements of each point of a boundary is the same for all the elements meeting at that boundary. The constitutive equations 3.2 are used for calculating the strains from the stresses. For the purpose of the method of analysis envisaged here, the strains are split up into an elastic part ε^{E} and an initial part ε^{I}. The elastic strains are those which would occur if the material displayed ideal linearly elastic behaviour (see Section 2.3).

$$\varepsilon_{ij} = \varepsilon_{ij}^{E} + \varepsilon_{ij}^{I}$$
$$\varepsilon_{ij}^{E} = F_{ijkl}\sigma_{kl} = F_{ijkl}P_{kl\alpha}\beta_{\alpha} \qquad (3.9)$$
$$\varepsilon_{ij} = F_{ijkl}P_{kl\alpha}\beta_{\alpha} + \varepsilon_{ij}^{I}$$

For linearly elastic materials the flexibility tensor F is the inverse of the stiffness tensor D in equation 3.2. The displacements in the element should satisfy the kinematic equations 3.3 and 3.4. In general, the chosen displacement field cannot exactly satisfy these equations. Therefore these two conditions are replaced by the condition that the integrals of the product of these conditions with a number of weighting functions must become zero. Since we are here concerned with the weighting of strains and displacements, the co-ordinate functions P of the stress field are chosen for the weighting functions. The substitutive kinematic conditions per element are:

$$\iiint_{V_e}\{\varepsilon_{ij} - \tfrac{1}{2}(u_{i,j} + u_{j,i})\}P_{ij\alpha}dV + \int_{A_e}(u_i - u_i^{o})e_j P_{ij\alpha}dA = 0 \qquad (3.10)$$
$$(\alpha = 1,..,m)$$

where Ve denotes the volume of the element and Ae denotes the area of the boundaries.
For the purpose of further working out the volume integrals, 3.10 is rewritten as:

$$\iiint_{V_e}\varepsilon_{ij}P_{ij\alpha}dV - \iiint_{V_e}u_{i,j}P_{ij\alpha}dV + \iiint_{V_e}\tfrac{1}{2}(u_{i,j} - u_{j,i})P_{ij\alpha}dV + \qquad (3.11)$$
$$\int_{A_e}u_i e_j P_{ij\alpha}dA - \int_{A_e}u_i^{o}e_j P_{ij\alpha}dA = 0$$

After partial integration, the second term on the left-hand side becomes:

$$\iiint_{V_e}u_{i,j}P_{ij\alpha}dV = \int_{A_e}u_i e_j P_{ij\alpha}dV - \iiint_{V_e}u_i P_{ij\alpha,i}dV \qquad (3.12)$$

Substitution of the equations 3.6, 3.7, 3.8, 3.9 and 3.12 into 3.11 gives:

$$\beta_\zeta\iiint_{V_e}P_{kl\zeta}F_{klij}P_{ij\alpha}dV + \iiint_{V_e}\varepsilon_{ij}^{I}P_{ij\alpha}dV + V_\delta\iiint_{V_e}Q_{i\delta}P_{ij\alpha,i}dV + \qquad (3.13)$$
$$V_\delta\iiint_{V_e}\tfrac{1}{2}(Q_{i\delta,j} - Q_{j\delta,i})P_{ij\alpha}dV - V_\gamma^{o}\int_{A_e}L_{i\gamma}e_j P_{ij\alpha}dA = 0$$

The equations 3.13 represent the relationships between the stress parameters β and the displacement quantities V and V^{o}. For the sake of obtaining a compact notation, the various integrals are substituted into 3.13,

$$F_{\zeta\alpha} = \iiint_{V_e}P_{kl\zeta}F_{klij}P_{ij\alpha}dV$$
$$Z_\alpha = \iiint_{V_e}\varepsilon_{ij}^{I}P_{ij\alpha}dV$$
$$B_{\delta\alpha} = \iiint_{V_e}Q_{i\delta}P_{ij\alpha,i}dV + \iiint_{V_e}\tfrac{1}{2}(Q_{i\delta,j} - Q_{j\delta,i})P_{ij\alpha}dV$$
$$D_{\gamma\alpha} = \int_{A_e}L_{i\gamma}e_j P_{ij\alpha}dA$$

With these expressions, 3.13 can be written as follows:

$$\boxed{\beta_\zeta F_{\zeta\alpha} + Z_\alpha + V_\delta B_{\delta\alpha} - V_\gamma^{o} D_{\gamma\alpha} = 0} \qquad (3.14)$$

After the constitutive equations and the kinematic conditions there still remain the equilibrium conditions to be satisfied. In conformity with the procedure followed with regard to the kinematic conditions, the equilibrium conditions for each point are replaced by the requirement that the integrals

(over the volume of the element) of the equilibrium equations multiplied by a number of weighting functions must be zero. The interpolation functions of the displacements in the element are used as weighting functions:

$$\iint_{V_e} (q_{ij,i} - q_i)Q_{i\delta}dV + \iint_{V_e} c_{ij}\tfrac{1}{2}(Q_{i\delta,j} - Q_{j\delta,i})dV = 0 \qquad (3.15)$$

$$(\delta = 1,..,k)$$

The first integral relates to the equilibrium of forces and the second integral relates to the equilibrium of moments. Substitution of equation 3.6 (for the stresses) into equation 3.15 gives:

$$\beta_\alpha B_{\delta\alpha} - R_\delta = 0 \qquad (3.16)$$

For the meaning of $B_{\delta\alpha}$ see equation 3.14.

$$R_\delta = \iint_{V_e} q_i Q_{i\delta}dV$$

By combination of the equations 3.14 and 3.16 the displacement quantities V can be eliminated from the relations between the stress parameters β and the displacement quantities V^o at the element boundaries:

$$\boxed{\beta_\zeta = H_{\zeta\alpha}\{D_{\gamma\alpha}V^o_\gamma - Z_\alpha\} + Y_{\zeta\delta}R_\delta} \qquad (3.17)$$

where:

$$H_{\zeta\alpha} = F^{-1}_{\zeta\alpha} - F^{-1}_{\zeta\nu}B_{\delta\nu}(B_{\delta\gamma}F^{-1}_{\gamma\varepsilon}B_{\lambda\varepsilon})^{-1}B_{\lambda\mu}F^{-1}_{\mu\alpha}$$

$$Y_{\zeta\delta} = F^{-1}_{\zeta\nu}B_{\lambda\nu}(B_{\lambda\gamma}F^{-1}_{\gamma\varepsilon}B_{\delta\varepsilon})^{-1}$$

In this derivation it is clearly manifest that per element the calculated stresses and the volume loadings need not to be in exact equilibrium at every point and that the displacements, too, only approximately need to satisfy the kinematic conditions. If the volume loadings are zero and if the chosen stress functions always satisfy the equilibrium conditions exactly, then the tensors B and R are zero. The distribution of the displacements in the element will then have no influence at all on the derivation and on the relationships finally arrived at. The displacement fields in the element here only perform the function of weighting the errors in the equilibrium equations. This is taken into account in making the choise of these displacement fields. In the displacement method the relationships between the displacements of a number of points at the element boundaries and the stress resultants at those points are utilized. These stress resultants K are uniquely determinable from the stresses. The requirement is that, for a small displacement of the element boundaries, these resultants do the same work as is done by the stresses at the boundaries.

$$\int_{A_e} q_{ij}e_j\delta u^o_i dA = K_\gamma\delta V^c_\gamma \qquad (3.18)$$

On substitution into this equation of the equations 3.6 and 3.8 it becomes:

$$\beta_\alpha D_{\alpha\gamma}\delta V^o_\gamma = K_\gamma\delta V^o_\gamma \qquad (3.19)$$

This must be valid for any variation δV^o, so that:

$$\beta_\alpha D_{\alpha\gamma} = K_\gamma \qquad (3.20)$$

Substitution of the equations 3.17 gives:

$$D_{\alpha\gamma}{}^{H}{}_{\alpha\delta} D_{\delta\lambda} V^{o}_{\lambda} = K_{\gamma} + D_{\alpha\gamma}{}^{H}{}_{\alpha\delta} Z_{\delta} - D_{\alpha\gamma}{}^{Y}{}_{\alpha\delta} R_{\delta} \qquad (3.21)$$

The choise of the number of stress parameters (m) and the numbers of displacement quantities (n) and (k) are closely interconnected. This clearly emerges on considering the equations 3.14. In these, m stress parameters β are dependent on $n + k$ displacement quantities V and V^{o}. If $n + k$ exceeds m, there are at least $n + k - m$ non-zero combinations of displacement quantities for which all the stress parameters become zero. In reality there are l of these displacement possibilities, these being the possibilities of displacement of the element as a rigid (undeformed) body. If it is desired to restrict the stressless displacement possibilities to these (l) rigid-body displacements, then the minimum requirement is expressed by:

$$n + k - m \leqslant l \qquad (3.22)$$

3.3 ADDITIONAL SYSTEM OF EQUATIONS

In Chapter 2.2 it was already stated that, if an element is intersected by one or two cracks, extra stress fields and extra displacement unknowns at the element perimeter are used for describing the stresses distributed discontinuously across the crack.
These extra degrees of freedom are not included in the original system of equations, but in a separate (additional) system. In this section the relationships between the various types of degrees of freedom and the types of stress parameters will be derived. Since the directions and patial derivatives are sufficiently evident from the tensor notation used in the preceding section in connection with general derivation given there, here only the even more compact matrix notation will be adopted. The designations of the matrices and vectors employed here correspond entirely to those of the tensors previously employed.

For the description of the stresses in a cracked element an extra stress field $P_2\beta_2$ is added to the stress field $P_1\beta_1$:

$$\sigma = P_1\beta_1 + P_2\beta_2 \qquad (3.23)$$

The displacements of the element boundaries which are intersected by a crack are described in terms of the general displacement distribution $L_A V^{o}_A$ and an extra distribution $L_B V^{o}_B$:

$$u^{o} = L_A V^{o}_A + L_B V^{o}_B \qquad (3.24)$$

Substitution of these functions into the equations 3.14 gives:

$$\beta_1 F_{11} + \beta_2 F_{21} + Z_1 + B_1 V - D_{1A} V^{o}_A - D_{1B} V^{o}_B = 0 \qquad (3.25a)$$

$$\beta_1 F_{12} + \beta_2 F_{22} + Z_2 + B_2 V - D_{2A} V^{o}_A - D_{2B} V^{o}_B = 0 \qquad (3.25b)$$

The interpolation functions P_2 and L_B are so chosen that in the equations the matrices F_{12} and D_{1B} become zero.

In Section 3.2 the displacement quantities V were eliminated from the equations 3.14 with the aid of the generalized equilibrium conditions 3.16. For the sake of splitting up the stress parameters β_1 and β_2 as much as possible, it is here required that the field $P_1\beta_1$ is approximately in equilibrium with the volume loading q.

The generalized equilibrium conditions 3.16 thus becomes:

$$\beta_1 B_1 - R = 0 \tag{3.26a}$$

$$\beta_2 B_2 = 0 \tag{3.26b}$$

With the aid of these equations the equations 3.25 can be rewritten as follow:

$$\beta_1 = H_{11}\{ D_{1A} V_A^o - Z_1 \} + Y_1 R \tag{3.27a}$$

$$\beta_2 = H_{22}\{ D_{2A} V_A^o + D_{2B} V_B^o - Z_2 \} \tag{3.27b}$$

The generalized nodal forces K can be calculated from the stress parameters with the aid of equation 3.20:

$$D_{1A}^T \beta_1 + D_{2A}^T \beta_2 = K_A \tag{3.28a}$$

$$D_{2B}^T \beta_2 = K_B \tag{3.28b}$$

The relationships between the generalized nodal forces and the displacement quantities at the element boundaries now become:

$$D_{1A}^T H_{11} D_{1A} V_A^o = K_A + D_{1A}^T H_{11} Z_1 - D_{1A}^T Y_1 R - D_{2A}^T \beta_2 \tag{3.29a}$$

$$D_{2B}^T H_{22} D_{2B} V_B^o = K_B + D_{2B}^T H_{22} Z_2 - D_{2B}^T H_{22} D_{2A} V_A^o \tag{3.29b}$$

These two systems of equations are separately established and solved. In each fresh iteration, first the displacements V_A^o are calculated with the aid of the initial strains Z_1 and the secondary stresses β_2 from the preceding iteration. Then the displacements V_B^o are calculated with the aid of the initial strains Z_2 from the preceding iteration and the newly calculated displacements V_A^o. This procedure of splitting up into two systems of equations has been chosen in order to avoid having to establish the original system of equations afresh every time a crack occurs.
Choosing the interpolation functions P_2 and L_B so that the matrices F_{21} and D_{1B} become zero is done by adopting the following expressions for these functions:

$$P_2 = (P_1 A + P_2^*) \tag{3.30}$$

$$L_B = (L_A \bar{A} + L_B^*) \tag{3.31}$$

The matrices A and $\bar{A}$ can always be so determined that the matrices F_{21} and D_{1B} are zero. This is done in order to have the least possible intercoupling between the various stress fields and the various displacement quantities.

3.4 TRIANGULAR THIN PLATE ELEMENT

In the uncracked element, linear interpolation functions are used for the stresses and the displacements of the boundaries. In order to satisfy the condition 3.22 with the numbers of stress parameters and displacement quantities, it is not presupposed that σ_{xy} is equal to σ_{yx}. This is allowed because the weighting function for this moment equilibrium condition ($\sigma_{xy} - \sigma_{yx} = 0$) is already incorporated in the derivation given in Section 3.2 .

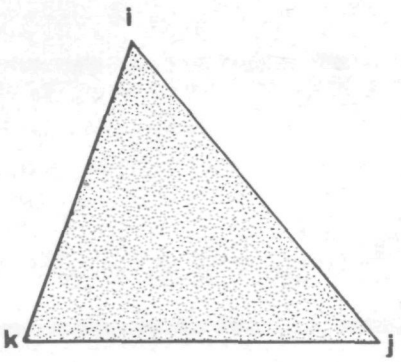

FIGURE 3.1 : Triangular thin plate element

The stresses at any particular point of the element are expressed in the 12 stress parameters $\beta_1(1)$ to $\beta_1(12)$.

$$\begin{bmatrix} \sigma_{xx} \\ \sigma_{yy} \\ \sigma_{xy} \\ \sigma_{yx} \end{bmatrix} = \begin{bmatrix} A_i & o & o & o & A_j & o & o & o & A_k & o & o & o \\ o & A_i & o & o & o & A_j & o & o & o & A_k & o & o \\ o & o & A_i & o & o & o & A_j & o & o & o & A_k & o \\ o & o & o & A_i & o & o & o & A_j & o & o & o & A_k \end{bmatrix} \begin{bmatrix} \beta_1(1) \\ \\ \\ \beta_1(12) \end{bmatrix} \qquad (3.32)$$

$$\sigma = P_1 \beta_1$$

The functions $A_l(x,y)$ are first-degree polynomials in x and y.

$$A_l(x,y) = a_l x + b_l y + c_l$$

The coefficients a_l, b_l and c_l have been so determined that A_l has the value unity at the corner l and is zero at the other corners.
As a result of formulating the interpolation functions P_1 with these polynomials A_l the parameters β become equal to the stresses at the corners of the element.

$$\left[\beta_1\right]^T = \left[\sigma_{xx}^{\,i}, \sigma_{yy}^{\,i}, \sigma_{xy}^{\,i}, \sigma_{yx}^{\,i}, \sigma_{xx}^{\,j}, \sigma_{yy}^{\,j}, \sigma_{xy}^{\,j}, \sigma_{yx}^{\,j}, \sigma_{xx}^{\,k}, \sigma_{yy}^{\,k}, \sigma_{xy}^{\,k}, \sigma_{yx}^{\,k}\right]$$

The displacements of the element boundaries are written for each boundary as linear functions of the four displacement quantities at the boundary concerned.

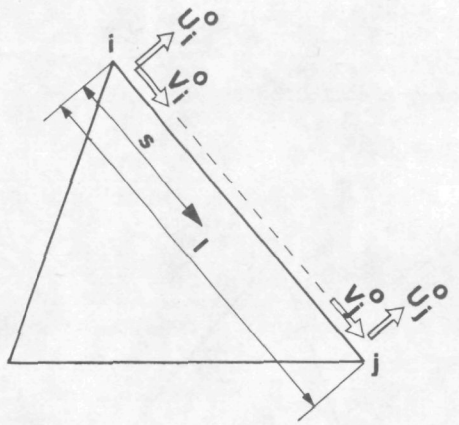

FIGURE 3.2 : Displacement unknowns at the plate element boundary

$$\begin{bmatrix} u^o(s) \\ v^o(s) \end{bmatrix} = \begin{bmatrix} B_i & o & B_j & o \\ o & B_i & o & B_j \end{bmatrix} \begin{bmatrix} u_i^o \\ v_i^o \\ u_j^o \\ v_j^o \end{bmatrix} \qquad u^o(s) = L_A V_A^o \qquad (3.33)$$

where the functions B_i and B_j are:

$$B_i = \frac{l - s}{l}$$

$$B_j = \frac{s}{l}$$

The functions for the description of the displacements in the element are used only for the weighting of the equilibrium conditions. These functions have been taken as follows:

$$\begin{bmatrix} u(x,y) \\ v(x,y) \end{bmatrix} = \begin{bmatrix} 1 & 0 & -y \\ 0 & 1 & x \end{bmatrix} \begin{bmatrix} u \\ v \\ \omega \end{bmatrix} \qquad u(x,y) = QV \qquad (3.34)$$

Only the three possibilities of deformation as a rigid body have been included in these displacement functions. For the equilibrium conditions this has the consequence that these conditions are satisfied, on an average, over the element. Since a linear distribution is adopted for the stresses, the equilibrium conditions are nevertheless exactly satisfied for a volume loading that is constant over the element. These equilibrium conditions are:

$$\sigma_{xx,x} + \sigma_{xy,y} = q_x$$

$$\sigma_{yx,x} + \sigma_{yy,y} = q_y$$

For the shear stresses the following remains valid:

$$\iiint_{V_e} (\sigma_{xy} - \sigma_{yx}) dV = 0$$

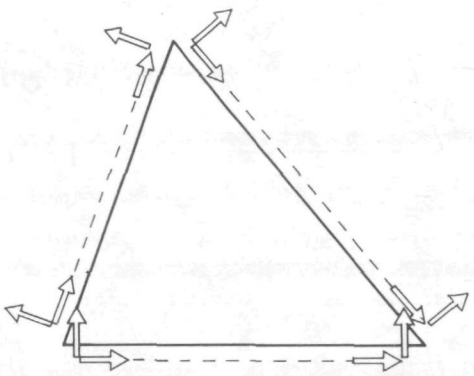

FIGURE 3.3 : Degrees of freedom of an uncracked plate element

If a crack forms in the element, extra stress fields are added to the fields $P_1\beta_1$ already present in the element. Apart from the addition P_1A_2 (see section 3.3) needed for making the matrix F_{12} zero, these extra fields $P_2^*\beta_2$ have been so chosen that they produce a constant boundary stress along the various boundary portions; this boundary stress is not equal on either side of a crack (see Fig. 3.4).

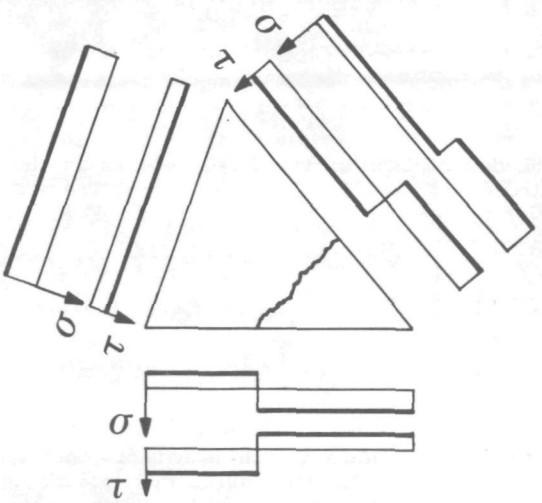

FIGURE 3.4a : Distribution of stresses along the boundaries of a plate element with one crack

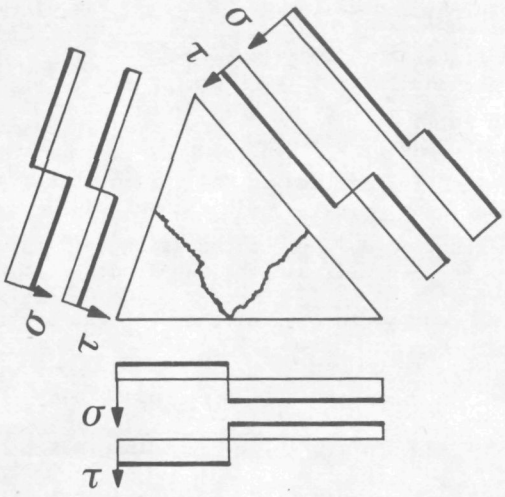

FIGURE 3.4b : Distribution of stresses along the boundaries of a plate element with two cracks

If there is one crack in the element the extra stress fields are:

$$\begin{bmatrix} \sigma_{xx} \\ \sigma_{yy} \\ \sigma_{xy} \\ \sigma_{yx} \end{bmatrix} = \begin{bmatrix} C & 0 & 0 & 0 & \cos^2\alpha(D-A_I) & \cos^2\beta(D-A_{III}) \\ 0 & C & 0 & 0 & \sin^2\alpha(D-A_I) & \sin^2\beta(D-A_{III}) \\ 0 & 0 & C & 0 & \sin\alpha\cos\alpha(D-A_I) & \sin\beta\cos\beta(D-A_{III}) \\ 0 & 0 & 0 & C & \sin\alpha\cos\alpha(D-A_I) & \sin\beta\cos\beta(D-A_{III}) \end{bmatrix} \begin{bmatrix} \beta_2(1) \\ \\ \\ \beta_2(6) \end{bmatrix}$$

$$\sigma_{extra} = P_2^* \beta_2 \qquad (3.35)$$

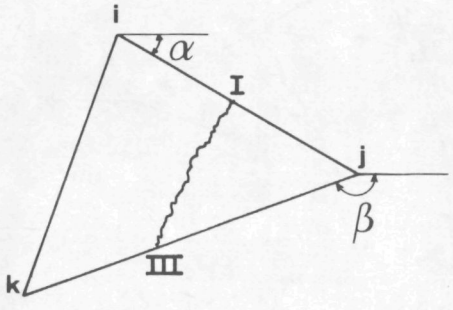

FIGURE 3.5 : Plate element with one crack

The functions C, D, A_I and A_{III} used in equation 3.35 are defined thus:

- C = 1 in the quadrilateral i, I, III k
  outside this quadrilateral : C = 0.
- D = 1 in the triangle I, j, III
  outside this triangle: D = 0
- A_I is a linear function defined in the triangle I, j, III and has the magnitude 1. at point I and the magnitude 0 at points j and III.
- A_{III} is a linear function defined in the triangle I, j, III and has the magnitude 1. at point III and the magnitude 0. at points I and j.

If the element is intersected by two cracks, then the extra stress fields are:

$$\begin{bmatrix} \sigma_{xx} \\ \sigma_{yy} \\ \sigma_{xy} \\ \sigma_{yx} \end{bmatrix} = \begin{bmatrix} C & 0 & 0 & 0 & \cos^2\alpha(D-A_I) & \cos^2\beta(D-A_{III}) \\ 0 & C & 0 & 0 & \sin^2\alpha(D-A_I) & \sin^2\beta(D-A_{III}) \\ 0 & 0 & C & 0 & \sin\alpha\cos\alpha(D-A_I) & \sin\beta\cos\beta(D-A_{III}) \\ 0 & 0 & 0 & C & \sin\alpha\cos\alpha(D-A_I) & \sin\beta\cos\beta(D-A_{III}) \end{bmatrix}$$

$$\begin{bmatrix} \cos^2\alpha(E-A_I^*) & \cos^2\gamma(E-A_{II}) \\ \sin^2\alpha(E-A_I^*) & \sin^2\gamma(E-A_{II}) \\ \sin\alpha\cos\alpha(E-A_I^*) & \sin\gamma\cos\gamma(E-A_{II}) \\ \sin\alpha\cos\alpha(E-A_I^*) & \sin\gamma\cos\gamma(E-A_{II}) \end{bmatrix} \begin{bmatrix} \beta_2(1) \\ \\ \\ \beta_2(8) \end{bmatrix}$$

$$\sigma_{extra} = P_2^* \beta_2 \qquad (3.36)$$

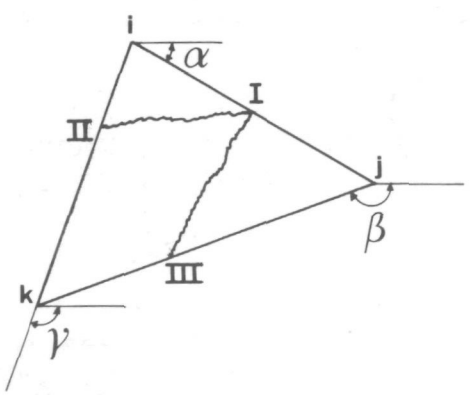

FIGURE 3.6 : Plate element with two cracks

The functions C, D, E, A_I, A_I^*, A_{II} and A_{III} used in equation 3.36 are defined as follows:

- C = 1 in the quadrilateral II, I, III, k; outside it: C = 0.
- E = 1 in the triangle i, I, II; outside it: E = 0.
- the definations of D, A_I and A_{III} are the same as in equation 3.35.
- A_I^* is a linear function defined in the triangle i, I, II which has the magnitude 1. at point I and the magnitude 0. at points i and II.
- A_{II} is a linear function defined in the triangle i, I, II which has the magnitude 1. at point II and the magnitude 0. at points i and I.

In Section 3.3 it has already been noted that the matrix F_{12} can be made zero by the addition of the functions $P_1 A$ to the functions P_2^*.
This is the case if the following is adopted for the matrix A:

$$A = - F_{11}^{-1} \iint_{V_e} P_1^T F P_2^* dV$$

The stress field $(P_1 A + P_2^*)\,\beta_2$ is then orthogonal with respect to the strain in consequence of the stresses $P_1\,\beta_1$.
In order to continue to satisfy exactly the equilibrium at the element boundaries, the displacement functions for the boundaries intersected by a crack should be extended with an extra displacement. Just as at uncracked boundaries, this displacement should agree with the stress distribution at these boundaries. The interpolation function for these extra boundary displacements is:

$$\begin{bmatrix} \Delta u^o(s) \\ \Delta v^o(s) \end{bmatrix} = \begin{bmatrix} \langle s - a \rangle^o + c_1 + c_2 s & 0 \\ 0 & \langle s - a \rangle^o + c_1 + c_2 s \end{bmatrix} \begin{bmatrix} \Delta u^o \\ \Delta v^o \end{bmatrix} \quad (3.37)$$

where:

$$c_1 = -1 + 4\frac{a}{l} - 3\frac{a^2}{l^2}$$

$$c_2 = -6\frac{a}{l^2} + 6\frac{a^2}{l^3}$$

$$\langle s - a \rangle^o \equiv 0 \qquad s<a$$

$$\langle s - a \rangle^o \equiv 1 \qquad s>a$$

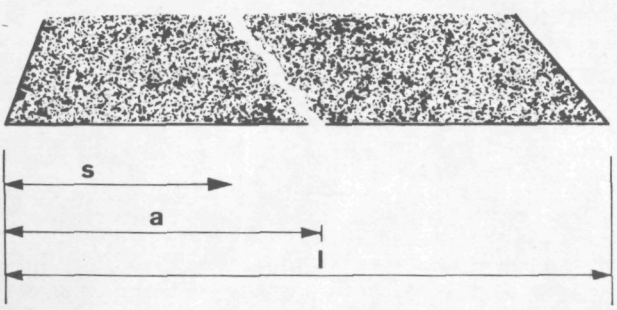

FIGURE 3.7 : Element boundary intersected by a crack

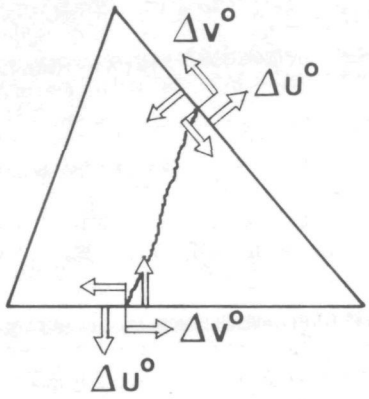

FIGURE 3.8 : Extra degrees of freedom at cracked element boundaries

The extra displacements in equation 3.37 are orthogonal with respect to the boundary stresses due to the function $P_1\ \beta_1$, so that the matrix D_{1B} becomes zero.

3.5 BAR ELEMENT

A bar element is used for the schematization of the embedded steel, i.e., the reinforcing bars and/or prestressing tendons. This element has a stiffness with respect to change in length (extensional stiffness) and with respect to deformation by shear force. Also, the properties of the contact zone between steel and concrete are included in the relationships for this element, so that no additional boundary layer elements are required. For this boundary layer a stiffness with respect to shear deformation and a stiffness with respect to indentation are taken into account. These last-mentioned stiffness characteristics of the boundary layer have been included in the model in order to enable it to deal with dowel forces and the consequences of non-linear bar geometry. The distribution of the forces in the bar element is adjusted for the distribution of the stresses along the boundaries of the triangular plate element with which these bar elements are to be associated. A linear stress distribution has been adopted in the uncracked plate element; to this corresponds a quadratic distribution for the normal force (F) and shear force (S) in the bar element. The functions $P_1\ \beta_1$ in an uncracked bar element are:

$$\begin{bmatrix} F \\ S \end{bmatrix} = \begin{bmatrix} 1 & s & s^2 & 0 & 0 \\ 0 & 0 & 0 & l^2 - 3s^2 & 2sl - 3s^2 \end{bmatrix} \begin{bmatrix} \beta_1(1) \\ \beta_1(5) \end{bmatrix} \qquad (3.38)$$

The distribution of the shaer force in an element has been so chosen that the average shear force is always zero. This ensures that the bending moments in the bar remain small and that they are zero at the ends of the bar. Accordingly, no rotational degree of freedom is needed at the ends. The constitutive equations for the combined steel/boundary layer element are

$$\begin{bmatrix} \varepsilon \\ \Delta_{//} \\ \gamma \\ \Delta_{\perp} \end{bmatrix} = \begin{bmatrix} \frac{1}{AE} & 0 & 0 & 0 \\ 0 & \frac{1}{K} & 0 & 0 \\ 0 & 0 & \frac{1}{GD} & 0 \\ 0 & 0 & 0 & \frac{1}{B} \end{bmatrix} \begin{bmatrix} F \\ \frac{dF}{ds} \\ S \\ \frac{dS}{ds} \end{bmatrix} \qquad (3.39)$$

where: ε = strain of the steel
$\Delta_{//}$ = displacement in boundary layer
γ = deformation due to shear force
$\Delta_{\perp}$ = indentation of boundary layer
A = cross-sectional area of steel
E = modulus of elasticity of steel
K = elastic stiffness of boundary layer with respect to displacement
D = dowel rigidity
G = shear modulus of steel
B = elastic stiffness of boundary layer with respect to indentation

The displacements at the element boundaries are descripted with the aid of the displacement quantities u_i^o, v_i^o, u_j^o, v_j^o on the outside of the boundary layer and the displacements $\bar{u}_i^o$, $\bar{v}_i^o$, $\bar{u}_j^o$ and $\bar{u}_j^o$ of the extreme points of the steel bar.

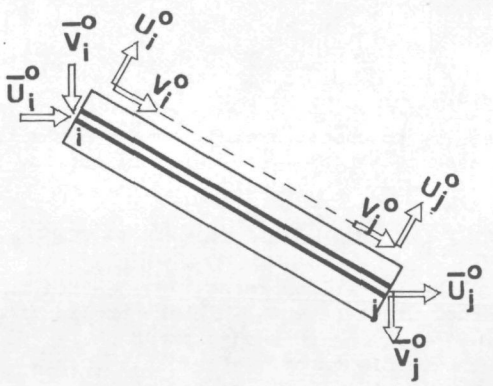

FIGURE 3.9 : Degrees of freedom of an uncracked bar element

If the bar element is intersected by a crack, then - as in the plate element - the stress functions and displacement functions are extended by the addition of extra fields.
The extra stress field $P_2^* \beta_2$ is:

$$\begin{bmatrix} F \\ S \end{bmatrix} = \begin{bmatrix} \langle s-a \rangle & 0 \\ 0 & 2\langle s-a \rangle - (1 - \frac{a}{l})^2 l \end{bmatrix} \begin{bmatrix} \beta_2^{(1)} \\ \beta_2^{(2)} \end{bmatrix} \qquad (3.40)$$

$$\langle s - a \rangle \equiv 0 \qquad s<a$$

$$\langle s - a \rangle \equiv (s - a) \qquad s>a$$

For this function, too, the average shear force per element is zero. In order to ensure that the matrix F_{12} becomes zero, the field $P_1 A\beta_2$ is added to this field $P_2^* \beta_2$, in the same way as is done in the case of the plate element. The matrix A is:

$$A = -F_{11}^{-1} \iint_{V_e} P_1 F P_2^* dV$$

The extra displacement field along the boundary layer corresponds entirely to the extra displacement fields along the boundaries of a cracked triangular element.

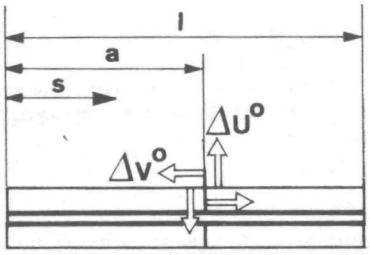

FIGURE 3.10 : Extra degrees of freedom at a cracked boundary layer

$$\begin{bmatrix} \Delta u^o(s) \\ \Delta v^o(s) \end{bmatrix} = \begin{bmatrix} \langle s-a \rangle^o + C_1 + C_2 s & 0 \\ 0 & \langle s-a \rangle^o + C_1 + C_2 s \end{bmatrix} \cdot \begin{bmatrix} \Delta u^o \\ \Delta v^o \end{bmatrix} \qquad (3.37)$$

(see Section 3.4)

Here it is not necessary to choose a displacement distribution in the element, since the assumed stress fields exactly satisfy the equilibrium conditions.

3.6 TAKING ACCOUNT OF CRACKS IN THE STIFFNESS MATRIX

In order to speed up the iteration process, whenever a number of new cracks have formed, the normal displacements in these are incorporated into the stiffness matrices. In applying this adjustment it is necessary to bear in mind that it must be possible to correct negative crack widths and that uniqueness of the crack widths is desirable.

In this procedure the normal displacements in a crack are split up into two parts:

$$V_{cr} = V_{cr}^1 + V_{cr}^2 \qquad (3.41)$$

The part V_{cr}^2 is, according to the normal procedure, accommodated in the initial strain vector Z_1 and the contribution of the part V_{cr}^1 is written explicitly in the formulas 3.27a for the stress parameters β_1:

$$\beta_1 = H_{11} D_{1A} V_A^o - H_{11} C_1 V_{cr}^1 - H_{11} Z_1 + Y_1 R \qquad (3.42)$$

where C_1 is the boundary integral over the crack of the interpolation functions P_1.
The stress resultants in the directions of the crack displacements V^1_{cr} are

$$C_1^T\beta_1 = C_1^T H_{11} D_{1A} V_A^o - C_1^T H_{11} C_1 V^1_{cr} - C_1^T H_{11} Z_1 + C_1^T Y_1 R \qquad (3.43)$$

It is assumed that when the crack width is non zero the normal stresses in a crack and consequently these stress resultants vanish.

Equations 3.43 are split up into

$$C_1^T H_{11} D_{1A} V_A^o - C_1^T H_{11} C_1 V^1_{cr} = 0 \qquad (3.44a)$$

$$- C_1^T H_{11} Z_1 + C_1^T Y_1 R = 0 \qquad (3.44b)$$

This means that the crack displacement V^1_{cr} only depend on the element boundary displacements V^o_A. The part V^2_{cr} only depends on the other initial strains in the element and the volume load.

From equation 3.44a it follows that

$$V^1_{cr} = (C_1^T H_{11} C_1)^{-1} C_1^T H_{11} D_{1A} V_A^o \qquad (3.45)$$

Substitution of 3.45 into 3.42 gives

$$\beta_1 = \left[H_{11} - H_{11} C_1 (C_1^T H_{11} C_1)^{-1} C_1^T H_{11} \right] D_{1A} V_A^o - H_{11} Z_1 + Y_1 R \qquad (3.46)$$

For the equations 3.29a which indicate the relationship between the generalized nodal forces K_A and the nodal displacements V^o_A is now substituted the equation

$$D_{1A}^T \left[H_{11} - H_{11} C_1 (C_1^T H_{11} C_1)^{-1} C_1^T H_{11} \right] D_{1A} V_A^o = K_A + D_{1A}^T (H_{11} Z_1 - Y_1 R) + D_{2A}^T \beta_2 \qquad (3.47)$$

Analysis of the part V^2_{cr} is performed with the visco-plastic model described in Section 2.3. After each iteration the total displacements V_{cr} are calculated with equation 3.41. These total crack displacements are incorporated as a whole in the initial strains for the determination of Z_2 (see equation 3.29b). This ensures that the same crack displacements are taken into account in both systems. If the crack widths V^1_{cr} become negative, this will be compensated by the part V^2_{cr} without necessitating re-adaption of the matrices.

MATERIAL MODELS

4.1 INTRODUCTION

The behaviour of a material is always described with the aid of a number of models, each of which describes a particular aspect of the behaviour. These models are here called the basic or material models, in order to distinguish them from the overall models for the analysis of a structure, such as the MICRO model, in which the basic models are used. The latest knowledge concerning the behaviour of the materials is embodied in the basic models. More particularly with regard to concrete, however, the available knowledge of its behaviour under various conditions is still very incomplete, and research on the subject is still in full swing. The MICRO model has therefore been so conceived that the basic models can quite simply be replaced by others or be increased in number.

The MICRO model comprises basic models for the following material properties:

for concrete:
- a non-linear stress-strain relationship;
- a cracking criterion;
- a crushing criterion;
- a shrinkage model;
- a creep model;
- a model for aggregate interlock in a crack.

for steel:
- a non-linear stress-strain relationship.

for the boundary layer between steel and concrete:
- a non-linear shear stress-displacement relationship;
- a linear normal stress-displacement relationship

For some material properties alternative models have been included, from among which the user can make a choice according to his own judgment. No experimental research into the behaviour of the materials has been undertaken within the context of this study. With the exception of the model for aggregate interlock in a crack have the basic models for the description of the concrete properties been taken from the literature. Where several models are reported in the literature, a choice has been made on the basis of agreement with experiments and of the serviceability of such models in the MICRO model. Pending the results of research after the force-displacement relations in a crack and after the co-operation between steel and concrete which are performed within the framework of the project "Concrete Analysis" (see Section 1.1), simple linear elastic and elasto-plastic models for these properties have been adopted. No models have been included for describing the relaxation of prestressing steel and the time-dependent deformations at a crack and in the boundary layer. The reason for not (yet) taking account of the two last-mentioned creep deformations is the existing lack of knowledge concerning these

deformations. In comparison with the creep of concrete, the relaxation of steel is such a rapid process that it is assumed to have been completely accomplished before the concrete starts its creep.

4.2 NON-LINEAR STRESS-STRAIN RELATIONSHIP OF CONCRETE

4.2.1 *LINK'S MODEL*

This model is based on results of experimental research by Kupfer et al. [4.1] concerning the behaviour of concrete under two-dimensional states of stress. Basing himself on these results, Link [4.2] developed formulas for the calculation of the strains (ε) associated with any (arbitary) two-dimensional state of stress. These formulas define the total strains depending on the actual stresses, the uniaxial compressive strength of concrete, the initial modulas of stiffness and the initial value of Poisson's ratio. Presupposing coincidence of the orientation of the principal directions of the stress tensor and the strain tensor, and assuming symmetry of the stress-strain relationship, Link formulates the constitutive relationship as follows:

$$\begin{bmatrix} \varepsilon_{11} \\ \\ \varepsilon_{22} \end{bmatrix} = \begin{bmatrix} \frac{1}{E_1^s} & -\frac{\nu_1^s}{E_1^s} \\ \\ -\frac{\nu_2^s}{E_2^s} & \frac{1}{E_2^s} \end{bmatrix} \begin{bmatrix} \sigma_{11} \\ \\ \sigma_{22} \end{bmatrix} \qquad (4.1)$$

On account of the above-mentioned symmetry, the following expression holds:

$$\frac{\nu_1^s}{E_1^s} = \frac{\nu_2^s}{E_2^s} \qquad (4.2)$$

The symbols in the formulas 4.1 have the following meanings;

E_i^s = secant modulus of stiffness in the principal direction i

ν_i^s = secant value of Poisson's ratio in the principal direction i

σ_{ii} principal stress in the direction i

ε_{ii} principal strain in the direction i

For the very elaborate formulas for E_i^s and ν_i^s the relevant literature should be referred to [4.2] .
The model is in good agreement with the experimental results of various investigators. Besides this advantage, it has some disadvantages, however, namely:

- the model is purely elastic and therefore takes no account of the permanent deformations that remain on unloading, nor of the dependence of the strains upon the stress path followed;
- the assumptions made in deriving the formulas have yet to be investigated as to their validity;
- the elaboration and precision of the formulas suggests an accuracy which is decidedly unrealistic with reference to a material such as concrete.

hold-request-slip

Bibliotheek TU Delft
Prometheusplein 1
2600 MG Delft
Verlenging: 015-2784510
Informatie: 015-2785678

* L O O P B O N V O O R B O E K A A N V R A G E N *

Aangevraagd op: 07 Juli 1998 Tijd: 1513

Uiterlijk terugbezorgen op (stempel datum):

Documentgegevens (auteur/titel)
Grootenboer, H.J..: FINITE ELEMENT ANALYSIS OF
TWO-DIMENSIONAL REINFORCED CONCRETE STRUCTURES, TALKING

Plaatsnummer(s)		Exemplaarnummer(s)
- 11504273	CBmg (cB)	273232
-		
-		
-		
-		
-		

Opmerkingen:

==========

Gebruikers-ID: 72670 Categorie: 02

Rijss, E.
Raam 20
2611 LS Delft

Bezorglokatie: CBmg (cB)

4.2.2 *BUYUKOZTURK'S MODEL*

Link's model (see Section 4.2.1) may prove inadequate for analysing the behaviour of structures which, after being loaded, are unloaded or on which the various loads are not simultaneously increased monotonically. A constitutive model for concrete which does take account of permanent deformations and also of the dependence of the strains upon the "stress history" is that of Buyukozturk [1.17]. This model is based on the conception of elasto-plastic material behaviour supplemented with istotropic strain hardening in consequence of plastic deformations. For the yielding surface (F) Buyukozturk uses what he calls a "generalized Mohr-Coulomb" formula:

$$F = 3(3J_2 + \bar{\sigma} J_1 + J_1^2/5)^{\frac{1}{2}} - \bar{\sigma} = 0 \qquad (4.3)$$

For two-dimensional states of stress the symbols in this formula denote:

$$J_1 = \sigma_{xx} + \sigma_{yy}$$

$$J_2 = (\sigma_{xx}^2 + \sigma_{yy}^2 - \sigma_{xx}\sigma_{yy})/3 + \sigma_{xy}\sigma_{xy}$$

$\bar{\sigma}$ = equivalent stress

The strain hardening rule adopted here is that the equivalent stress ($\bar{\sigma}$) is dependent on the equivalent plastic strain ($\bar{\varepsilon}^p$):

$$\bar{\sigma} = H(\bar{\varepsilon}^p) \qquad (4.4)$$

For the increase of the plastic strains (ε^p) the following formula is used:

$$d\varepsilon^p = d\bar{\varepsilon}^p \{\frac{\partial F}{\partial \sigma}\}$$

$$d\bar{\varepsilon}^p \equiv 0 \text{ als } F \leq 0 \qquad (4.5)$$

$$d\bar{\varepsilon}^p > 0 \text{ als } F > 0$$

This formula is based on the Prandtl-Reuss assumption with isotropic hardening. This means that the plastic strain increases ($d\varepsilon^p$) are perpendicular to the surface(F). In his model Buyukozturk takes account of the plastic deformations only if one or both of the principal stresses are negative (compression) and uses a relationship between the equivalent stress ($\bar{\sigma}$) and the equivalent strain ($\bar{\varepsilon}^p$) which depends on the two principal stresses and the "stress history" (see Fig. 4.1).

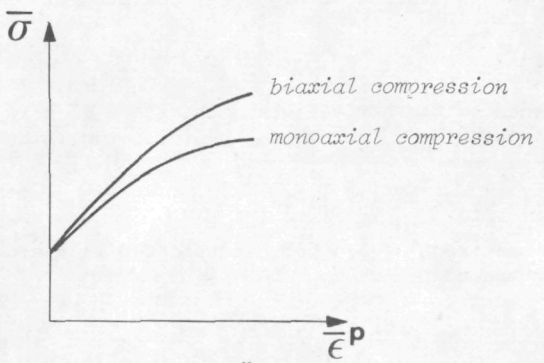

FIGURE 4.1 : Relationship between $\bar{\sigma}$ and $\bar{\varepsilon}^p$ for different stress conditions

In his description of the model Buyukozturk gives no formula for the strain hardening function H. Therefore in the MICRO program a parabalic relation between the equivalent stress ($\bar{\sigma}$) and the equivalent plastic strain ($\bar{\varepsilon}^p$) has been assumed. Also has the calculation of the equivalent plastic strain been modified so that the dependence of the strain hardening on the state of stress has been taken account of and the model can be used for all states of stress. With these modifications, Buyukozturk's plastic model has been implemented as a visco-plastic model. The formula for the rate of visco-plastic deformations is:

$$\dot{\varepsilon}^{vp} = \gamma < \frac{F}{F_o} > \frac{\partial F}{\partial \sigma} \tag{4.6}$$

where: $\dot{\varepsilon}^{vp}$ = visco-plastic strain rate

γ = viscous constant

F_o = reference value of F to make the expression dimensionless

If the state of stress is within the yielding surface, the material will behave elastically. Therefore the following must hold:

$$< \frac{F}{F_o} > \equiv 0 \qquad \text{if } F < 0$$

$$< \frac{F}{F_o} > = (\frac{F}{F_o}) \qquad \text{if } F \geq 0 \tag{4.7}$$

It has already been pointed out that the strain hardening function H depends on the state of stress and on the stress history. In order to take account of these two aspects in the strain hardening model, the equivalent strain is calculated, not from the total visco-plastic strains, but from a summation of all the increases in (n) stages of analysis:

$$\bar{\varepsilon}^p = \sum_{i=1}^{n} \alpha_i (d\bar{\varepsilon}^p)_i \tag{4.8}$$

The increase of the equivalent strain ($d\bar{\varepsilon}^p$) per stage is here defined as:

$$d\bar{\varepsilon}^p = \sqrt{\frac{2}{3} d\varepsilon_{ij}^{vp} d\varepsilon_{ij}^{vp}} \tag{4.9}$$

The interdependence of the hardening and the state of stress is incorporated in the multiplying factor α, for which the following formula is employed:

$$\alpha = \bar{\sigma} / \sqrt{\sigma_{11}^2 + \sigma_{22}^2 - 1{,}5\, \sigma_{11}\, \sigma_{22}} \tag{4.10}$$

In Fig. 4.2 the magnitude of $1/\alpha$ has been plotted in the two-dimensional principal stress space.

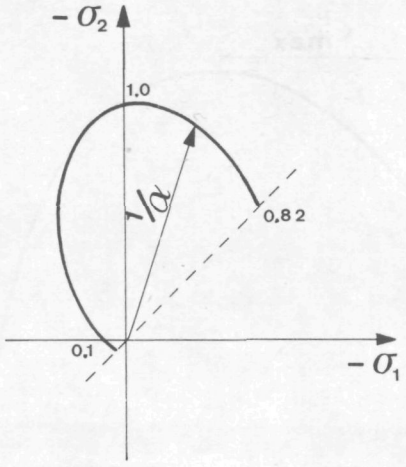

FIGURE 4.2 : Function $1/\alpha$

The smaller the value of $1/\alpha$, the greater is the kinematic hardening and the smaller will the plastic deformations remain. The function α has been so chosen that in the case of biaxial compressive loading the plastic deformations are about 20% less than in the case of monoaxial compressive loading. For any particular value of the equivalent stress $\bar{\sigma}$ the plastic deformations in the case of tensile loading are between 5 and 10% of the plastic deformations in the case of compressive loading.

The relationship between $\bar{\sigma}$ and $\bar{\varepsilon}^P$ (see equation 4.4) is described in the MICRO model by a second-order polynomial:

$$\bar{\sigma} = a_o + a_1 \bar{\varepsilon}^P + a_2 (\bar{\varepsilon}^P)^2 \qquad (4.11)$$

It is assumed that when a state of stress attains the crushing criterion (see Section 4.4.2) the concrete can nevertheless still transmit some stress. On attainment of the crushing criterion there occurs a transition from an isotropic hardening model to an isotropic softening model. For this the same procedure and formulas are used as for the hardening model, except for formula 4.11, which now becomes:

$$\bar{\sigma} = \langle H^*(\bar{\varepsilon}^P) \rangle = \langle a_o + a_1 (2\bar{\varepsilon}^P_{max} - \bar{\varepsilon}^P) + a_2 (2\, \bar{\varepsilon}^P_{max} - \bar{\varepsilon}^P)^2 \rangle \qquad (4.12)$$

The value $\bar{\varepsilon}^P_{max}$ corresponds to the crushing criterion. For the equivalent stress $\bar{\sigma}$ in formula 4.12 the following holds:

$\bar{\sigma} \equiv H^*(\bar{\varepsilon}^P)$ if $H^*(\bar{\varepsilon}^P) > 0$

$\bar{\sigma} \equiv 0$ if $H^*(\bar{\varepsilon}^P) < 0$

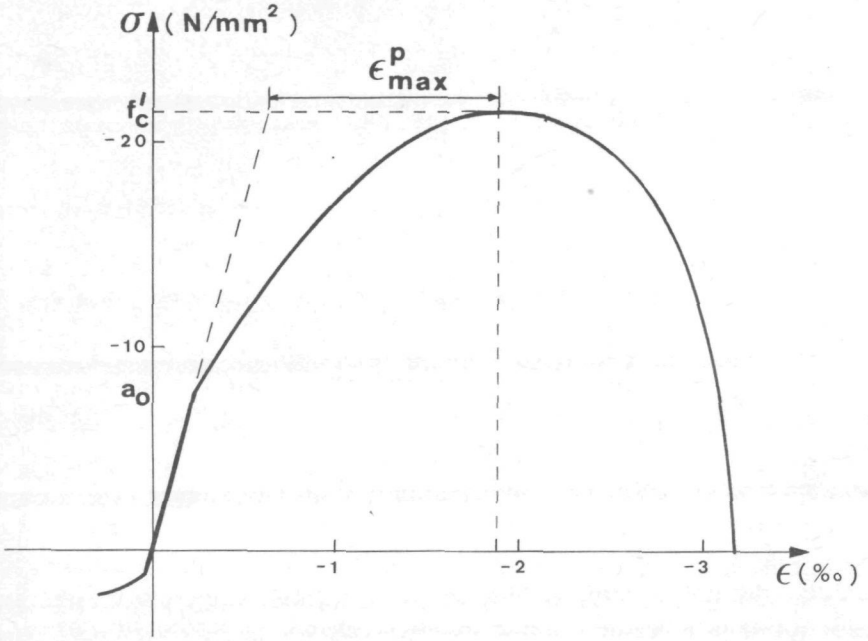

FIGURE 4.3 : Stress- strain diagram for uniaxial state of stress analysed with the modified Buyukozturk's model

It must be pointed out that the validity of the various assumptions adopted in the analysis has not yet been sufficiently verified by experimental results. From the limited amount of comparative information available it does, however, already emerge that the supposed orthogonality of the increase of the plastic strains and the yielding surface is not correct.

4.3 CRACKING CRITERION FOR CONCRETE

In considering the behaviour of concrete subjected to two-dimensional states of stress a distinction is drawn between the crushing and the cracking of the concrete. By cracking is here understood the formation of cracks in the concrete perpendicularly to the plane of the two-dimensional state of stress. These cracks develop if one of the principal stresses is positive (tensile stress) or if both of them are positive. Many authors [1.17, 4.3, 4.4] make use of a stress envelope as shown in Fig. 4.4 for describing the states of stress for which these cracks arise.

The values SB, SA and tan(α) are needed for describing this criterion. The points A mark the transition from the cracking criterion to the region where crushing of the concrete occurs. Experimental results indicate for tan(α) value ranging from 1/10 (Nelissen [4.4]) to 1/15 (Kupfer [4.1.]).
For the calculations performed for this thesis the following have been adopted:

$S_A = f_c$ = uniaxial tensile strength of concrete

$S_B = f'_c$ = uniaxial compressive strength of concrete

$\tan(\alpha) = \frac{1}{15}$

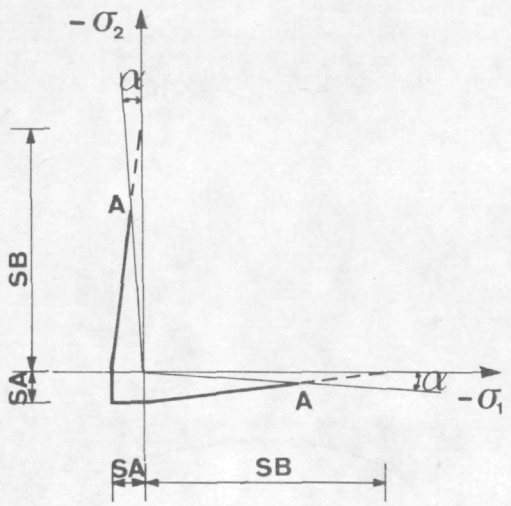

FIGURE 4.4 : Criterion for cracking

It is assumed that if the stresses attain a value located on this cracking stress envelope, a crack is formed perpendicularly to the larger principal stress (= tensile stress) and the stresses at right angles to this crack have to become zero.

4.4 CRUSHING OF CONCRETE

By crushing of concrete is here understood the formation of cracks both in and perpendicularly to the plane of the two-dimensional state of stress. This type of cracking occurs if one or both of the principal stresses are approximately equal to the monoaxial compressive strength of concrete. As a result of such cracking the ability of the concrete to transmit large compressive stresses reduce. In the original constitutive models of concrete by Link and Buyukozturk no account have been taken of this post crushing strength. The model of Buyukozturk has therefore been modified to this. A modification of the constitutive model by Link has been omitted. Just as was done for describing the constitutive behaviour of concrete, so here too the models of Link [4.2] and Buyukozturk [1.17] will be used for describing the criterion for crushing. In both models the shape of the crushing envelope is independent of the concrete quality.

4.4.1 *LINK'S MODEL*

The model for the failure criterion of concrete according to Link [4.2] is, like his constitutive model, based on the tests of Kupfer et al. [4.1] . This criterion is valid both for failure in cracking and for failure in crushing. In the MICRO model this model according to Link is used only to describe the crushing of concrete. The transition from cracking criterion to crushing criterion is located at the points A for which the value of $\tan(\alpha)$ is equal to 1/15 (see also Section 4.3). Using the method of "curve fitting", Link has established a number of formulas for the failure envelope for

various kinds of concrete. As a generally-applicable formula for normal weight concrete he recommends:

$$Y = 0.1203 + 0.3682X - 0.1910X^2 + 2.8430X^3 - 5.4875X^4 + 3.7567X^5 +$$
$$- 1.0154X^6 + 0.06664X^7 + 0.4335 * (0.594SIN(1.847996X) -$$
$$+ 0.00192TAN(.951998X))$$

$$X = 0.5\sqrt{2}(\sigma_{11} + \sigma_{22})/f'_c \qquad (4.13)$$
$$Y = -0.5\sqrt{2}(\sigma_{11} - \sigma_{22})/f'_c$$

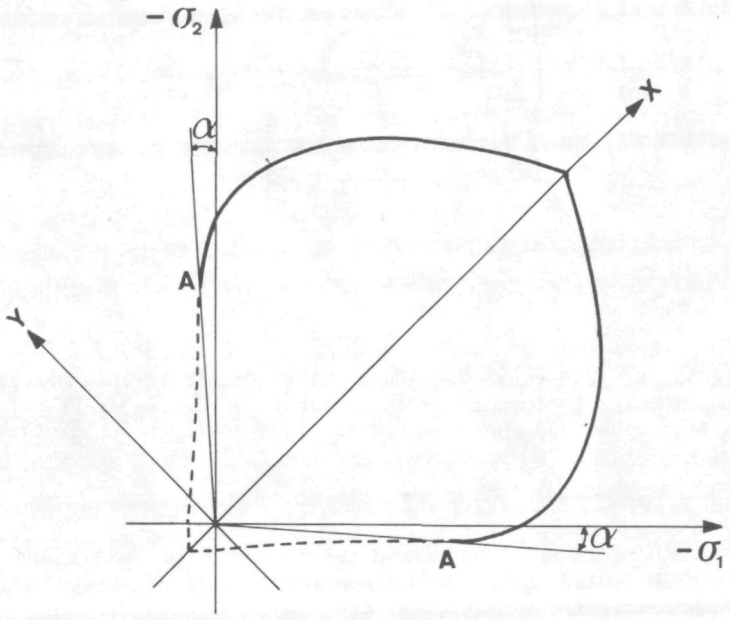

FIGURE 4.5 : Link's failure envelope

The model is in good agreement with the experimental results of Kupfer et al. However, this model likewise has the drawback of taking no account of the stress history and of giving an exaggerated impression of accuracy.

4.4.2 *BUYUKOZTURK'S MODEL*

Buyukozturk's failure criterion ties up with his constitutive model. If the equivalent stress $\bar{\sigma}$ becomes equal to the compressive strength f'_c, the yielding criterion (4.3) turns into the failure criterion:

$$3J_2 + f'_c J_1 + 0.2J_1^2 = (f'_c)^2/9 \qquad (4.14)$$

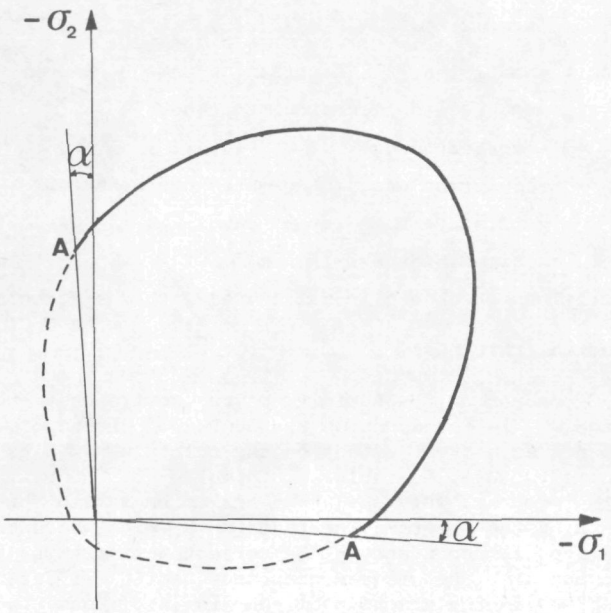

FIGURE 4.6 : Buyukozturk's failure envelope

In the relationship between the equivalent stress and the equivalent strain, as employed here, the attainment of the crushing criterion corresponds to a maximum value for the equivalent strain ($\bar{\varepsilon}^p = \bar{\varepsilon}^p_{max}$). Buyukozturk tests this formula against Kupfer's experimental results. He applies this criterion only in the case where both principal stresses are negative (compression). For the compressive/tensile and the tensile/tensile region he adopts the cracking criterion of Section 4.3. In this approach the transition from crushing with cracks is considered to occur at a value of -15 and -1/15, respectively, for the ratio σ_{11}/σ_{22} (see point A in Fig. 4.4).

4.5 SHRINKAGE OF CONCRETE

The shrinkage deformation of concrete is here considered independently of the state of stress and of the creep deformation. Recent research shows that there is indeed a connection between shrinkage and creep. These investigations have, however, not yet resulted in a model that can be incorporated into an overall model. The model for shrinkage employed here is based on CEB Report 111 (1975) [4.5, 4.6].

The shrinkage deformation is determined with the formula:

$$\varepsilon_{shrinkage}(j) = \sum_{i=1}^{j} \varepsilon_{b\ shrinkage}\{R(i)\} * \left[K_s(F_{dk} t_{c1}\ \{i+1\}) + \right.$$

$$\left. - K_s\ (F_{dk} t_{c1}\{i\}) \right] \qquad (4.15)$$

where:

$\varepsilon_{shrinkage}(j)$ = shrinkage strain after the j^{th} day

$\varepsilon_{bshrinkage}\{R(i)\}$ = basic shrinkage (final shrinkage value)

F_{dk} = corrected fictitious thickness

$t_{c1}(i)$ = corrected age

$K_s(F_{dk}, t_{c1})$ = function describing shrinkage behaviour

$R(i)$ = relative humidity at day i

j and i = time in days

The corrected fictitious thickness is calculated with the formula:

$$F_{dk} = k_w * \text{actual thickness}$$

The factor k_w is dependent on the humidity of the environment (see [4.6]). The basic shrinkage ε_{bs} is dependent on the degree of drying of the concrete, which in turn depends to a great extent on the relative humidity of the environment of the structure. No tables or formulas for the basic shrinkage are included in the program. This shrinkage has to be stated for each period of time by the user of the program. The function K_s with which the shrinkage behaviour is described is dependent on the corrected fictitious thickness F_{dk} and the corrected age t_{c1}. The program comprises tables for determining K_s; these tables are based on the graphs published in [4.6] (see Fig. 4.7)

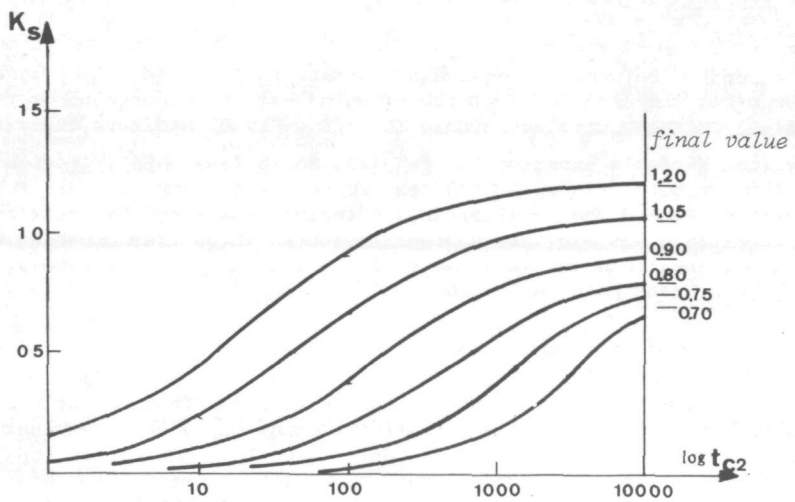

FIGURE 4.7 : Function K_s

The corrected age is determined with the formulas:

$$t_{c1}(j) = \sum_{i=1}^{j} \frac{T(i) + 10^{o}}{30^{o}} \Delta t_i \qquad (4.16)$$

where T(i) is the temperature in degrees centigrade on day i.

For each period of time the following quantities have to be introduced into the program:

- the basic shrinkage — ε_{cb} shrinkage
- the temperature — T
- the end time of the period — j
- the correction factor for the thickness — k_w

4.6 CREEP OF CONCRETE

Like the model for shrinkage (see Section 4.5), the model for creep is based on CEB Report 111 (1975) [4.5, 4.6]. Creep deformation is determined by applying a multiplying factor ϕ to the non-time-dependent non-linear deformation. By basing the calculation of creep deformation on the total non-time-dependent deformation it is ensured that at high compressive stresses (> 0.5 compressive strength) the creep deformation is no longer proportional the stress, but increases progressively.

The creep model comprises two parts;
- the recoverable creep, sometimes referred to as the delayed elastic deformation;
- the irrecoverable creep.

The creep deformation after day j is determined with the formula (4.17)

$$\varepsilon_{creep}(j) = \sum_{i=1}^{j} \varepsilon^{*}(i) \left[\phi_p * (K_p \{F_{dk}, t_{c2}(i+1)\} - K_p \{F_{dk}, t_{c2}(i)\}) + \right.$$

$$\left. + \phi_r * (K_r \{t_{c2}(i+1) - t_{c2}(i)\}) * (1 - K_r \{t_{c2}(j+1) - t_{c2}(i+1)\}) \right]$$

where:

$\varepsilon_{creep}(j)$ = vector with creep strains after day j

$\varepsilon^{*}(i)$ = vector with non-time-dependent non-linear strains at day i

ϕ_p = final value of irrecoverable creep deformation

ϕ_r = final value of recoverable creep deformation

$K_p(F_{dk}, t_{c2})$ = function describing irrecoverable creep behaviour

$K_r(t_{c2})$ = function describing recoverable creep behaviour

F_{dk} = corrected fictitious thickness

$t_{c2}(j)$ = corrected age

The quantities ϕ_p and F_{dk} are dependent on the relative humidity of the environment of the structure. As in the case of shrinkage, no tables or formulas for the values ϕ_p and ϕ_r have been included in the program. The program user has to state these quantities for each period of time. The corrected fictitious thickness is calculated with the formula:

$$F_{dk} = k_w * \text{actual thickness} \qquad (4.18)$$

The factor k_w is dependent on the humidity of the environment. The corrected age t_{c2} is dependent on the temperature and on the type of cement.

The following formula has been adopted for determining t_{c2}:

$$t_{c2}(j) = k_z \sum_{i=1}^{j} \frac{T(i) + 10^o}{30^o} \Delta t_i \qquad (4.19)$$

where T(i) is the temperature in degrees centigrade on day i and k_z is a factor depending on the type of cement employed.
Graphs for the functions K_p and K_r are given in [4.6]. The graphs for K_p are incorporated in the form of a table in the program.

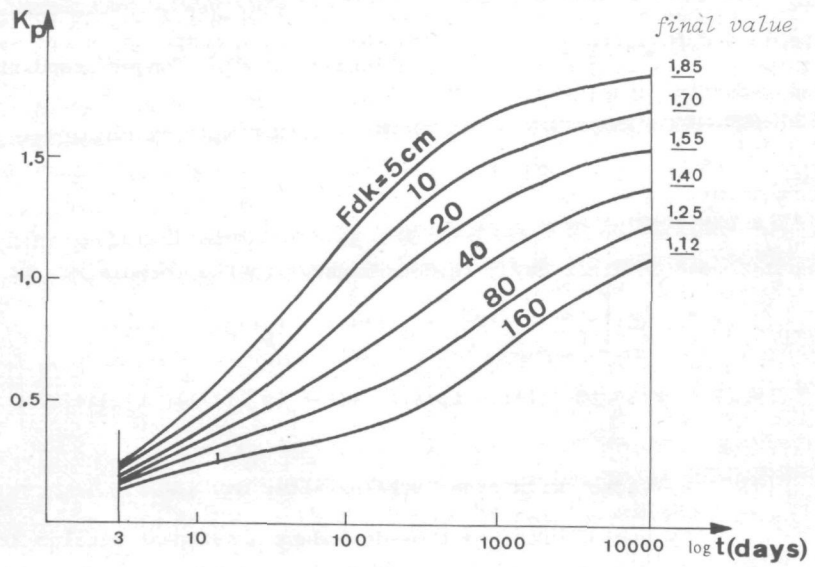

FIGURE 4.8 : Function K_p

The graph representing the behaviour of K_r has been converted into the formula:

$$K_r = (1 - e^{-\alpha (t_{c2} - t_o)}) \qquad (4.20)$$

The numerical value of the factor α can be stated by the user; α= 0.09 is recommended.

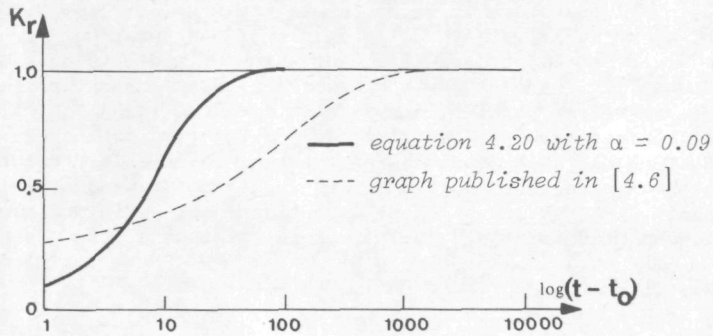

FIGURE 4.9 : Function K_r

By describing the recoverable creep with the aid of a Kelvin element this creep can, per period of time, be completely determined from the stresses and the recoverable creep that has already occurred at the beginning of the period. Hence it is not necessary to remember the whole stress history. The increase in creep deformation thus becomes:

$$\varepsilon_{creep}(j+1) - \varepsilon_{creep}(j) = \Delta\varepsilon_{creep}(j+1) = \overset{*}{\varepsilon}(j+1)\Big[\phi_p * (K_p\{F_{dk}, t_{c2}(j+2)\} - K_p\{F_{dk}, t_{c2}(j+1)\})\Big] + \sum_{i=1}^{j+1} \overset{*}{\varepsilon}(i)\Big[\phi_r * (1-e^{-\alpha t_{c2}(i+1)} * e^{\alpha t_{c2}(i)})(e^{-\alpha t_{c2}(j+2)} * e^{\alpha t_{c2}(i+1)})\Big] - \sum_{i=1}^{j} \overset{*}{\varepsilon}(i)\Big[\phi_r * e^{-\alpha t_{c2}(j+1)} * (e^{\alpha t_{c2}(i+1)} - e^{\alpha t_{c2}(i)})\Big] \tag{4.21}$$

$$\Delta\varepsilon_{creep}(j+1) = \overset{*}{\varepsilon}(j+1)\,\phi_p * \Delta K_p + \overset{*}{\varepsilon}(j+1)\,\phi_r * (1-e^{-\alpha t_{c2}(j+2)} * e^{\alpha t_{cr}(j+1)})\,\varepsilon_r(j) * (e^{-\alpha t_{c2}(j+2)} - e^{-\alpha t_{c2}(j+1)}) \tag{4.22}$$

In this formula for the creep deformation increase the symbol $\varepsilon_r(j)$ denotes the recoverable creep deformation after the j^{th} day. For each period of time the following quantities have to be introduced into the program:

- the final value of the irrecoverable creep ϕ_p
- the final value of the recoverable creep ϕ_r
- the temperature T
- the correction factor for the thickness k_w
- the correction factor for fictitious time k_z

4.7 AGGREGATE INTERLOCK IN A CRACK

A crack that develops in concrete is never completely straight, nor are its two faces smooth. As a result, sliding of the crack faces relatively to each other encounters a resistance, the magnitude of which will depend on the width of the crack because with increasing width fewer and fewer irregularities on the faces are able to resist parallel displacement. At the Technological University of Delft a research project [1.1, 4.7] currently in progress, is concerned with finding out the relationships between, inter alia, the crack width, the parallel displacement and the forces required for producing this displacement. Pending the results of those investigations, a rigid-plastic model will here be adopted for the parallel displacement at a crack (see Fig. 4.11).

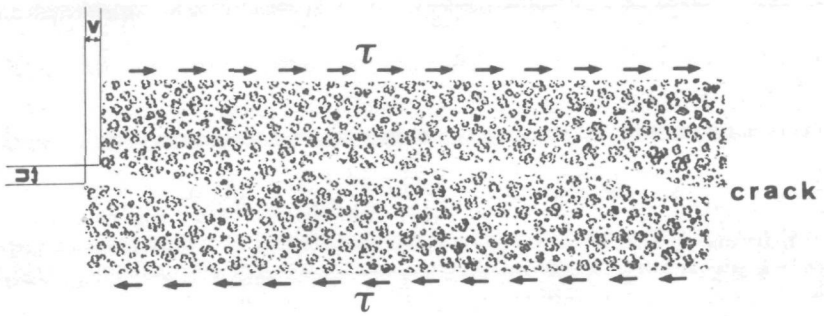

FIGURE 4.10 : Irregularities on crack faces

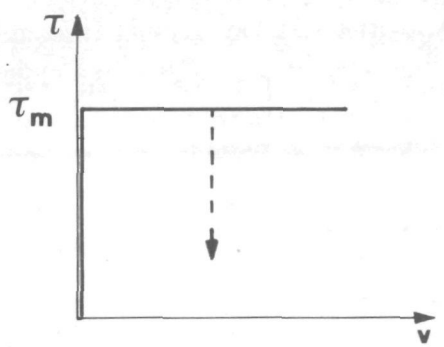

FIGURE 4.11 : Rigid-plastic model for aggregate interlock in a crack

The following formula is adopted for the magnitude of the maximum shear stress (τ_m) that can be transmitted in a crack:

$$\tau_{max} = \frac{1}{Ku} \qquad (4.23)$$

where: u = width of the crack
K = a constant

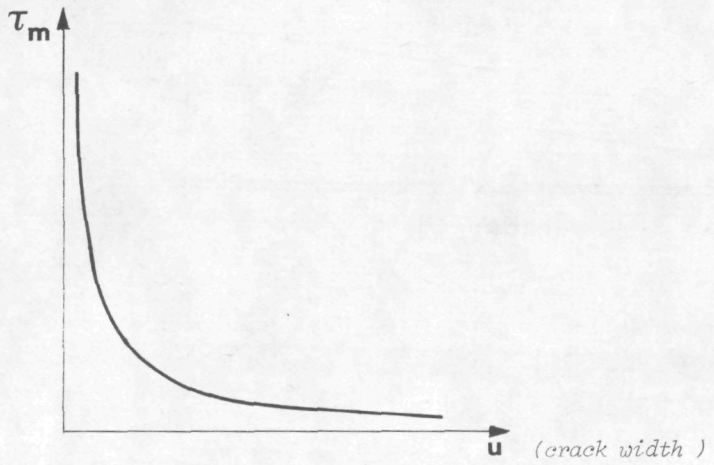

FIGURE 4.12 : Maximum shear stress as a function of crack width

4.8 BEHAVIOUR OF THE STEEL

The program incorporates two different models for describing the behaviour of the reinforcing steel or prestressing steel, namely:

- the ideal elasto-plastic model for steel with a pronounced yield range;
- the non-linear elasto-plastic model for steels without a pronounced yield range.

Any flexural stresses that may be acting in the steel are not taken into account in either model.

4.8.1 *IDEAL ELASTO-PLASTIC MODEL*

It is assumed that yielding of the steel bar can occur only at a crack in the concrete. Here the yield deformation of the steel is highly concentrated locally, so that in the program a delta function is used to describe the plastic strain behaviour over the length of the bar.

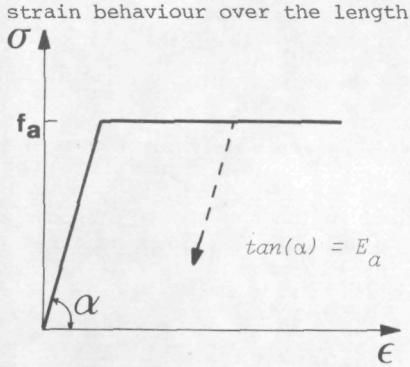

FIGURE 4.13 : Ideal elasto-plastic model for reinforcement

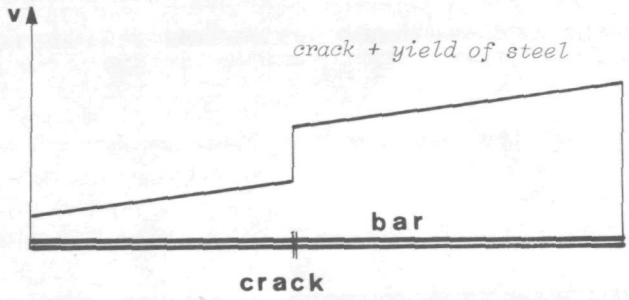

FIGURE 4.14 : Discontinuous behaviour of the displacements at a crack when yielding of the steel occurs

4.8.2 *NON-LINEAR ELASTO-PLASTIC MODEL*

The relationship between the stress (σ) and the strain (ε) is introduced for the purpose of this model. This relationship is represented in the form of a polygon.

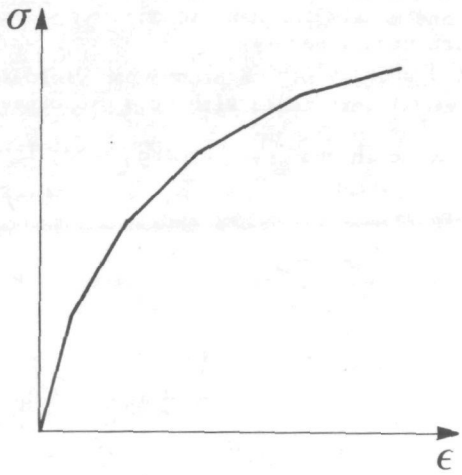

FIGURE 4.15 : Relationship between σ and ε in the non-linear elasto-plastic model for the reinforcement

Just as in the ideal elasto-plastic model, in the non-linear elasto-plastic model the tangent modulus of stiffness on unloading is taken as equal to the tangent modulus (E_o) at the origin.

4.9 BOND

The behaviour of the boundary layer between steel and concrete under a shear stress is descripted by an ideal elasto-plastic model.

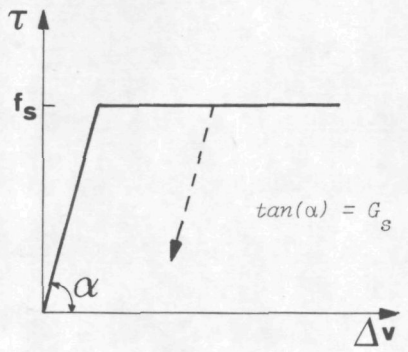

FIGURE 4.16 : Ideal elasto-plastic model for bond

4.10 DOWEL ACTION

Pending further research into the effect and magnitude of the dowel forces, only the linear elastic relationship between relative displacements perpendicular to the centre-line of the bar and forces acting on this centre-line has been adopted in the program.

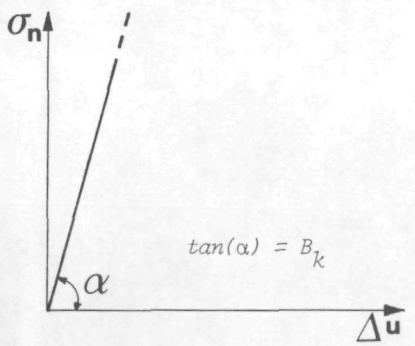

FIGURE 4.17 : Elastic model for dowel forces

COMPUTER PROGRAM

5.1 SEQUENCE OF CRACKING

In order to take account of the effect of cracking upon the stresses in the vicinity of the crack, only one crack in one element is introduced per iteration. In which element a new crack must be assumed is determined with the aid of the cracking potential. For each triangular element a cracking potential is calculated on the basis of the stresses at the centre of gravity of the triangle and the cracking criterion stated in Section 4.3. This potential indicates the factor by which the stresses are to be calculated in order to conform to the cracking criterion. Zero value of the cracking potential indicates that the stresses are in the range where crushing, not cracking, constitutes the maximum criterion (points A and B in Fig. 5.1). A potential of less than unity indicates that the stresses are still too small for exceeding the cracking criterion (point C in Fig. 5.1). A crack can develop only in an element having a cracking potential of not less than unity, i.e., ≥ 1 (point D in Fig. 5.1). A new crack is introduced into the element with the highest cracking potential of not less than unity.

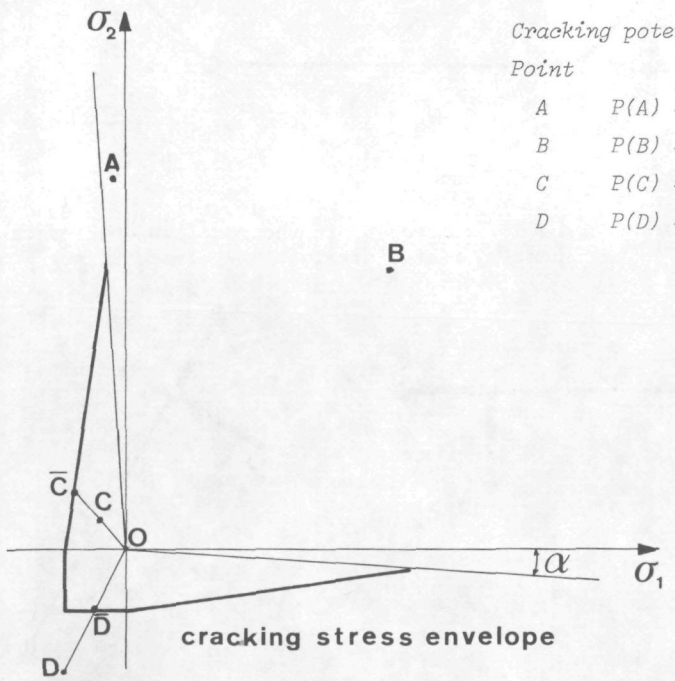

Cracking potential (P)

Point	
A	$P(A) = 0$
B	$P(B) = 0$
C	$P(C) = \overline{OC} \,/\, \overline{O\bar{C}} < 1$
D	$P(D) = \overline{OD} \,/\, \overline{O\bar{D}} > 1$

FIGURE 5.1 : Calculation of cracking potential

Local stress peaks are formed at the end of a crack. These cause further spreading of the crack, even if the average stresses in the vicinity therof - apart from the stress peaks - are below the cracking criterion. The highly localized stress fields associated with the notch stresses are not calculated in the MICRO model. The effect that, in an element adjacent to the end of an existing crack, a crack will develop at lower average stresses than it would if there were no crack present is here dealt with by multiplying the cracking potential of these elements by a factor larger than unity. The calculations that have been performed show a value of between 1.3 and 1.5 for this factor to be satisfactory.

5.2 CURVED BARS

Additional linear relationships between various degrees of freedom (displacements) can be introduced into the computer model. These relationships are specially intended to enable features of detailing, such as curves in bars and hooks at bar ends, to be suitably schematized. A curved bar is schematized to an assembly of straight linear portions (see Fig. 5.2).

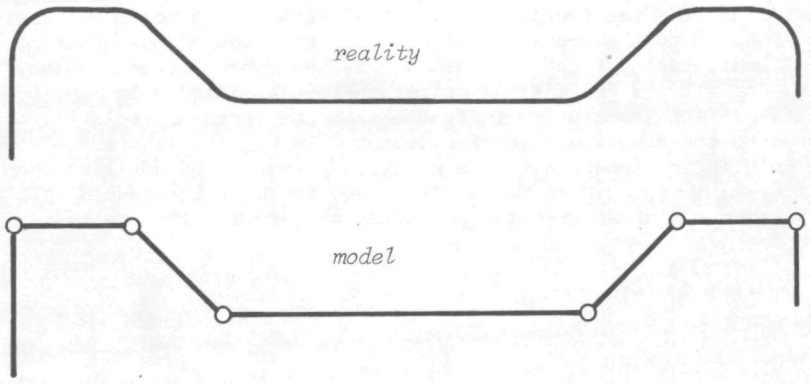

FIGURE 5.2 : Curved bar

In this way the curves or bends are reduced in the model to angular changes of direction located on the junction of two straight bar elements (see Fig. 5.3).

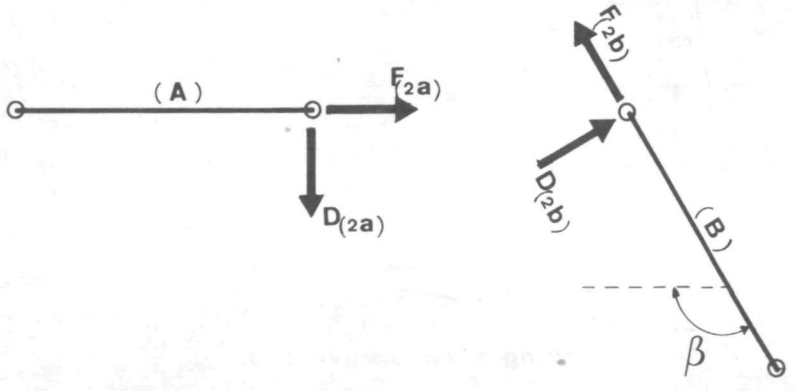

FIGURE 5.3 : Oblique junction of two bar elements

If the two bars A and B are interconnected at point 2, the equilibrium conditions for this point are:

$$F_{(2A)} + \cos(\beta)\, F_{(2B)} + \sin(\beta)\, D_{(2B)} = 0 \qquad (5.1)$$

$$D_{(2A)} - \sin(\beta)\, F_{(2B)} + \cos(\beta)\, D_{(2B)} = 0 \qquad (5.2)$$

Since the developed bar length at an angular junction point in the model is equal to zero, it is presupposed that the slip resistance at that point is likewise zero. In that case, however, the condition $F_{(2A)} = F_{(2B)}$ must be satisfied.
The above-mentioned extra condition for the junction point is duly taken care of by adding to the equilibrium conditions, already mentioned, the further condition that:

$$D_{(2B)} = -\frac{\cos(\beta) + 1}{\sin(\beta)} F_{(2B)} \qquad (5.3)$$

5.3 SCATTER OF MATERIAL PROPERTIES IN A STRUCTURE

The properties of concrete and steel are not constants, but stochastic quantities. Particularly for concrete it is true to say that its composition is liable to vary from one point to another in a structure. The effect that this scatter has upon the behaviour of a structure varies greatly according to the type of structure and according to the aspect of behaviour under consideration. Thus, the scatter in the tensile strength of the concrete has a different effect on the results of a series of direct tensile tests than on the results of a series of splitting tensile tests. If the dimensions of a structure are much larger than those of the inhomogeneities, it will in general be permissible to base the analysis of the overall structural behaviour upon a homogeneous material model. On the other hand, if the analysis is concerned with a small structure or with particular aspects of structural behaviour, the scatter will indeed have to be taken into account. This is exemplified by the effect of the scatter in the tensile strength of concrete and in the bond strength of concrete to steel upon crack spacings and crack widths.
Fig. 5.4b illustrates the pattern of cracks that was formed when a reinforced concrete tie member as shown in Fig. 5.4a was tested in tension. The order in which the cracks developed is indicated by the numbers written beside them. The diagram clearly reveals the differences in the crack spacings and the irregularity in the order in which cracking occured. These effects are due to the scatter in the tensile strength of the concrete both in the longitudinal and in the transverse direction of the test specimen.

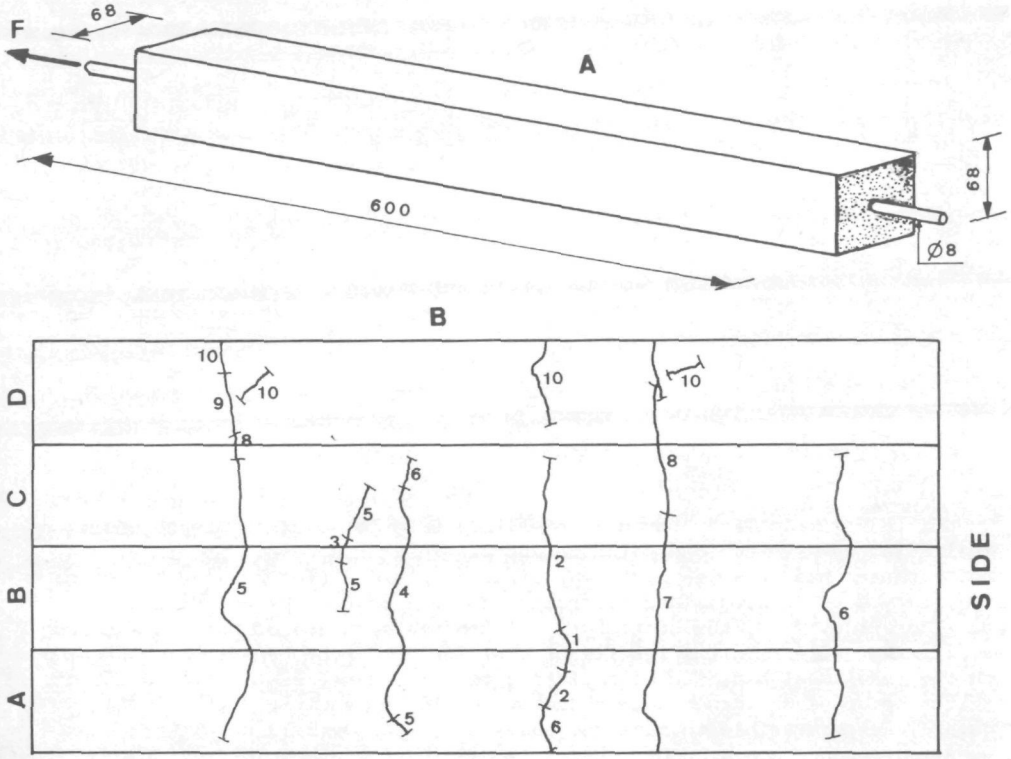

FIGURE 5.4 : Tie member with pattern of cracks

This tie member was analysed as one of the tests for the MICRO program. In the first analysis the tensile strength of the concrete was taken as equal in all the elements. The result was a very regular crack pattern and a practically unvarying crack width in all parts of the specimen (see Fig. 5.5).
In the second analysis, each element is assumed to have a different tensile strength, determined with the aid of the Monte Carlo method from a normal distribution of these strengths. The generated strengths together with the results of the analysis are presented in Fig. 5.6. The standard deviation of the normal distribution has been taken as 0.15 times the mean tensile strength.
In Fig. 5.6 the generated tensile strength per element is indicated as the quality designation. The "plus" sign denotes a tensile strength above, the "minus" sign a tensile strength below the mean.

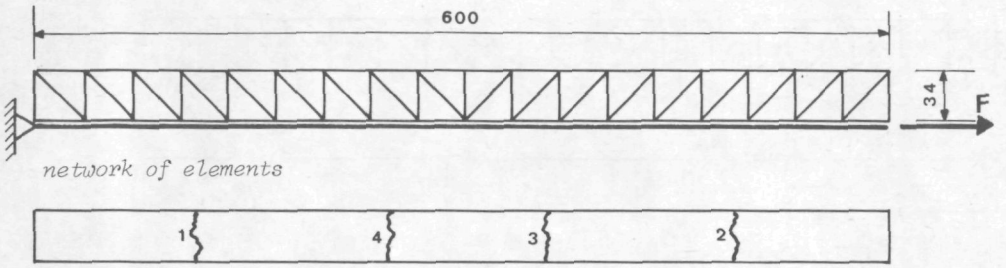

network of elements

pattern of cracks

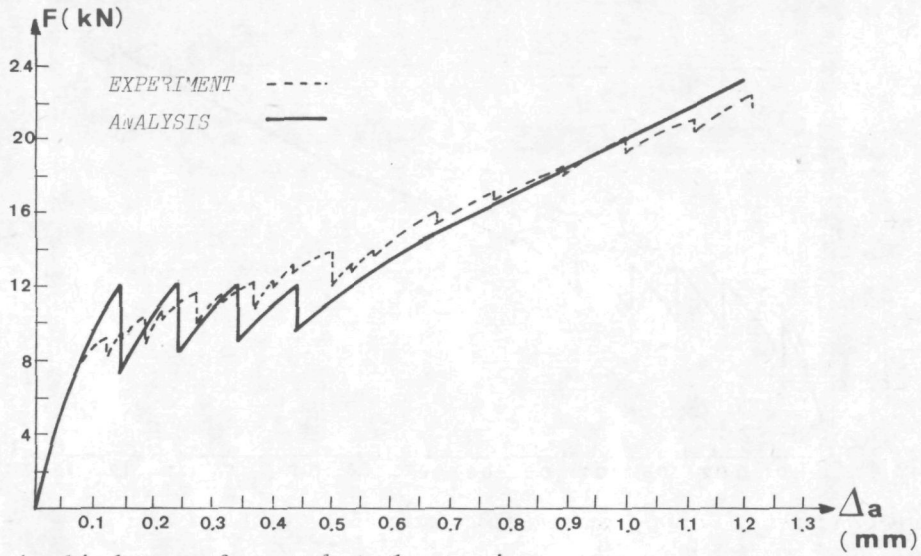

relationship between force and steel extension

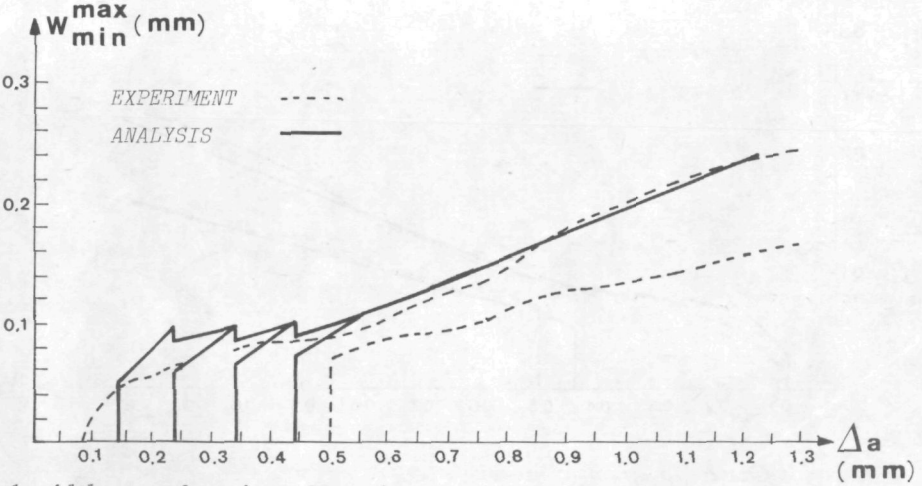

crack width as a function of steel extension
FIGURE 5.5 :

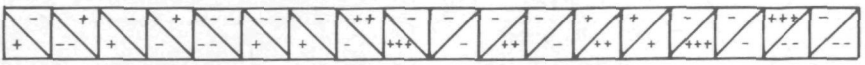

quality

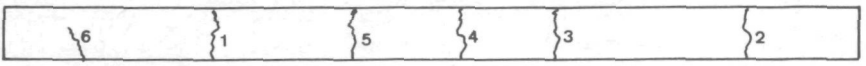

pattern of cracks

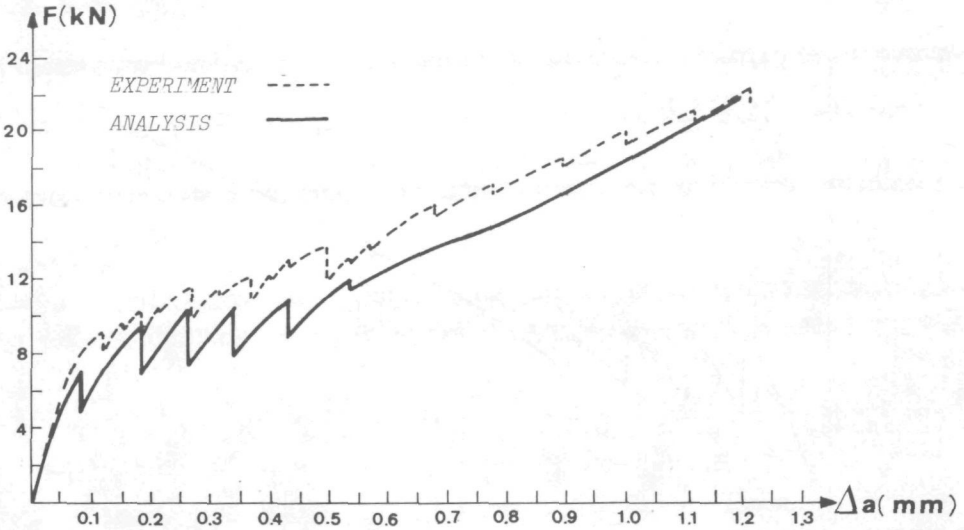

relationship between force and steel extension

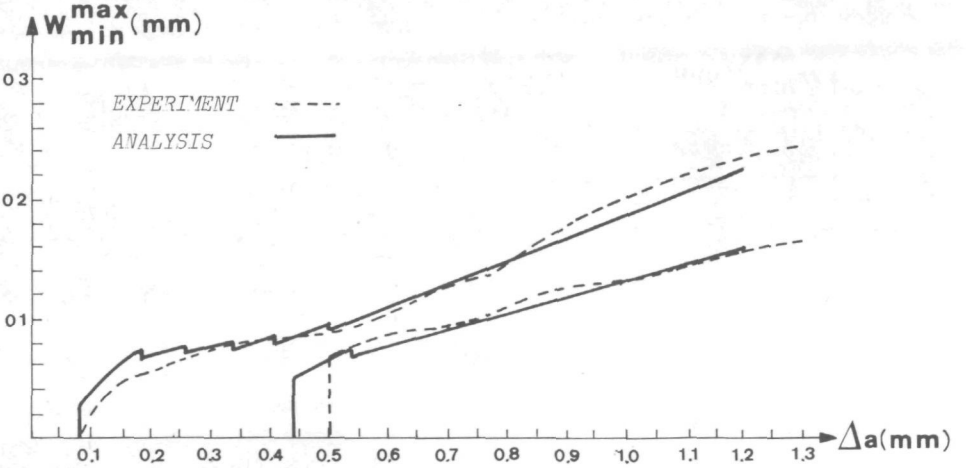

crack width as a function of steel extension

FIGURE 5.6 :

Comparison of the results of the two analyses shows the effect of the scatter in the tensile strength of the concrete upon the force-deformation behaviour to be slight. Of greater influence are the number of cracks, the crack spacing and the crack widths. The properties of steel and concrete adopted in these analyses where taken from [5.1] , while the most suitable maximum bond stress (f_s) was determined by preliminary calculations.

CONCRETE:

f_b = 2.5 N/mm^2

E_b = 28000. N/mm^2

STEEL:

E_a = 192300. N/mm^2

BOND:

f_s = 7.5 N/mm^2

G_s = 1590. N/mm^3

For studying the effect of scatter upon the behaviour of small structures this simulation method is an acceptable technique. For larger structures, however, it is impracticable because it involves a number of non-linear analyses. Fortunately, the effect of the scatter in the properties of the materials upon the overall structural behaviour is usually quite small.

5.4 PROGRAM

The MICRO program operates as a so-called subsystem under the conctrol of the Genesys system [5.2]and is programmed in Gentran. Input of this program is done with tables and commands which are defined in the Genesys manner and which can be stated unformated. For a detailed description of input and output the reader is referred to [5.3].
The numbering of the degrees of freedom and the manner of solving the ultimate system of equations are based on the wave front method [2.1] . The modified Crout algorithm [5.4] is used for solving the system of equations. This algorithm is so programmed that during decomposition only the system triangle is present in the working storage. The output is selective and may take the form of tables and/or diagrams. Fig. 5.7 presents an overall flowchart.

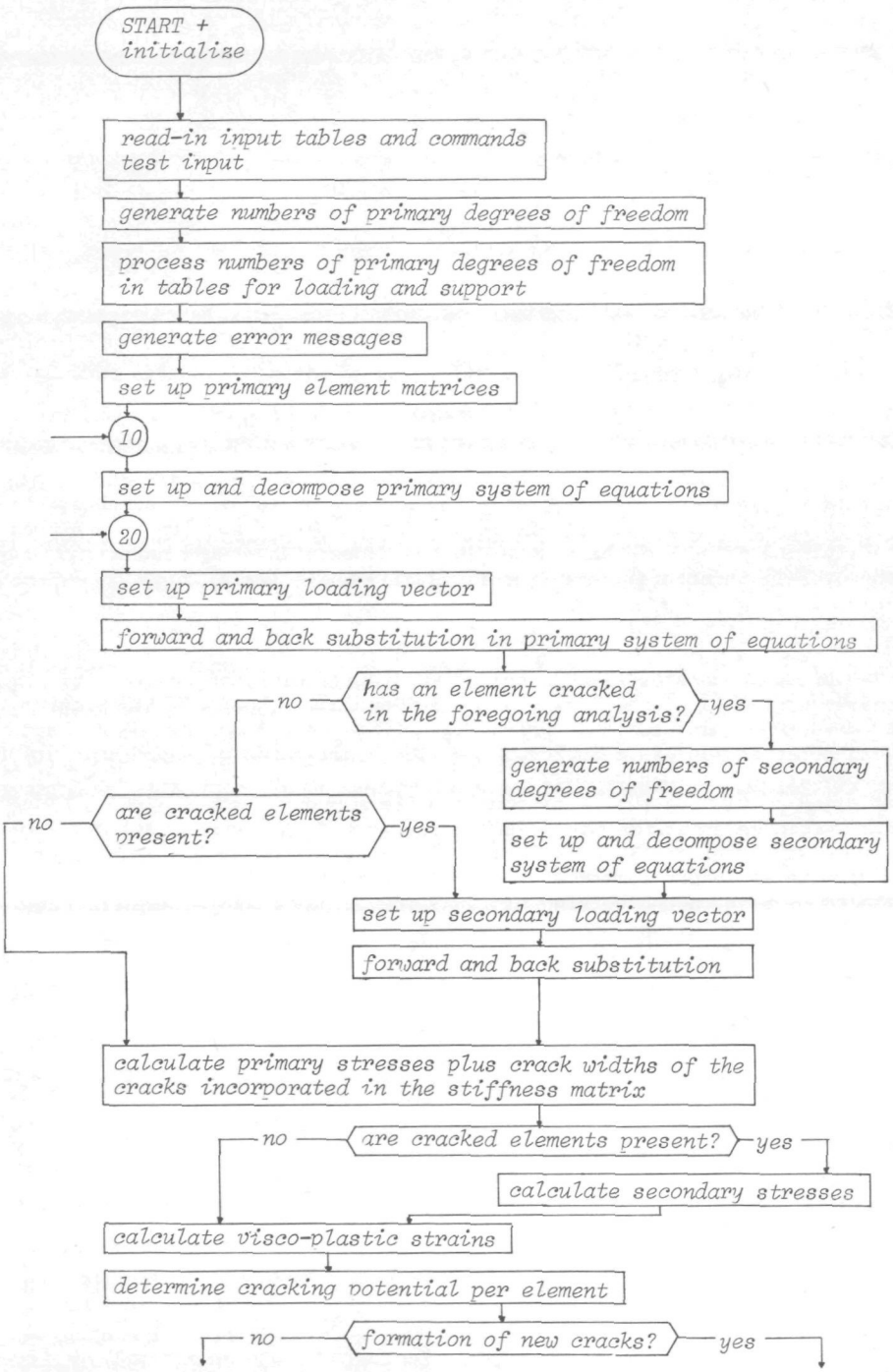

FIGURE 5.7a : Overall flowchart of the MICRO program

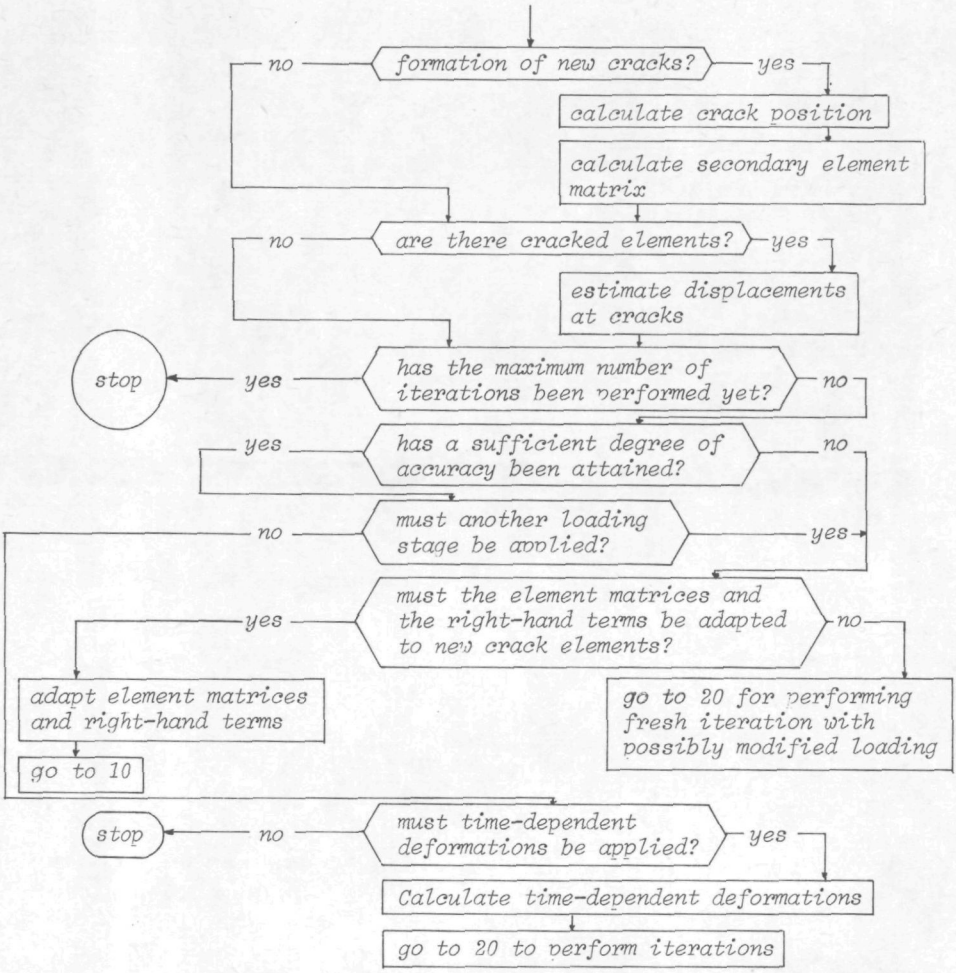

FIGURE 5.7b : Continuation overall flowchart of the MICRO program

6

ANALYSES PERFORMED

6.1 INTRODUCTION

In order to test the MICRO model with regard to its serviceability and ability to meet the objectives, a number of structures whose experimental behaviour has been described in the literature were analysed with the aid of the model. Since only a limited number of analyses were performed, it was not practicable to check all the possibilities of the model. In the analyses the time-dependent behaviour and the behaviour under alternating load were not considered. Although the possible occurrence of dowel forces in the reinforcement and of parallel displacement at a crack was allowed for in the model, neither of these phenomena occurred to any significant extent in the four structures analysed.
In Section 5.3 the results of the analysis of a tie member, i.e., a structural member loaded in tension only, have already been compared with the experimental data. As distinct from the approach adopted in analysing that tie member, in the present chapter no variations of the parameters have been introduced, because parameter studies can be performed better and more quickly on appropriately selected structural details than on the examples described here. Just as in performing an experiment, an analysis based on a prescribed displacement offers advantages in comparison with an analysis based on a prescribed loading. Thus, in the prescribed displacement method any retrograde changes in the load-deflection diagram can be detected, where as this is not possible in an analysis based on a prescribed loading. Also, the first-mentioned method is advantageous in a case where the structure develops ideally plastic or very nearly ideally plastic behaviour. In an analysis based on a prescribed displacement the iteration process will, in such a case, still converge reasonably rapidly, whereas in the prescribed loading method there will be very poor convergence or indeed none at all.
Unfortunately, an analysis based on a prescribed displacement is not always possible. If a structure is subjected to a number of point loads or a uniformly distributed load which are of variable magnitude, it will be necessary to perform the analysis with a prescribed magnitude of the loading.

6.2 BEAM LOADED IN BENDING

One condition for successfully employing a computer program for the analysis of structures having a complex internal pattern of forces is that a numerical model of his kind should correctly analyse the basic cases with regard to loadbearing capacity.
After the tie member already described in Section 5.3, the second basic case to be analysed was a reinforced concrete beam loaded in bending. This beam was one of a series of beams with varying percentages of reinforcement and subjected to four-point loading tests as reported by Monnier in [6.1] . The beam selected for the present purpose was No. 8 with a proportion of tensile reinforcement equivalent to 0.47% of the cross-sectional area of the beam. The dimensions of this test specimen and the manner of loading are indicated in Fig. 6.1.

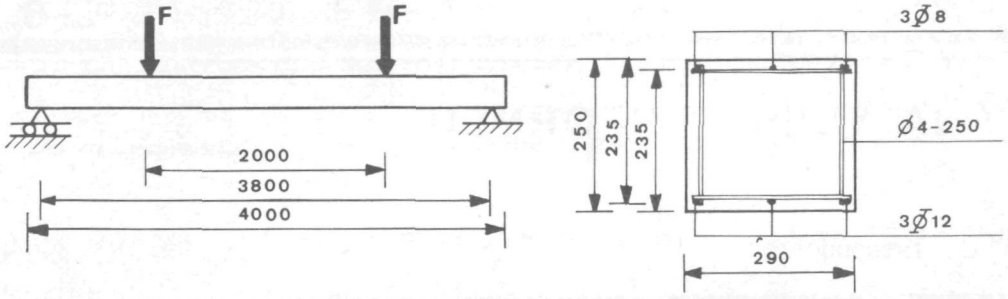

FIGURE 6.1 : Four-point bending test on beam No. 8 in [6.1] (dimensions mm)

In order not to have to consider the effect of shear force in this analysis, the latter was confined to the behaviour of the region between the two point loads, where the bending moment is constant.
For analysing the behaviour in pure bending it will suffice to consider only a short portion of the beam. This portion should, however, be chosen sufficiently large to ensure that several cracks will develop in it, so that both the state of stress at a crack and the state of stress between two cracks are comprised in the analysis. Accordingly, for an expected maximum crack spacing of 140 mm, a 350 mm long portion of beam was adopted for the analysis. At its left-hand end this portion is loaded with a prescribed angular rotation ψ, whereas rotation is prevented at the right-hand end. In order to be able to apply this angular rotation ψ without imposing restraint upon change in length of the beam and without affecting the position of the neutral axis or causing a disturbance in behaviour in consequence of the introduction of the bending moment, the beam portion under consideration is assumed to be extended by a 160 mm long rigid portion at its left-hand end. The network of elements, the manner of support and the loading on the rigid portion (shown shaded) are indicated in Fig. 6.2. In order to keep the stresses and strains in the rigid portion small in relation to the rest of the beam and in order to obviate cracking in this portion, the thickness of the elements in it is 1000 times the thickness of the elements in the (non-shaded) rest of the beam. The effect of the concrete cover to the bottom reinforcement has not been taken into account in the analysis. This omission can result in 13% over-estimation of the concrete stresses in the uncracked beam. When cracks develop in the beam, however, the effect of ignoring the bottom cover is negligible.

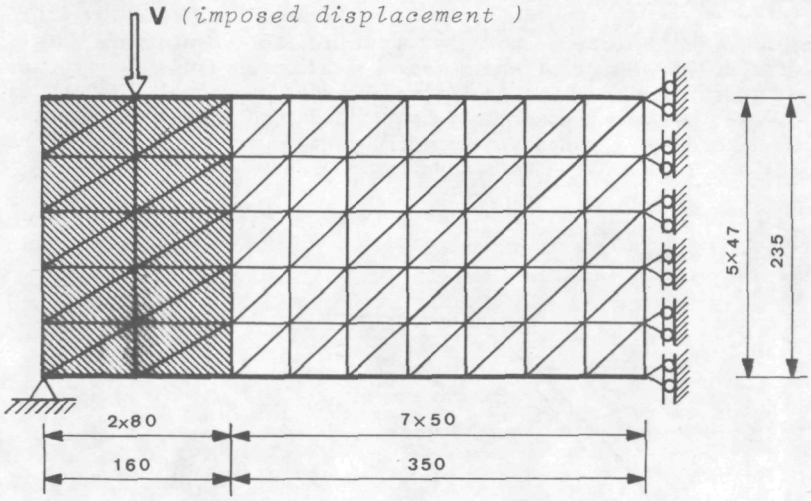

FIGURE 6.2 : Element model and manner of loading

The experiment was, in the main, based on an imposed load, so that the decline in loadbearing capacity in consequence of cracking was not recorded. During load increase, up to the point where yielding of the reinforcement began, the beam was unloaded once. Since this once-only load alternation can have had little effect on the subsequent behaviour, it has been ignored in the analysis. Instead, a monotonically increasing angular rotation of the end of the beam has been assumed.

Furthermore, the analysis has been based on the under-mentioned material properties, as reported in [6.1]. The properties of the boundary layer between steel and concrete have been estimated.

CONCRETE: non-linear behaviour: Link's model

f'_b = -31.1 N/mm^2

f_b = 3.75 N/mm^2

E_b = 30000. N/mm^2

ν_b = 0

STEEL; ideal elasto-plastic model

f_a = 441. N/mm^2

E_a = 218500. N/mm^2

BOND:

f_s = 3.75 N/mm^2

G_s = 3500. N/mm^3

The experimentally determined and the calculated moment-curvature relationships are presented in Fig. 6.3. The bending moment at which the first crack occurs is 10 kNm in the experiment and 11 kNm in the analysis (see Fig. 6.6). Whenever a crack is formed, there is, according to the analysis, a slight decrease in the magnitude of the moment for a somewhat greater angular rotation. These decreases in bending moment are not manifest in the experiment because it was performed under load-controlled conditions. The bending moment at which yielding of the tensile reinforcement occurs is 32 kNm in the experiment and 33.5 kNm in the analysis.

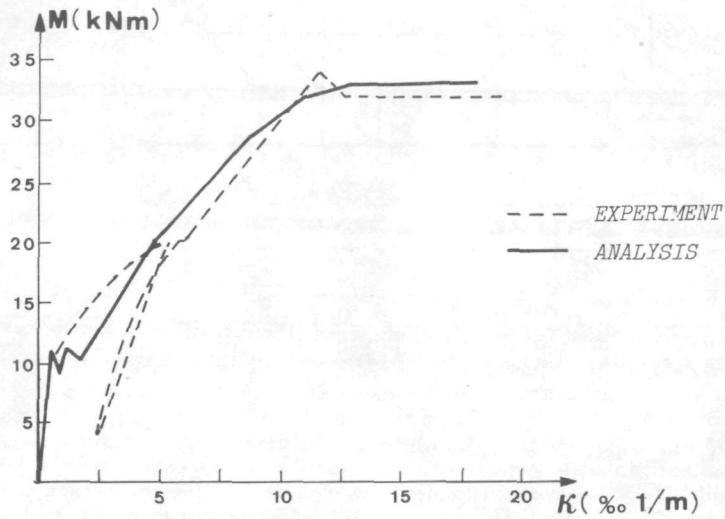

FIGURE 6.3 : Moment-curvature diagram

The relation between the average (tensile) stress in the bottom reinforcement and the bending moment as determined in the experiment and in the analysis is indicated in Fig. 6.4. On comparing experiment and analysis, the abrupt increase in the average steel stress as calculated in the analysis after the occurrence of the first crack is notable. This difference between experiment and analysis is due to the fact that in the experiment a longer portion of the beam is considered and the cracks develop only gradually between a moment of 10 kNm and 24 kNm (see Fig. 6.6). In the analysis, on the other hand, the three big flexural cracks all occur at the same bending moment of 11 kNm. The fact that in the experiment these cracks do not all occur at the same load must be due to internal scatter (variation) in the tensile strength of the concrete and/or to scatter in the bond between concrete and steel.

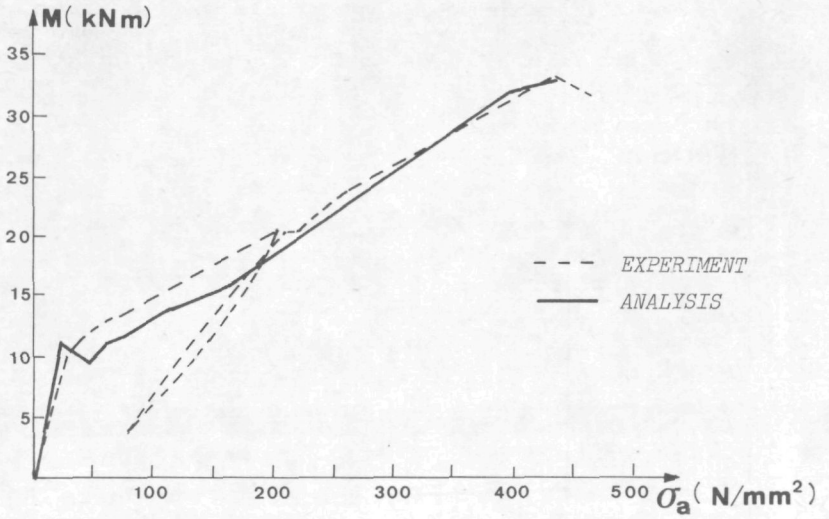

FIGURE 6.4 : Average stress in the bottom reinforcement as a function of the bending moment

The relationship between the bending moment and the average compressive stress in the concrete at the top of the beam is indicated in Fig. 6.5.

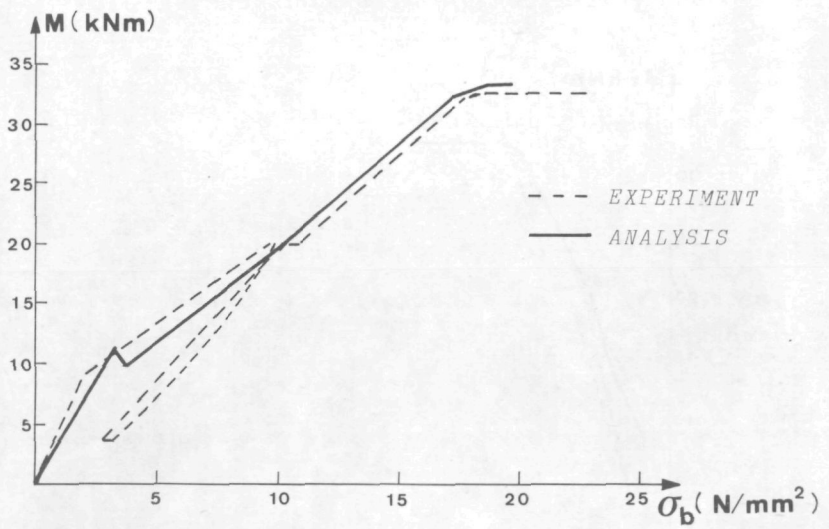

FIGURE 6.5 : Average stress in the concrete at the top of the beam as a function of the bending moment

The average crack spacing and maximum crack spacing are indicated in Fig. 6.6. According to the analysis, the cracks are spaced regularly at 150 mm, a value which is very close to the maximum spacing of 140 mm found experimentally. This agreement is also manifest in Fig. 6.7, where the relationship between the maximum crack width and the bending moment is presented for experiment and analysis respectively.

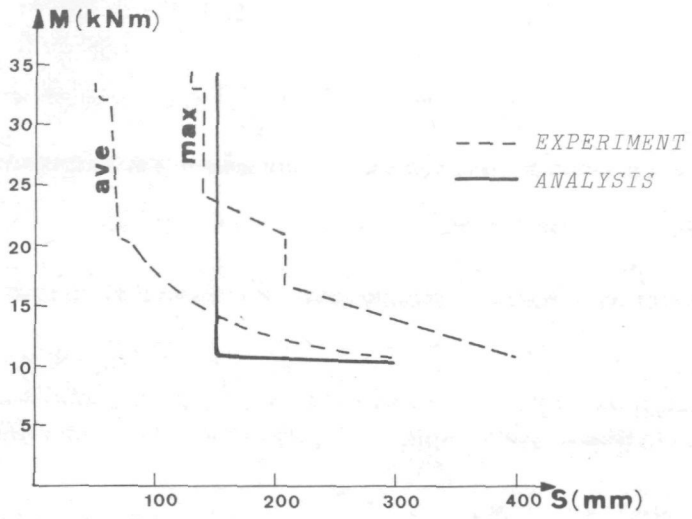

FIGURE 6.6 : Average crack spacing and maximum crack spacing as as a function of the bending moment

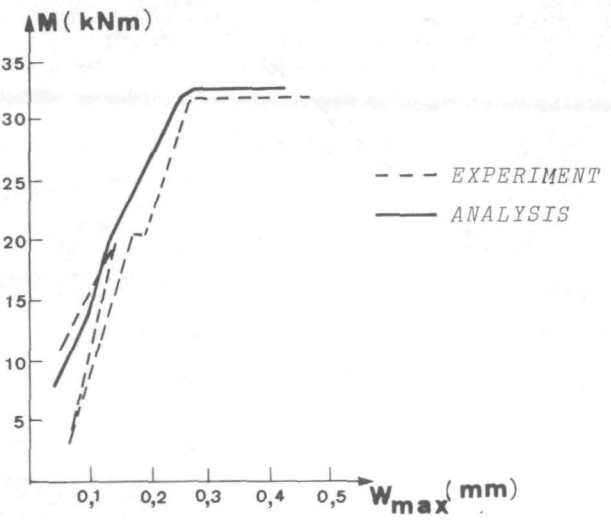

FIGURE 6.7 : Maximum crack width as a function of the bending moment

With regard to the stress in the bottom reinforcement it has already been mentioned that in the experiment the cracks were formed at different external loads. This was attributed to scatter in the properties of the concrete in the beam. The effect of this scatter manifests itself not only in the differences in bending moment at which the cracks occur, but also in the scatter in the crack spacings. The crack patterns obtained experimentally and by analysis, at a load at which yielding of the bottom reinforcement occurs, are shown in Fig. 6.8. It is notable that in both crases there are horizontal cracks high up in the beam. The reason why, in the analysis, there is an absence of smaller vertical cracks between the large cracks has already been discussed above.

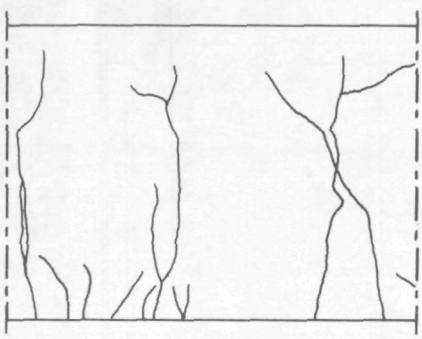

Crack pattern in the region of constant bending moment according to experiment

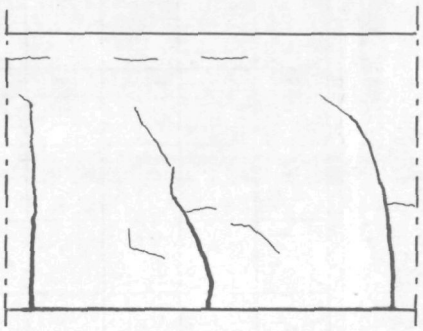

Crack pattern according to analysis

FIGURE 6.8 : Crack pattern associated with yielding of the bottom reinforcement

CONCLUSION

From the comparison of analysis and experiment it appears that the behaviour of a beam loaded in bending can be satisfactorily analysed with the MICRO model. In making this comparison, much attention has been paid to the differences between the calculated and the experimentally determined results in consequence of the scatter in the actual material properties. This scatter, however, has little effect on the overall behaviour and on the magnitude of the steel and concrete stresses. It is significant only in so far as the average crack spacing and crack widths are concerned. The homogeneous material model gives good results for the maximum crack spacing and maximum crack widths.

6.3 PLATE LOADED AT UPPER EDGE

In Section 1.3 it was stated, as one of the aims of the MICRO model, that this model should be suitable for the analysis of structures in which only a few dominant cracks determine the behaviour. The reason for this aim is that models with "smeared-out" cracks do not do sufficient justice to these dominant cracks. With reference to such models, Schnobrich states in [1.11]:"This added flexibility is paid for by the tendency of the procedure to diffuse the cracking system and constrain it so that no one crack could dominate the behaviour. This has some implications in investigating shear failure development in some members."
An example of a structure in which only a few dominant cracks determine the behaviour is the plate WT2 in the series of tests on various types of plate

structure described by Leonhardt and Walther in [1.5].
The plate in question is loaded along its upper edge, as shown in Fig. 6.9.

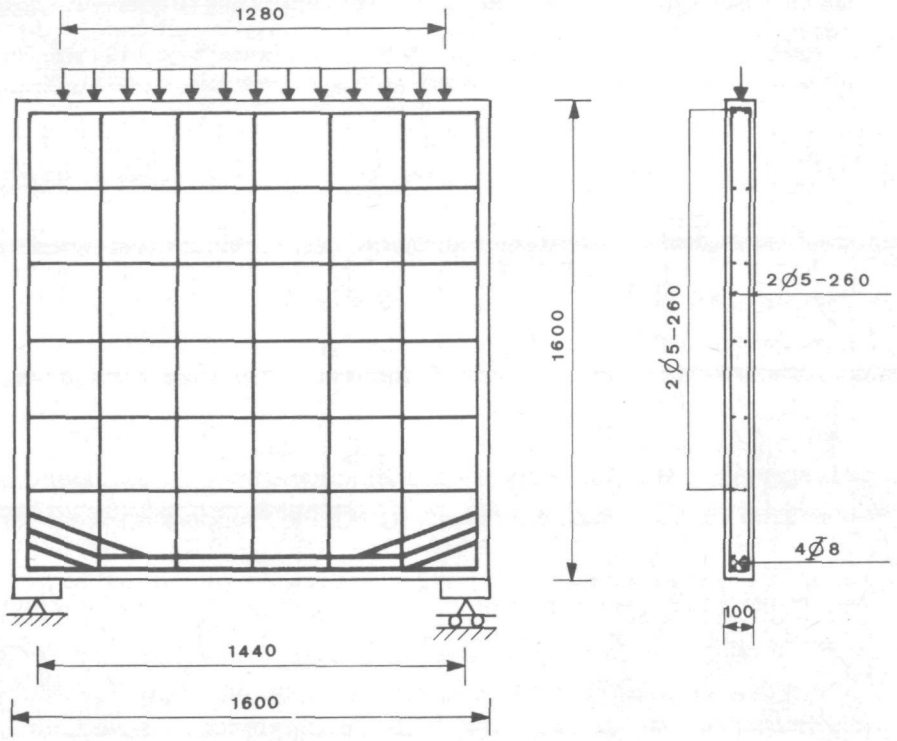

FIGURE 6.9 : Shape, reinforcement and manner of loading the plate WT2 reported in [1.5]

On account of symmetry of the structure and of the boundary conditions, it is sufficient to confine the analysis to one half of the structure. For analysing the half plate the boundary condition on the right-hand side is the symmetry condition that the horizontal displacement of the plate midway between the two bearing must be zero. The network of elements for the concrete and for the reinforcing bars, respectively, is indicated in Fig. 6.10, as well as the manner of loading and support.

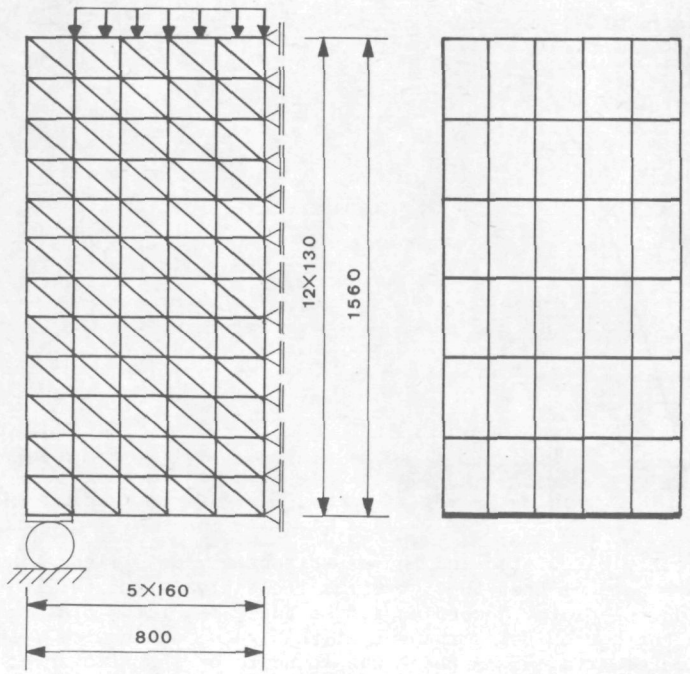

Concrete elements *Reinforcement elements*

FIGURE 6.10 : Element model for the analysis of half the plate

Since the structure is subjected to a uniformly distributed load, the analysis has had to be performed with a stepwise increasing load applied to the top of the plate. The drawbacks of this method of loading have already been described in Section 6.1. The following material properties have been adopted in the analysis:

CONCRETE: non-linear behaviour: Link's model

$f_b' = -30.1 \ N/mm^2$

$f_b = 3.5 \ N/mm^2$

$E_b = 32000. \ N/mm^2$

$\nu_b = 0.2$

STEEL: non-linear elasto-plastic model (see Fig. 6.11)

$E_a = 210000. \ N/mm^2$

BOND: $f_s = 4.7 \ N/mm^2$

$G_s = 47. \ N/mm^3$

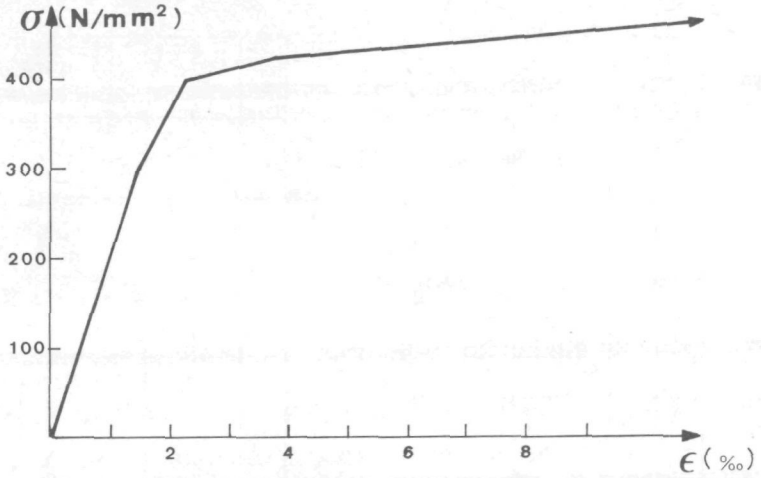

FIGURE 6.11 : Stress-strain diagram for bottom reinforcement

The analytically calculated and the experimentally determined load-deflection diagrams have been plotted in Fig. 6.12. The analysis was terminated at a load of 1075 kN on the plate. According to the analysis, large plastic strains occurred in the bottom reinforcement at that value of the load, and with the next load increment of 25 kN there was found to be insufficient convergence even after 25 iterations, indicating practically ideal plastic behaviour of the structure under load of that magnitude. The failure load determined in the experiment was 1195 kN.

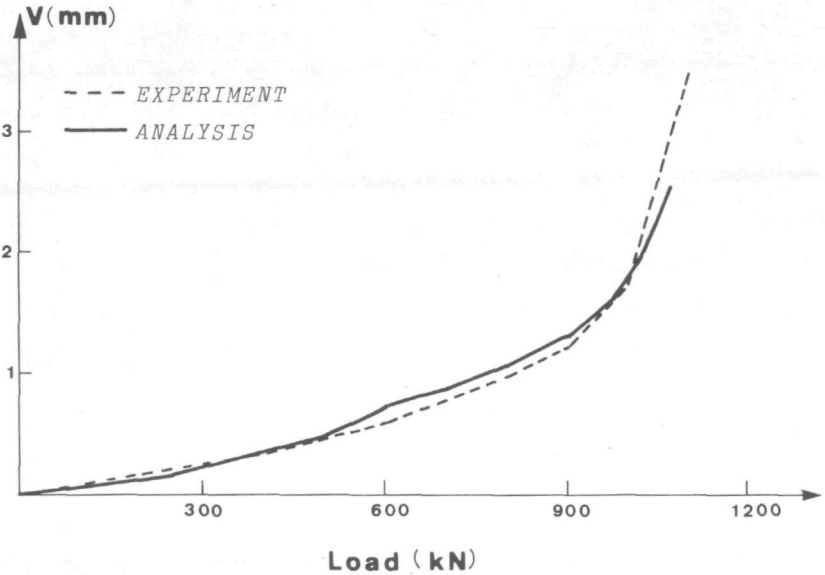

FIGURE 6.12 : Load-deflection diagram

The crack patterns found in the experiment and in the analysis are shown in Fig. 6.13.

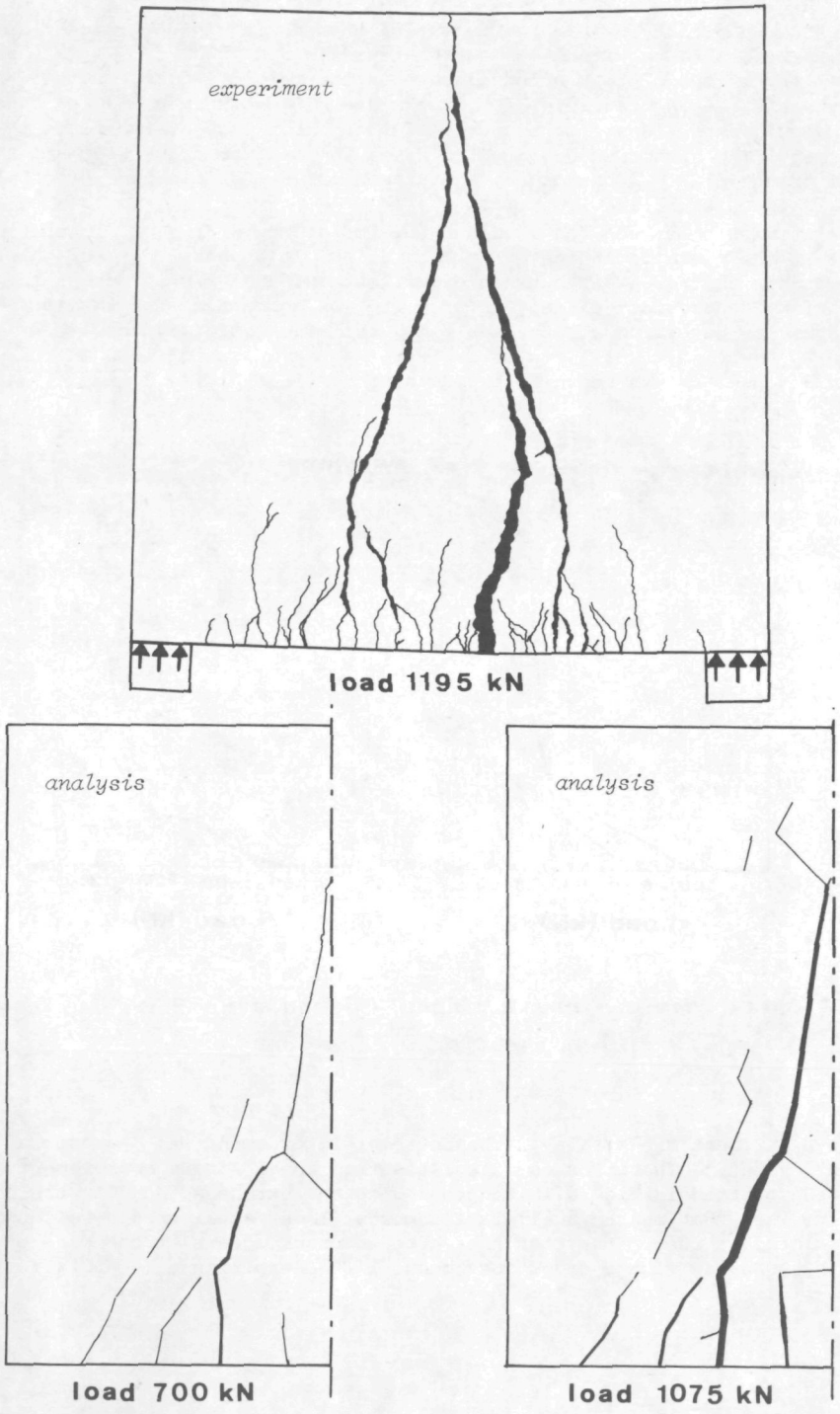

FIGURE 6.13 : Crack patterns according to experiment and analysis

Both patterns clearly reveal the formation of a few dominant flexural cracks which start beside the middle of the plate and curve upwards towards the axis of symmetry of the plate. In consequence of the relative course network of elements and the adopted rule of only one crack crossing per element boundary the analysis shows fewer minor cracks at the bottom edge of the plate than the experiment. The higher value calculated for the maximum crack width at the bottom of the plate is bound up with the smaller number of these cracks in the analysis (see Fig. 6.14a).

The relationship between the load and the sum of the widths of all the bottom cracks in the plate is indicated in Fig. 6.14b. It appears that for this relationship the agreement between experiment and analysis is better than for the maximum crack width already referred to. On account of the smaller number of cracks, as determined in the analysis, the crack deformations are evidently concentrated at this smaller number of cracks. At a load of 1000 kN the widths of the dominant cracks begin to predominate considerably.

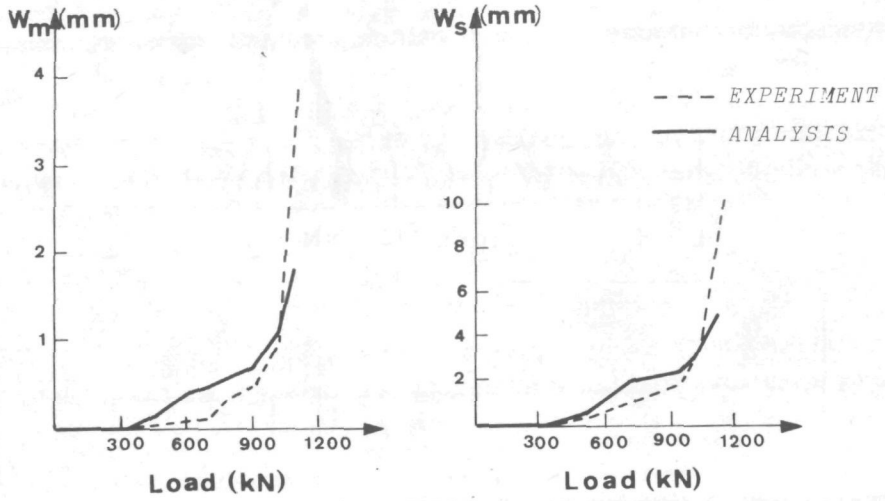

FIGURE 6.14 : Maximum crack width (W_m) and summed crack widths (W_s) as a function of the load

In the experiment the strain in the bottom reinforcement was measured at the axis of symmetry. The stresses calculated from these strain measurements have been plotted in Fig. 6.15,together with the stresses found in the analysis. The fact that in the analysis a somewhat lower steel stress is found at higher loads is due to the fact that here no crack occurs at the axis of symmetry, whereas such a crack does occur in the experiment (see Fig. 6.13).

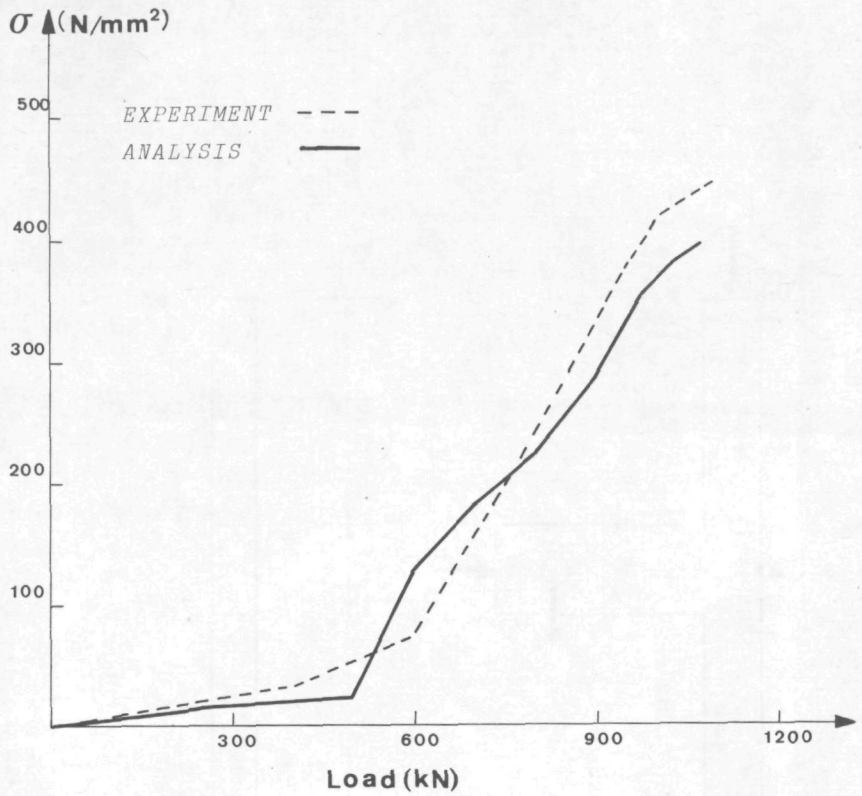

FIGURE 6.15 : Stress in bottom reinforcement at the axis of symmetry as a function of the load

CONCLUSION

Analysis and experiment both reveal only a few dominant cracks which start at the bottom of the plate, between the axis of symmetry and the support, and which in the upward direction bend towards the centre of the plate. The analytically calculated width of these cracks is likewise in sufficiently good agreement with the measured widths. It does, however, emerge from the crack pattern determined by analysis and by experiment, respectively, that the number of elements in the analysis is to small to prescribe the correct crack spacing in the bottom edge of the plate. Since the number of smaller cracks which would develop at the bottom edge of the plate have only little effect on the overall behaviour, the load-deflection curves according to experiment and according to analysis are in excellent agreement.

6.4 BEAM-TO-COLUMN CONNECTION

As the final check for the MICRO model a structure has been analysed in which, besides flexural cracks, there also occur shear cracks.

This structure is one which was investigated in the Stevin Laboratory in a program of research on the strength and rigidity of various types of beam-to-column connections. These tests are more particularly of interest because they showed these specimens to fail at a lower value of the load than had been anticipated on the basis of the failure loads of the sections of the beam and of the connected columns. Test specimen No. 1402 in this series of beam-to-column connections described in [6.2] has been analysed. The structural dimensions and the manner of loading and support are shown in Fig. 6.16.

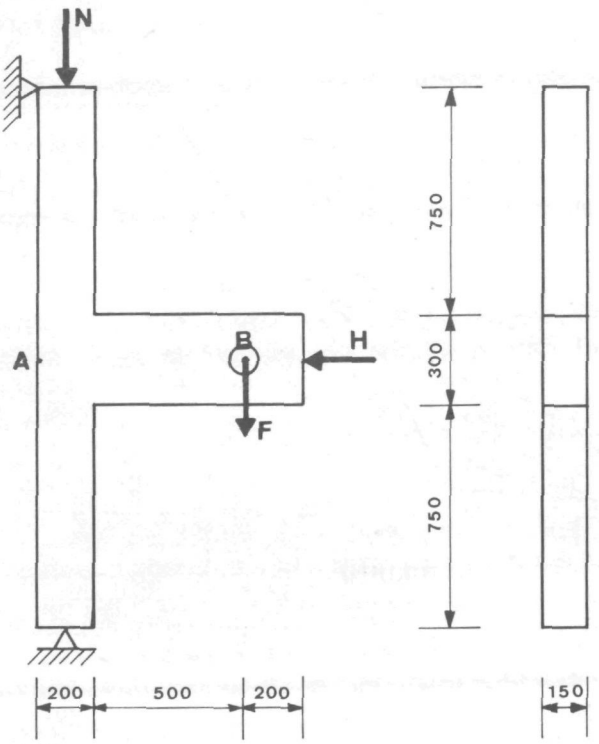

FIGURE 6.16 : Shape and manner of loading of specimen 1402 as described in [6.2]

The reinforcement in the column and beam is illustrated in Fig. 6.17.

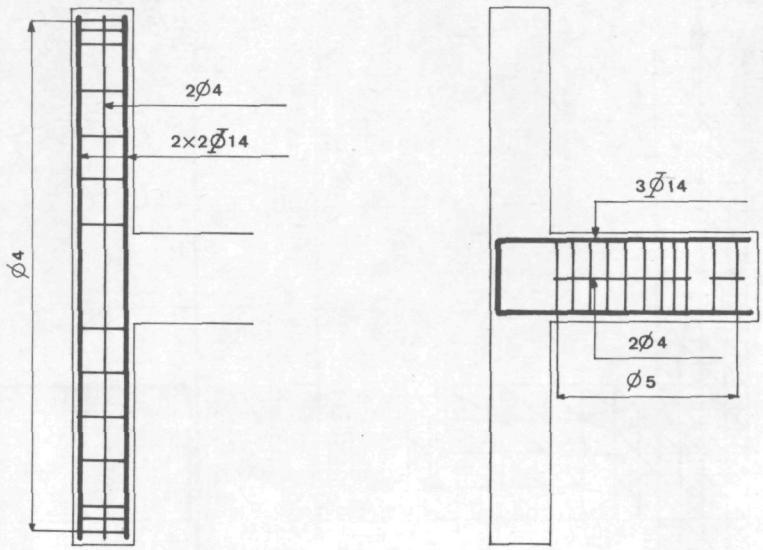

FIGURE 6.17 : Reinforcement of beam and column in the specimen

In the test the load (N) on the column and the load (F) on the end of the beam were increased simultaneously. The horizontal load (H) on the end of the beam was made so large that point A on the outside of the column (see Fig. 6.16) underwent no horizontal displacement. From the load-deflection diagram for the beam end B (see Fig. 6.20) it appears that in the experiment the tangential rigidity of the structure decreases greatly when the load (F) exceeds 85% of the failure load (F_u).
In the introduction to this chapter it has already been pointed out that, if the tangential rigidity becomes low, it is advisable to base the analysis on an imposed displacement instead of a given external force. Since the magnitude of the load is not known in advance in a case where a prescribed displacement is applied, the loading procedure applied in the test cannot be adopted in the analysis. For the above-mentioned reasons, the analysis, as distinct from the experiment, has been based on a constant load (N) of 45 kN acting on the column, restraint of horizontal displacement at the beam end at mid-depth of the beam (point B, Fig. 6.16), and a monotonically increasing vertical displacement of the beam end. Restraint to prevent horizontal displacement at point B is, if this structural connection is assumend to be attached to a rigid core, in better agreement with reality than restraint to prevent horizontal displacement at point A. The network of elements employed in this analysis and the manner of support and loading are shown in Fig. 6.18. Where the beam reinforcement is bent, it has been assumed in the analysis that the normal force in the bar is equal on each side of the point of change of direction (see Section 5.2).

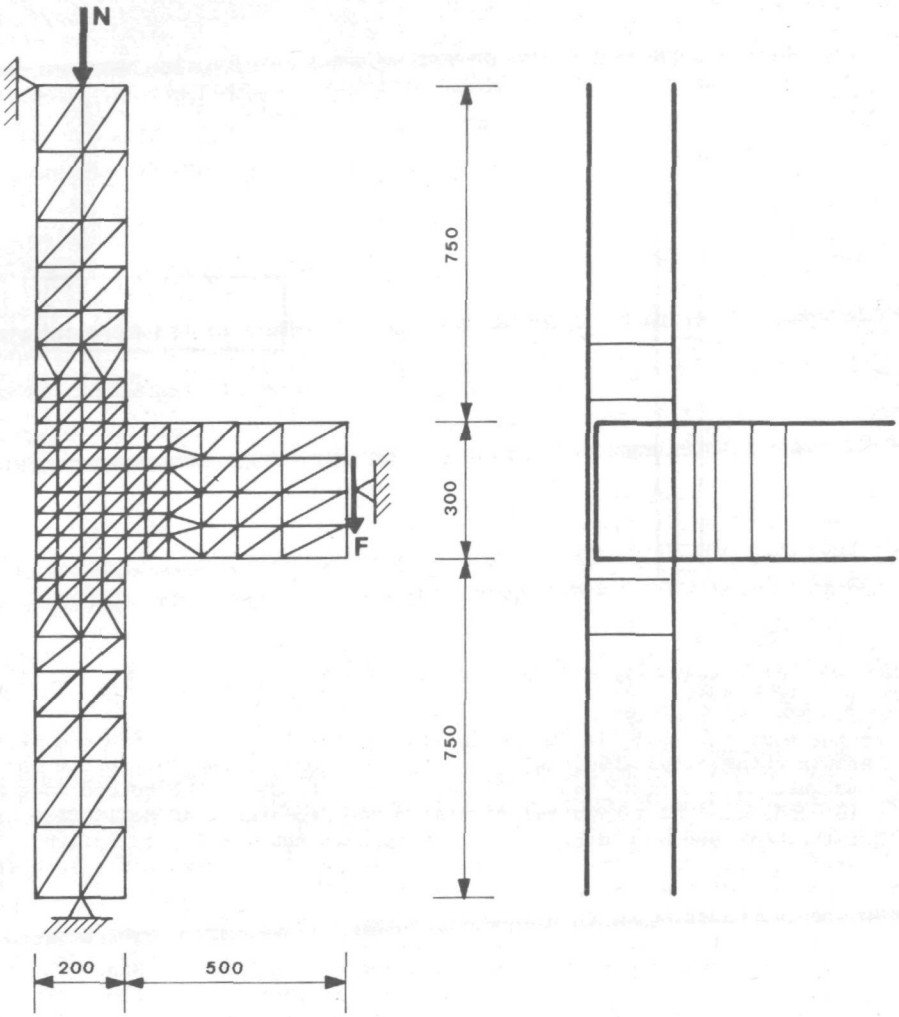

Concrete elements *Reinforcement elements*

FIGURE 6.18 : Network of elements

The following material properties have been adopted in the analysis:

CONCRETE: non-linear behaviour: Link's model

f_b	=	-24.7	N/mm^2
f_b	=	2.38	N/mm^2
E_b	=	24000.	N/mm^2
ν_b	=	0.15	
K	=	5.	

STEEL: ideal elasto-plastic model

	f_a	= 420.	N/mm^2	
	E_a	= 210000.	N/mm^2	
BOND:	f_s	= 5.5	N/mm^2	beam reinforcement
	f_s	= 6.75	N/mm^2	column reinforcement
	G_s	= 55.	N/mm^3	beam reinforcement
	G_s	= 67.5	N/mm^3	column reinforcement
	B_k	= G_s		

The failure loads according to the experiment and the analysis are given in Table 6.1.

	failure load	
	experiment	analysis
F_u	65.3 kN	61.5 kN
N_u	48.0 kN	45.0 kN
H_u	9.1 kN	18.5 kN

TABLE 6.1 : Failure load according to experiment and analysis

It appears from this table that according to the analysis a larger force H is required for preventing horizontal displacement of point B in Fig. 6.16 than according to the experiment is required for preventing horizontal displacement of point A.
On considering the analytically calculated deformation of the structure (see Fig. 6.19a) this difference in the force H seems plausible because according to the analysis, with the boundary conditions to be satisfied there, point A is displaced to the left in consequence of cracking. Directly associated with the magnitude of the horizontal force H is the distribution of the bending moment from the beam to the upper and lower column. At the failure load this distribution was in the proportions of 31% and 69% according to the experiment and of 40% and 60% according to the analysis. As a result of this difference in distribution of the beam moment to the connected columns, the failure moment of the lower column was 8% higher in the analysis than in the experiment, whereas the failure load (F_u) was 5% lower in the analysis than in the experiment. A calculation of the failure load of the structure based on the failure loads of the sections of the beam and columns and a distribution of the internal forces in accordance with the linear elastic theory gives a failure load (F_u) of 90 kN.

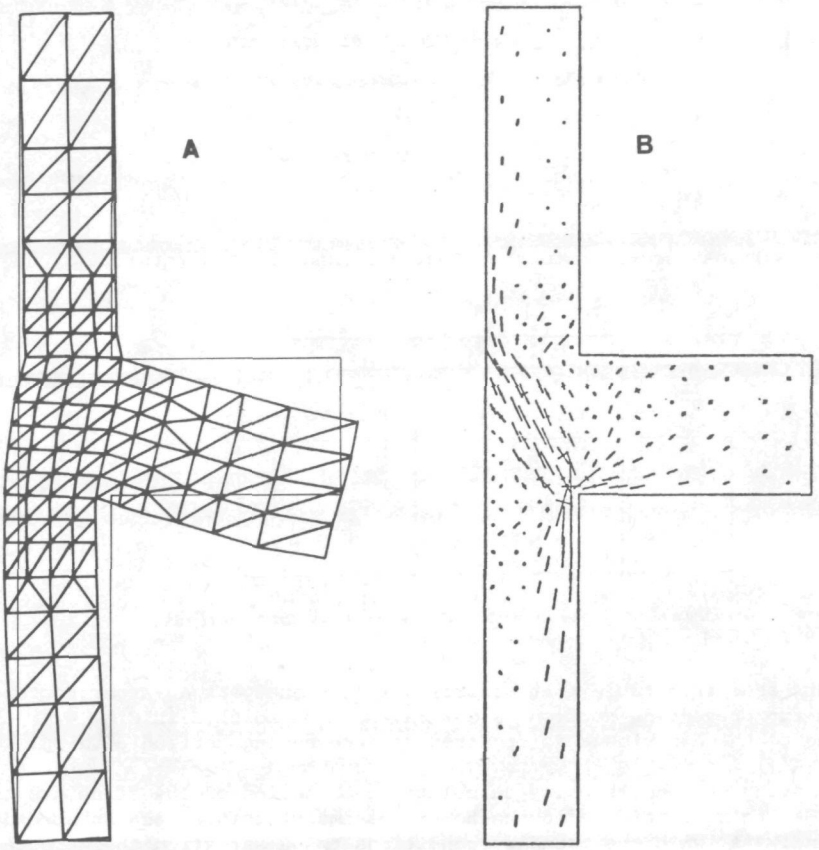

*Deformation of the network of elements under failure load (shown 20 * magnified)*

Directions and magnitudes of principal stresses in the concrete at failure load

FIGURE 6.19 :

The directions and magnitudes of the principal stresses in the concrete at failure load are indicated in Fig. 6.19b. The compression diagonal in the connection, and the absence due to cracking of large tensile stresses, are distinctly discernible in this diagram.
In Fig. 6.20 the load-deflection diagrams for the end of the beam have been plotted. There is seen to be very good agreement between the diagrams for the experiment and for the analysis.

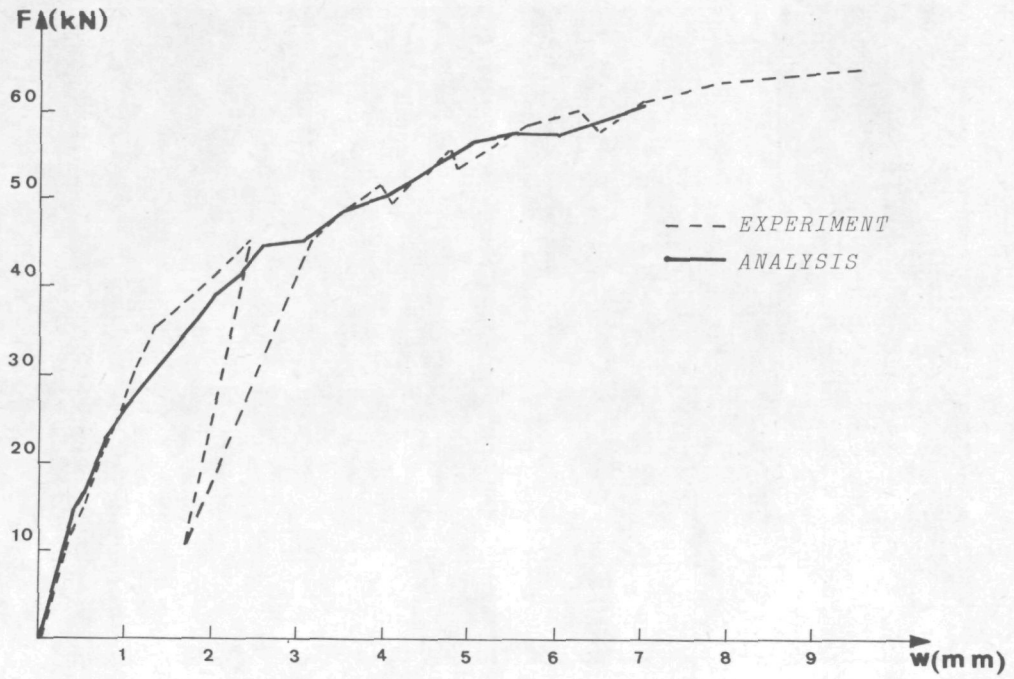

FIGURE 6.20 : Load-deflection diagram

The analysis was terminated at 7 mm deflection of the beam, because for this value the analysis indicates that crushing occurs in the concrete in the compressive zone of the lower column directly under the beam. Such crushing in that region is also found to occur in the test specimen, as Fig. 6.21 shows. Besides the above-mentioned crushing, at failure of the specimen the concrete cover to the left-hand column reinforcement is detached by spalling. This phenomenon is not manifested in the analysis, since the latter does not take the cover into account.

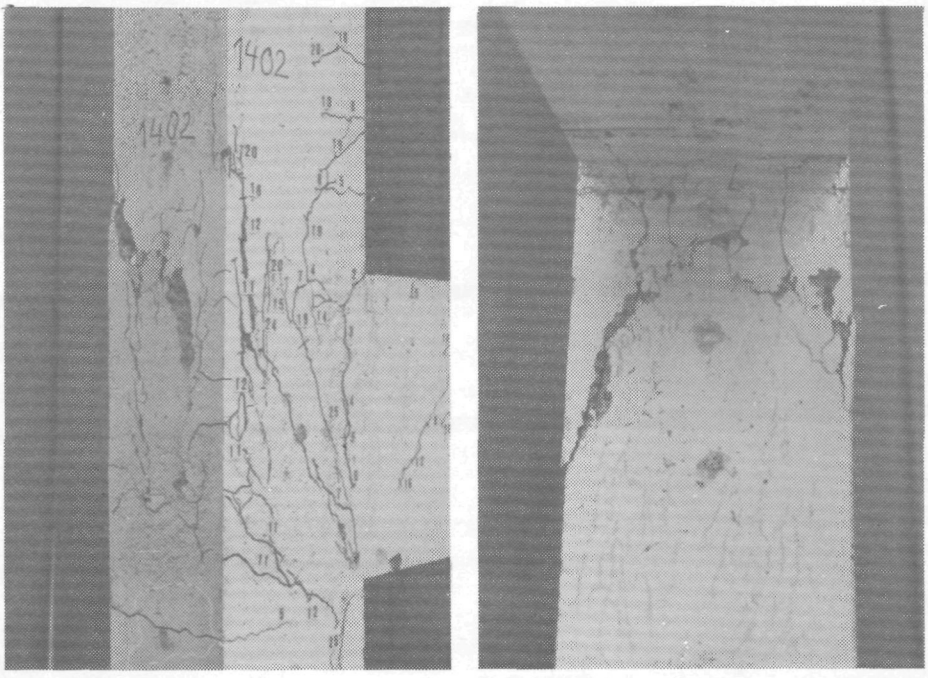

FIGURE 6.21 : Details of the specimen after failure

In Fig. 6.22 the crack pattern determined in the experiment and the crack pattern found in the analysis are shown side by side. In both cases the pattern after failure of the structure is illustrated. Both distinctly reveal the diagonal shear cracks which developed in the connection. In comparison with the experiment the analysis shows more flexural cracks in the lower column and fewer of such cracks in the upper column. This is very probably due to the heavier loading of the lower column in the analysis, a feature what has already been noted in the discussion of the moment distribution. Also, in both crack patterns there is a vertical flexural crack in the beam at its junction with the column. Both in the experiment and in the analysis this is the first crack to be formed.

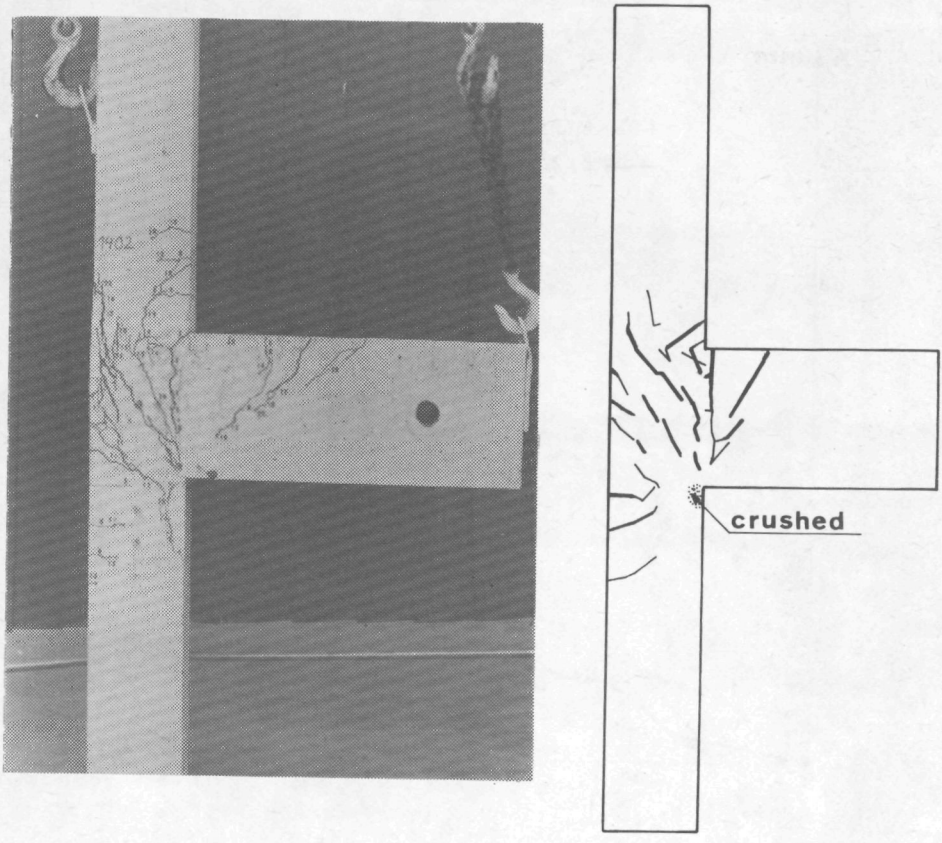

FIGURE 6.22 : Crack patterns according to experiment and analysis

In the experiment the width of the crack at the upper corner of the junction of beam and column was recorded. In Fig. 6.23 the width of this crack is compared with the analytically calculated width for various values of the load applied at the end of the beam.

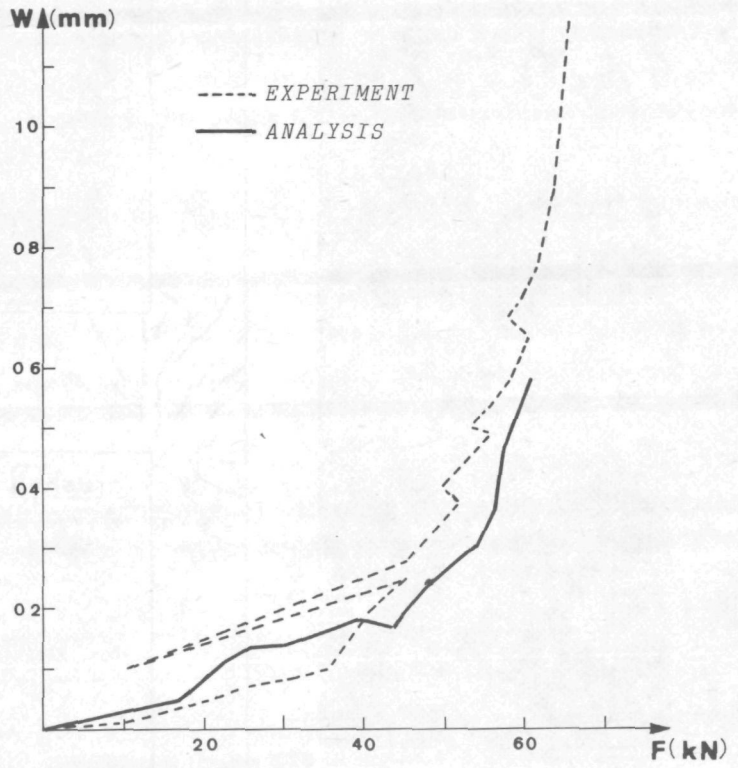

FIGURE 6.23 : Width of crack at upper corner of junction between beam and column

The analytically calculated forces and stresses in the bottom reinforcement and top reinforcement of the beam are presented in Figs. 6.24 and 6.25. In these figures is also indicated which part of the reinforcement slips in the concrete. Comparison with the test specimen in this respect is not possible because no steel strains were measured in the experiment. From the steel stress diagrams it appears that the yield stress of the reinforcement ($420\ N/mm^2$) is nowhere exceeded. For 3.5 mm deflection of the end of the beam the maximum bond stress occurs along the top reinforcement in the beam in the region where this reinforcement is anchored horizontally in the column. Any further increase in the tensile force in this reinforcement is resisted by the bond of the vertically bent-down end portions of these bars in the column.

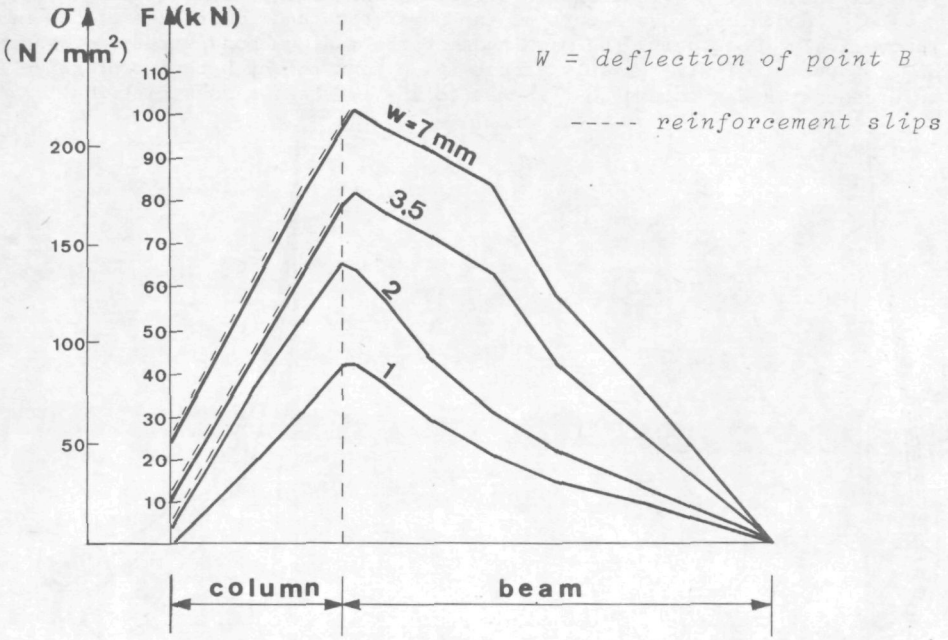

FIGURE 6.24 : Forces and stresses in top reinforcement of beam

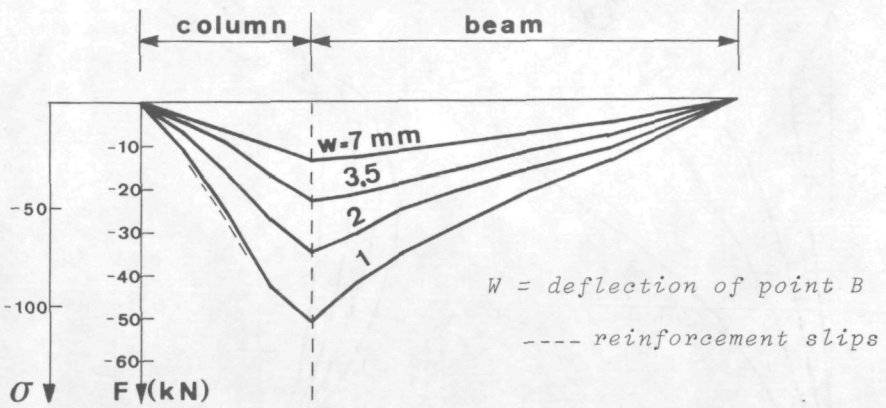

FIGURE 6.25 : Forces and stresses in bottom reinforcement of beam

In the experiment the stresses in the column reinforcement were not measured. The stresses in this reinforcement and the part which slips in the concrete as calculated in the analysis are presented in Fig. 6.26. This diagram shows that at the failure load there was slip of both the left-hand and right-hand column reinforcement at the beam, so that the maximum compressive forces in these bars occur, not at the most severely loaded sections, but higher up in the upper and lower down in the lower column.

For all loads the maximum tensile stress in this reinforcement at the most severely loaded sections occurs at the upper face and lower face of the beam respectively. Obviously, the magnitude of the maximum bond stress between steel and concrete (f_s) will greatly affect the extent to which the compressive reinforcement in the column contributes to the internal stress distribution.

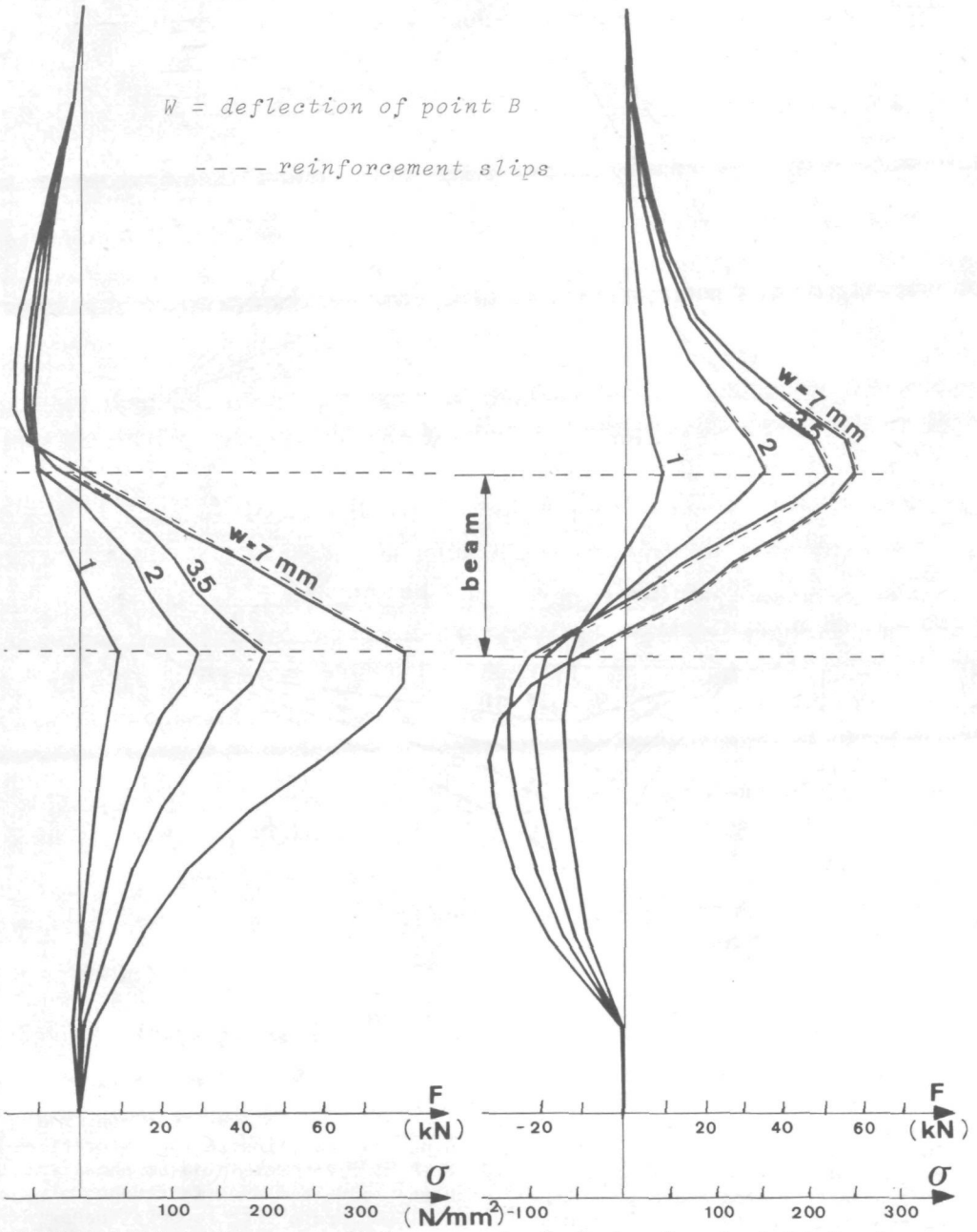

FIGURE 6.26 : Forces and stresses in left-hand and right-hand reinforcement in the column

CONCLUSION

Despite the somewhat adjusted boundary conditions and the manner of loading, there is very good agreement between experiment and analysis. The latter clearly reveals the effect of reinforcement slip upon the internal stress distribution. In consequence of this slip it is not possible to rely on the development of steel stresses of such magnitude as would be calculated from an analysis of the sections of the structural members concerned.
Fig. 6.26 shows that more particularly the compressive reinforcement in the lower column at the most severely loaded section contributes only little to the loadbearing capacity. As a result, the concrete at that section is more severely loaded than had been anticipated, so that failure of this concrete occurs.

7

CONCLUSIONS

As stated in Section 1.4, the aim of this study has been the development of a numerical model with which the behaviour of two-dimensional structures loaded within their own plane can be analysed.

By this behaviour to be analysed is understood:
- the deformation of the structure at a particular magnitude of the load;
- the magnitude of the load at which cracks are formed in the structure;
- the crack spacing and crack widths;
- the slip of the reinforcement;
- the stresses in the concrete and in the reinforcing steel at a particular magnitude of the load;
- the magnitude of the failure load.

In the analysis it is necessary to take account of the non-linear and possibly time-dependent behaviour of concrete, the non-linear behaviour of steel, the non-linear behaviour in the zone of contact between these two materials, and the possibility of transfer of stress across a crack in the concrete. On comparing the results of analyses with those of experiments it appears that the MICRO model can provide a good insight into the above-mentioned behaviour characteristics. This is true both of structures with fairly well distributed cracking (such as the tie member in Section 5.3 and the beam loaded purely in bending in Section 6.2) and of structures with only a few dominant cracks (such as the plate loaded at its upper edge in Section 6.3). From the analysis of the beam-to-column connection (Section 6.4) it emerges that the slip of the reinforcement is of major influence upon the internal stress distribution, the magnitude of the failure load and the deformation of the structure. Also, the development of a few dominant cracks, with large widths, in the plate loaded at its upper edge is possible only because the bottom reinforcement in this plate can slip in relation to the concrete.
The slip of the reinforcing steel as well as the associated development of dominant cracks are well reproduced in the analyses. From the results of the analyses it furthermore appears that the elements developed on the basis of the hybrid method with natural boundary displacements provide a good insight into the stresses and deformations even if the structure is divided into a limited number of elements. The scatter of the tensile strength of the concrete in the structure is found to be of major influence on the scatter in the crack widths and crack spacings. On the other hand, the effect of this scatter in the tensile strength upon the overall deformation of the structure is not significant. When a number of identical experiments are performed, the scatter in the measured crack widths will, however, likewise be greater than the scatter in the deformation.
On judging the differences between experiment and analysis it is necessary to take account of this scatter. An analysis based on the assumption that the tensile strength of the concrete does not vary from one part of the structure to another will suffice only if the object of the analysis is to obtain insight into the deformation, the average crack width and the average crack spacing.

The method adopted in the analyses, where the elements at the end of a crack will undergo cracking at lower stresses than elements not so situated, gives values for the crack penetration depth which are in good agreement with reality. It also appears that the continuity of the cracks in the analysis agrees well with the experimentally determined cracking behaviour. The satisfactory performance of the MICRO model with regard to the structures analysed here does not mean that this model or the material models employed do not require any further refinement. Since only a limited number of structures have been analysed, not all the possibilities of the model have been tested to an equal degree. Dowel action and transfer of shear across a crack were practically absent in the structures analysed.
For the analysis of the structures in which these latter aspects are of major influence it is to be expected that the material models in question will have to be adapted to the results of the "Concrete analysis" research project mentioned in Chapter 1.

SUMMARY

The increase in scale of civil engineering structures built of reinforced concrete or prestressed concrete, and the desire to construct them economically without detriment to structural safety, give rise to the need for a deeper insight into the behaviour of concrete structures and of the causes of this behaviour.
Numerical models with which the behaviour of such structures can be analysed are able to contribute substantially to gaining the necessary insight.
The object of the present study is to develop a numerical model with which the static behaviour of two-dimensional reinforced concrete or prestressed concrete structures with in-plane loading can be analysed. The behaviour of a structure can, inter alia, be understood to comprise:

- the deformation of the structure at a particular magnitude of the load;
- the magnitude of the load at which cracks are formed in the structure, as well as the position and direction of these cracks;
- the spacing of the cracks, their widths and the parallel displacement occuring at a crack;
- the displacement (slip) of the reinforcement in relation to the concrete;
- the stresses in the concrete and the reinforcing steel or prestressing steel;
- the magnitude of the failure load and the mechanism of failure.

Numerical models for the analysis of two-dimensional structures, as described in the literature,are briefly reviewed in Section 1.3. In general, the finite element method is adopted for these models, all of which devote considerable attention to cracking, since this is of major influence upon the behaviour of the structures. Two methods of schematizing the cracks are to be distinguished, namely: a method based on the possibility of discrete cracks along the boundaries of the elements, and a method in which the cracks are permitted to pass through the elements, but are assumed to be distributed over the element or over part thereof. The principal differnces between the two methods are:

The method with discrete cracks along the element boundaries

- gives better insight into the relative displacements at a crack;
- offers the possibility of describing the stress peaks and the dowel forces in the steel at a crack;
- can take account of the relationship between aggregate interlock and displacements at a crack;
- is often better able to schematize dominant cracks and their effect on behaviour.

The method with cracks "smeared out" in the element

- offers greater freedom with regard to possible crack directions;
- does not make it necessary to establish the system matrix over and over again and to invert or decompose it; also, the number of degrees of freedom remains constant throughout the analysis.

In the method of crack schematization developed in this thesis the advantages of both methods are combined. The model is based on the finite element approach. For describing the structure, two types of element have been developed: a triangular plate element for schematizing the concrete, and a bar element for describing the reinforcing steel or prestressing steel plus the bond zone with the surrounding concrete. Both these elements are based on the hybrid method with natural boundary displacements. The element relationships have been derived with the aid of Galerkin's method in Chapter 3. It is characteristic of these elements that the stresses at their boundaries are always in equilibrium with one another and with the internal loading. In the model, discrete cracks are considered, which may extend in any direction through the elements and which continue as much as possible across the element boundaries. Besides taking account of the discontinuity in the displacements on each side of a crack, the model also takes account of discontinuity across a crack of the normal stresses in the direction of the crack. Once they have formed, cracks remain present in the model. Transfer of compressive stresses across a crack is not possible except for zero crack width. A crack that has been squeezed shut will open immediately, as soon as a tensile stress acts across it. A crack width of less than zero is not possible. The method of initial strains is used for deeling with the non-linear behaviour of the materials, the displacement at the cracks and the slip of the reinforcement. Besides the possibility of treating the displacements at the cracks as initial displacements, in the MICRO model the element matrices of the cracked elements can, after a number of cracks have formed, be adapted to the dynamic boundary conditions which apply at the line of the crack.

Chapter 4 contains a description of the material models with which, in using the program, the behaviour of the materials can be explicitly described. These material models are:

- a non-linear stress-strain relationship for concrete;
- the cracking criterion for concrete;
- the crushing criterion for concrete;
- the shrinkage of concrete as a function of time;
- the creep of concrete as a function of time;
- the aggregate interlock in a crack;
- a non-linear stress-strain relationship for steel;
- a yielding criterion for steel;
- the bond between steel and concrete;
- the dowel action of the reinforcing steel.

Furthermore, the program can take account of angular changes in direction of the reinforcing bars and with scatter of the properties of concrete and steel in the structure.
The comparison, in Chapter 5 and 6, of structures analysed with the aid of the program, on the one hand, and the results of experiments, on the other, show that with the model developed in this thesis it is possible to obtain a good insight into the deformation, the crack pattern, the crack widths, the crack spacing, the intern stress distribution and the failure load of two-dimensional structures under in-plane static loading.

REFERENCES

1. 1 *WALRAVEN J.C./ VOS E./ REINHARDT H.W.*
"Experiment on Shear Transfer in Cracked Concrete" Preliminary Report IASS symposium, Nonlinear Behaviour of Reinforced Concrete Spatial Structures, Vol.1 p.p. 61-73, Darmstadt 1978.

1. 2 *NGO D./ SCORDELIS A.C.*
"Finite element analysis of reinforced concrete beams" ACI Journal, Proceedings Vol.64 no.3 March 1967 p.p. 152-163.

1. 3 *NILSON A.H.*
"Nonlinear analysis of reinforced concrete by the finite element method" ACI Journal, Proceedings Vol. 65 no.9 sept. 1968 p.p. 757-766.

1. 4 *STAUDER W.*
"Ein Beitrag zur Untersuchung von Stahlbetonscheiben mit Hilfe finiter Elemente unter Berücksichtigung eines wirklichkeits nahen Werkstoffverhaltes" Dissertation, TH Darmstadt, 1973.

1. 5 *LEONHARDT F./ WALTHER R.*
"Wandartige Trager" Deutscher Ausschuss für Stahlbeton Heft 178, Berlin 1966.

1. 6 *FRANKLIN H.A.*
"Nonlinear analysis of reinforced concrete frames and panels" Dissertation, Berkeley, 1970.

1. 7 *GOTO Y.*
"Cracks formed in Concrete around Deformed Tension Bars" ACI Journal, April 1971 p.p. 244-251.

1. 8 *EBBINGHAUS P.*
"Herleitung eines Verfahrens zur Berechnung von Stahlbetonscheiben unter Berücksichtigung der Riszentwirckling" Dissertation, RWTH Aachen, 1975.

1. 9 *CERVENKA V.*
"Inelastic finite analysis of reinforced concrete panels under inplane loads" Dissertation, University of Colorado, 1970.

1.10 *DORR K./ MEHLHORN G./ STAUDER W./ UHLISCH D.*
"Berechnung von Stahlbetonscheiben im Zustand II bei Annahme eines wirklichkeitsnahen Werkstoffverhaltens" Deutscher Ausschuss für Stahlbeton Heft 238,Berlin 1974.

1.11 *SCHNOBRICH W.C.*
"Behaviour of reinforced concrete structures predicted by the finite element method" Computers & Structures, Vol.7, no.3 June 1977 p.p. 365-376.

1.12 *HOSHINO M.*
"Ein Beitrag zur Untersuchung des Spannungszustandes an Arbeitsfugen mit Spannglied koppelungen von adschnittsweise in Ortbeton hergestellten Spannbetonbrücken" Dissertation, TH Darmstadt 1974.

1.13 *CEDOLIN L./ DEI POLI S.*
"Finite Element Nonlinear Analysis of Reinforced Concrete Bidimensional Structures" Technical Report N.40 ISIC 1974.

1.14 *VALLIAPPAN S./ DOOLAN T.F.*
"Nonlinear stress analysis of reinforced concrete" Journal of the Structural Division, Proceedings of the ASCE, Vol.98, no.ST 4, April 1972 p.p. 885-898.

1.15 *ZIENKIEWICZ O.C./ PHILLIPS D.V./ OWEN D.R.J.*
"Finite element analysis of some concrete non-Linearities-Theory and examples" IABSE Seminar on "Concrete structures subjected to triaxial stresses" May 1974, Bergamo Paper III-2.

1.16 *ARGYRIS J.H./ FAUST G./ SZIMMAT J./ WARNKE E.P./ WILLAM K.J.*
"Finite Element - Berechnung von Spannbeton - Reaktor - druckbehältern" Deutsche Ausschuss für Stahlbeton, No.278, Berlin 1977.

1.17 *BUYUKOZTURK O.*
"Nonlinear analysis of reinforced concrete structures" Computers & Structures Vol.7 no.1, Febr. 1977 p.p. 149-156.

1.18 *LIN C.S.*
"Nonlinear Analysis of reinforced concrete slabs and shells" Report no. UC SESM 73-7, University of California, 1973.

1.19 *SUIDAN M./ SCHNOBRICH W.C.*
"Finite Element Analysis of Reinforced Concrete" ACI Journal, October 1973, p.p. 2109-2122.

1.20 *HAND F.R./ PECKNOLD D.A./ SCHNOBRICH W.C.*
"Nonlinear Layered analysis of RC Plates and Shells" Journal of the Structural Division, Proceedings of the ASCE, Vol. 99 no. ST 7, July 1973, p.p. 1491-1505.

1.21 *KUSTERS G.M.A.*
"Niet-lineair materiaalgedrag van gewapend beton met behulp van de eindige elementenmethode" Instituut voor Bouwmaterialen en Bouwconstructies IBBC-TNO, rapport BI-77-36, Rijswijk 1977.

2. 1 *BLAAUWENDRAAD J.*
"Systematische bouw met directe methoden en variatieprincipes van continue en discrete mechanicamodellen" Dissertation TH Delft, 1973.

2. 2 *CARMEAU I.*
"Numerical stability in quasistatic elasto/visco-plastity". International Journal for numerical methods in engineering, 1975, vol.9, p.p. 109-127.

3. 1 *WOLF J.P.*
"Generalized Stress-Models for Finite-Element Analysis". Report no. 52, Institut für Baustatik ETH Zürich, 1974.

3. 2 *HUTTON S.G./ ANDERSON D.L.*
"Finite Element Method: A Galerkin Approach". Journal of the Engineering Mechanics Division, Proceedings of the ASCE, no. EM 5, October 1971, p.p. 1503-1520.

4. 1 *KUPFER H.*
"Das Verhalten des Betons unter mehrachsiger Kurzzeitbelastung unter besonderer Berücksichtigung der zweiachsigen Beanspruchung". Deutscher Ausschuss für Stahlbeton Heft 229, Berlin 1973.

4. 2 *LINK J.*
"Eine Formulierung des zweiaxalen Verformungs- und Bruchverhaltens von Beton und deren Anwendung auf die wirklichkeitsnahe Berechnung von Stahlbetonplatten". Deutscher Ausschuss für Stahlbeton Heft 270, Berlin 1976.

4. 3 *ROMSTAD K.M./ TAYLOR M.A./ HERRMAN L.R.*
"Numerical Biaxial Characterization for Concrete". Journal of the Engineering Mechanics Division of the ASCE, no. EM 5, October 1974, p.p. 935-947.

4. 4 *NELISSEN L.J.M.*
"Twee-assig onderzoek van grindbeton". Dissertation TH Delft, 1970.

4. 5 *RUSCH H./ JUNGWIRTH D./ HILSDORF H.*
"Kritische Sichtung der Verfahren zur Berücksichtigung der Einflüsse von Kriechen und Schwinden des Betons auf das Verhalten der Tragwerke". Beton und Stahlbetonbau, Heft 4, 1973, p.p. 76-86.

4. 6 *CEB*
"Systeme international de reglementation technique unifiee des structures". Bulletin d'information no. 111, October 1975.

4. 7 *WALRAVEN, J.C.*
"Mechanisms of shear transfer in cracks in concrete". Stevin-laboratory TH Delft, report 5-78-12, Delft 1978.

5. 1 *GIJSBERS F.B.J.*
"Enige trekproeven op gewapend beton" CUR-commissie A 26, report no. A 26/77-04, 1977.

5. 2 *THE GENESYS CENTRE*
"Reference manual". The Genesys Centre, 1972.

5. 3 *GROOTENBOER H.J.*
"Users Manual MICRO-program". To be published in 1979.

5. 4 *MONDKAR D.P./ POWELL G.H.*
"Toward optimal in-core equation solving" Computers & Structures vol 4, 1974, p.p. 531-548.

6. 1 *MONNIER Th.*
"The moment-curvature relation of reinforced concrete" Heron vol. 17, no. 2, 1970.

6. 2 *HOEKSTRA A.S.*
"De invloed van de wapeningsdetaillering op het gedrag van de doorgaande kolom-balkverbinding" Afdeling Civiele Techniek, TH Delft, 1977.

SAMENVATTING

Door de schaalvergroting bij civiel-technische constructies, van gewapend beton of voorgespannen beton, en de wens deze economisch te construeren zonder de veiligheid geweld aan te doen, ontstaat de behoefte aan een verdieping van het inzicht in het gedrag van betonconstructies en in de oorzaken van dit gedrag. Numerieke modellen waarmee het gedrag van betonconstructies kan worden berekend, kunnen in belangrijke mate bijdragen aan dit beoogde inzicht. Doel van deze studie is de ontwikkeling van een numeriek model waarmee het statisch gedrag van tweedimensionale in hun vlak belaste constructies, van gewapend beton of voorgespannen beton, kan worden geanalyseerd.
Onder het gedrag van een constructie wordt ondermeer verstaan:
- de vervorming van de constructie bij een bepaalde belasting,
- de grootte van de belasting waarbij in de constructie scheuren ontstaan alsmede de plaats en de richting van deze scheuren,
- de onderlinge afstanden tussen de scheuren, de scheurwijdten en de parallel verplaatsing in een scheur,
- de relatieve verplaatsing (slip) van de wapening ten opzichte van het beton,
- de spanningen in het beton en het wapeningsstaal of het voorspanstaal,
- de grootte van de bezwijklast en het bezwijkmechanisme.

In paragraaf 1.3 is een kort overzicht gegeven van in de literatuur beschreven numerieke modellen voor de berekening van tweedimensionale betonconstructies. Voor deze modellen wordt algemeen uitgegaan van de eindige elementenmethode. Aangezien de scheurvorming grote invloed heeft op het gedrag wordt in alle modellen hieraan veel aandacht geschonken.
In de wijze van schematisering van de scheuren zijn twee methoden te onderscheiden. Een methode gebaseerd op de mogelijkheid van discrete scheuren langs de randen van de elementen en een methode waarbij de scheuren door de elementen mogen lopen maar waarbij deze over een deel van het element of het gehele element verdeeld worden aangenomen.
De belangrijkste verschillen tussen de beide methoden zijn:

De methode met discrete scheuren langs de elementenranden,
- geeft meer inzicht in de relatieve verplaatsingen in een scheur,
- biedt de mogelijkheid tot het beschrijven van de spanningspieken en de deuvelkrachten in het staal ter plaatse van een scheur,
- kan rekening houden met het verband tussen de haakweerstand en de verplaatsingen in een scheur,
- kan dominante scheuren en hun invloed op het gedrag veelal beter schematiseren.

De methode met in het element uitgesmeerde scheuren,
- biedt een grotere vrijheid ten aanzien van de mogelijke scheurrichtingen,
- vraagt niet telkenmaal de systeemmatrix op te stellen en te inverteren of te decomponeren. Tevens blijft het aantal vrijheidsgraden tijdens de gehele berekening constant.

In de hier ontwikkelde methode van scheurschematisering worden de voordelen van beide methoden gecombineerd. Het model is gebaseerd op de eindige elementenmethode. Voor de beschrijving van de constructie zijn ontwikkeld een driehoekig schijfelement voor de schematisering van het beton en een staafelement voor de beschrijving van het wapeningsstaal of voorspanstaal plus de aanhechtzône met het omhullende beton. Beide elementen zijn gebaseerd op de Hybride methode met natuurlijke randverplaatsingen. De elementrelaties zijn in hoofdstuk 3 afgeleid met behulp van de methode Galerkin. Kenmerkend voor deze elementen is dat de spanningen op de randen van de elementen altijd in evenwicht zijn met elkaar en met de uitwendige belasting.

In het model wordt gerekend met discrete scheuren die in een willekeurige richting door de elementen kunnen lopen en over de elementranden zo veel mogelijk doorlopen. Naast de discontinuïteit in de verplaatsingen aan weerszijden van een scheur wordt eveneens rekening gehouden met een discontinuïteit over een scheur van de normaalspanningen in de richting van de scheur.

Scheuren die eenmaal zijn ontstaan blijven in het model aanwezig. Overdracht van drukspanningen via een scheur is eerst omgelijk bij een scheurwijdte van nul. Een dichtgedrukte scheur opent zich onmiddellijk zodra er een trekspanning op gaat werken. Een scheurwijdte kleiner dan nul is niet mogelijk.

Voor de verwerking van het niet lineaire gedrag van de materialen, de verplaatsingen in de scheuren en de slip van de wapening wordt de initiële rekkenmethode gebruikt. Naast de mogelijkheid om de verplaatsingen in de scheuren te verwerken als initiële verplaatsingen kunnen in het MICRO-model na het ontstaan van een aantal scheuren de elementmatrices van de gescheurde elementen worden aangepast aan de op de scheurlijn geldende dynamische randvoorwaarden.

In hoofdstuk 4 zijn beschreven de materiaalmodellen waarmee bij gebruik van het programma het gedrag van de materialen expliciet kan worden omschreven. Deze materiaalmodellen zijn:
- een niet lineaire spannings-rek relatie voor beton,
- het scheurcriterium voor beton,
- het criterium voor het verbrijzelen van beton,
- de krimp van beton in de tijd,
- de kruip van beton in de tijd,
- de haakweerstand in een scheur,
- een niet lineaire spannings-rek relatie voor staal,
- een vloeicriterium voor staal,
- de aanhechting tussen staal en beton,
- de deuvelwerking van het wapeningsstaal.

Verder kan in het programma rekening worden gehouden met geknikte vormen van de wapening en een spreiding van de beton en de staaleigenschappen in de constructie.

De vergelijking in hoofdstuk 5 en 6 van de met het programma berekende constructies met de uitkomsten van experimenten toont dat met het ontwikkelde model een goed inzicht kan worden verkregen in de vervorming, het scheurenpatroon, de scheurwijdten, de scheurafstanden, de interne spanningsverdeling en de bezwijkbelasting voor tweedimensionale in hun vlak belaste constructies onder een statische belasting.